DEVELOPMENT AND APPLICATION OF A MODEL DESCRIBING THE BIOACCUMULATION AND METABOLISM OF POLYCYCLIC AROMATIC HYDROCARBONS IN A MARINE BENTHIC FOOD WEB

by

Ryan William Stevenson
Bachelor of Science, UBC, 1995

A PROJECT SUBMITTED IN PARTIAL FULFILLMENT
OF THE REQUIREMENTS FOR THE DEGREE OF
MASTER OF RESOURCE MANAGEMENT

in the School of Resource and Environmental Management
Report No. 334

SIMON FRASER UNIVERSITY
July 2003

APPROVAL

Name: **Ryan William Stevenson**

Degree: **Master of Resource Management**

Title of Project: **Development and Application of a Model Describing the Bioaccumulation and Metabolism of Polycyclic Aromatic Hydrocarbons in a Marine Benthic Food Web**

Report No. **334**

Examining Committee:

Dr. Frank A.P.C. Gobas

Senior Supervisor
Associate Professor
School of Resource and Environmental Management
Simon Fraser University

Dr. Christopher J. Kennedy

Associate Professor
Department of Biological Sciences
Simon Fraser University

Date Approved:

ABSTRACT

Emission of polycyclic aromatic hydrocarbons (PAHs) to Kitimat Arm is of concern because PAHs persist in the environment and are known carcinogens. Despite their hydrophobicity, metabolic transformation within organisms is expected to limit food chain biomagnification of PAHs. However, metabolic transformation produces reactive Phase I metabolites, which are the primary cause of PAH-related carcinogenesis and other toxic effects. The goal of this research was to develop a model for assessing bioaccumulation of parent PAHs and PAH metabolites in marine organisms from Kitimat Arm.

A mechanistic bioaccumulation model was developed for non-metabolized substances in a representative benthic food web for the BC Coast. Following calibration, model predictions were within a factor of four of observed BSAFs for polychlorinated biphenyls in Dungeness crab from Kitimat Arm and False Creek, BC.

For PAHs, the model was modified to characterize metabolic transformation of PAHs, low bioavailability of PAHs due to soot-association, and the mass balance of Phase I PAH metabolites. Based on a literature review, metabolic rate constants for PAHs were expected to range from approximately 0.20/day in bivalve mollusks to 1-1.5/day in Dungeness crab and fish species. Model predictions were within a factor of three of observed BSAFs for PAHs in Dungeness crab from Kitimat Arm.

Model behaviour indicated trophic dilution of parent PAH body burdens in predatory organisms as a result of metabolic transformation within organisms and their prey species. The model also predicted trophic dilution of Phase I PAH metabolites, regardless of assumptions regarding the rates of Phase II conjugation and detoxification. Flux calculations determined that Phase I PAH metabolite body burdens were primarily the result of metabolite production within organisms rather than uptake of metabolites from prey and, therefore, closely linked to parent PAH body burdens.

Model application determined that bivalve mollusks have the highest expected dose of parent PAHs and Phase I PAH metabolites, suggesting potentially higher ecological risk for this organism class. The model also demonstrated that seafood criteria for the protection of human health need to consider residues of both parent PAHs and Phase I PAH metabolites that are present in harvested organisms from PAH-contaminated areas.

ACKNOWLEDGEMENTS

The completion of this research project marks the end of an exciting time of development and learning for me, at a personal, academic and professional level. I am especially grateful to my senior supervisor, Dr. Frank Gobas. Thank you, Frank, for your vision for this project, your unrelenting positive energy and your guidance with the many challenges that this research presented. I would also like to thank Dr. Chris Kennedy for offering his knowledge and suggestions, especially relating to PAH metabolism.

Funding for this project was a continued challenge and I am grateful to several funding sources. I am most grateful to Dr. Frank Gobas for providing funding from his research grants after the originally-planned funding fell through. Thank you also to the Faculty of Applied Sciences at SFU for the award of two Graduate Fellowships and the School of Resource Management for TA-ship opportunities. I would also like to thank Gary Mann of Azimuth Environmental Consulting Group for the several contracts which augmented my meager student income.

My time at REM has been enriched by the fabulous group of people who make up the faculty, staff and students here. It is the people in REM who make this place an exemplary learning institution and a fun place to be. Keep it up! I would especially like to thank Laurence, Rhonda, Bev, Sarah and Anissa for all the help, and members of the Toxlab for the valuable discussions and group learning.

Finally, I would like to thank Jamila and Tofino. Jam, your way of being in the world inspires me. Thank you for your love and support. Thank you, Tofino, for retrieving all those logs.

TABLE OF CONTENTS

LIST OF FIGURES

LIST OF TABLES

GLOSSARY

Bioaccumulation – the combined processes of chemical uptake at respiratory surfaces (bioconcentration) and in the gut (gastrointestinal magnification), and chemical elimination via gill elimination, faecal egestion, growth dilution and metabolic transformation. For hydrophobic chemicals, bioaccumulation often results in much higher concentrations in aquatic organisms relative to water (Gobas and Morrison, 2000)

Bioaccumulation Factor (BAF) – for pelagic organisms, it is the ratio of the chemical concentration in the organism (g/kg lipid) to that dissolved in water (g/kg; Gobas and Morrison, 2000).

Bioaccumulative (B) – the term used under the CEPA screening framework for chemicals which have a tendency to accumulate in organisms and transfer through the food chain (CEPA, 1999).

Bioavailability – the fraction of chemical present within a phase, that is available for uptake by organisms via either respiratory or dietary routes (Gobas and Morrison, 2000)

Bioconcentration – chemical uptake at gill or respiratory surfaces via passive diffusion (Gobas and Morrison, 2000)

Biota-Sediment Accumulation Factor (BSAF) – for benthically-coupled organisms, it is the ratio of the chemical concentration in the organism (g/kg lipid) to that in the sediment with which it is associated (g/kg OC; Gobas and Morrison, 2000).

Biotransformation – the process of chemical transformation within an organism, generally due to the action of the metabolic system of the organism (Gobas and Morrison, 2000). Also referred to as metabolic transformation or chemical metabolism.

Carcinogenesis – as a result of chemical exposure, the induction in organisms of neoplasms and tumours in forms that are not normally observed, at earlier stages than are usually observed, or at higher levels of incidence than are normally observed (IARC, 1982).

Cytochrome P-450 – the class of enzymes generally responsible for catalyzing the hydroxylation of drugs, hormones and chemicals via a mixed-function oxidation reaction (Gibson and Skett, 1986). Cytochrome P-450 is present in the endoplasmic reticulum of cells and is responsible for Phase I metabolic transformation of PAHs.

Ecological Risk Assessment (ERA) – the application of a formal framework to assess the potential impacts of human-created stressors (especially contaminants) on a natural resource. ERA typically involves the integration of an exposure

assessment, toxicological dose response information and receptor characteristics (US EPA, 1998).

Epifauna – For benthic marine systems, organisms which inhabit the sediment surface.

Food Chain Biomagnification – the phenomenon whereby chemical concentrations (on a lipid-normalized basis; g/kg lipid) increase through successive trophic levels in the food chain. Also referred to as Food Chain Bioaccumulation (Gobas and Morrison, 2000).

Fugacity (f) – the escaping tendency of a chemical from a phase or the *partial pressure* (Pascals) of a chemical within a phase (Mackay, 1991). Fugacity depends upon the chemical concentration within a phase (C; mol/m^3) and the capacity of the phase to absorb the chemical (Z; $Pa \cdot m^3/mol$) such that $f = C/Z$. Z varies with chemical and phase properties.

Gastrointestinal Magnification – chemical uptake from food in the gut. Gastrointestinal magnification results from the "fugacity pump" that is created as lipid is absorbed from digesta (lowering its fugacity capacity) and the volume of digesta decreases (increasing the chemical concentration; Gobas and Morrison, 2000).

Human Health Risk Assessment – the application of a formal framework to assess the likelihood that a given exposure to a chemical or stressor will cause health effects in humans.

Infauna – For benthic marine systems, organisms which burrow within and inhabit the zone below the sediment surface.

Model Bias (MB) – a statistic used to assess the systematic bias of model predictions (i.e., toward underprediction or overprediction) either as a function of, or independent of chemical properties such as K_{ow}. Refer to Equation 31.

Model Calibration – sensitivity analysis to obtain the set of conditions that (i) provide an accurate representation of the system being modelled and (ii) are scientifically defensible based on mechanistic considerations and empirical data. (Jackson et al. 2000; Connolly, 1991).

Neoplasm – an abnormal mass of tissue that results from chemical carcinogenesis. Synonymous with tumour.

Persistent (P) – the term used under the CEPA screening framework for chemicals which take a long time to break down in the environment (CEPA, 1999).

Porewater – water from the interstitial spaces of sediment, often assumed to be in equilibrium with sediment solids.

Sensitivity Analysis – the systematic varying of model parameters to examine the impact of parameter uncertainty on model behaviour and predictions

Steady State – the set of conditions whereby the total chemical influx of chemical in an organisms equals the total outflux of chemical, with no net change in mass or concentration of the chemical (Gobas and Morrison, 2000).

Toxic (T) – the term used under the CEPA screening framework for chemicals which enter the environment in amounts that may have a harmful effect on the environment or human health (CEPA, 1999).

Trophic Guild – an aggregation of species inhabiting a similar portion of the environment and similar position in the food web (i.e., with similar predators and prey).

ABBREVIATIONS

B(a)A – benz(a)anthracene

B(a)P – benzo(a)pyrene

BCF – bioconcentration factor

BPH – benzo(a)pyrene hydroxylase

CEPA – Canadian Environmental Protection Act

DNA – deoxyribonucleic acid

EH – epoxide hydroxylase

GST – glutathione *s* transferase

IRIS – Integrated Risk Information System

K_{ow} – octanol-water partition coefficient

K_{sc} – soot-carbon-water partition coefficient

MFO – mixed-function oxidase

NLOM – non-lipid organic matter

OC – organic carbon

PAH – polycyclic aromatic hydrocarbon

PBT – persistent, bioaccumulative and toxic

PCB – polychlorinated biphenyl

POP – persistent organic pollutant

SSQ – sum of squared deviations

US EPA – United States Environmental Protection Agency

1 INTRODUCTION

1.1 PERSISTENT ORGANIC POLLUTANTS IN CANADA

Persistent organic pollutants (POPs) are stable, long-lived chemicals that are environmentally persistent, prone to global atmospheric transport, and in some cases, accumulate in the food chain to levels that are potentially toxic to aquatic and terrestrial life (UNECE, 1998; Vallack et al., 1998). Associated with these consequences are potential economic costs, social impacts and degradation of ecosystems which provide important ecological services and are utilized for traditional hunting and gathering activities. Representative POPs include human-manufactured chemicals (e.g., PCBs, pesticides) as well as byproducts of industrial processes (e.g., PAHs, dioxins).

In Canada, POPs are regulated under the Canadian Environmental Protection Act (CEPA; 1999). The Act seeks to regulate substances on the Domestic Substances List that "enter the environment in amounts that may have an immediate or long-term harmful effect on the environment" (Environment Canada, 2000). The method for achieving this goal involves a framework of assessment designed to evaluate persistence (i.e., slow rates of breakdown in the environment), bioaccumulation (i.e., accumulation in living organisms) and toxicity (i.e., potentially harmful at environmentally relevant tissue residues). Substances which are deemed to be persistent, bioaccumulative and toxic (PBT), and which are primarily of anthropogenic origin, are categorized as Track 1 chemicals with management aimed at virtual elimination. For hydrophobic chemicals with a natural tendency to accumulate in organisms, biotransformation of parent chemical within the organism can be a significant elimination process, limiting bioaccumulation of parent chemical. However, there are no provisions under the CEPA screening framework for assessing the persistence, bioaccumulation and toxicity of the metabolites of POPs, some of which have known toxic potential.

Further study of the fate, bioaccumulation and toxicity of potential POPs including the implications of POP metabolism can provide useful information for the effective management of these substances. Integrating these processes through environmental

modelling improves scientific understanding so that the environmental implications of certain management policies can be more accurately predicted. This, in turn, improves the quality of scientific information available to policy makers attempting to balance economic, social, cultural and environmental values.

1.2 POLYCYCLIC AROMATIC HYDROCARBONS

Polycyclic aromatic hydrocarbons (PAHs) are hydrophobic organic substances composed of two or more benzene rings (CEPA, 1994, Eisler, 1987). PAHs enter the environment from many sources, both anthropogenic (e.g., oils spills, smelter emissions, coal-based energy) and natural (e.g., forest fires, volcanic eruptions). The largest point source of PAHs in the Northern Hemisphere is aluminum smelters utilizing Soderburg technologies (CEPA, 1994). Low molecular weight PAHs (PAHs comprised of two or three benzene rings) are known to be acutely and chronically toxic to aquatic organisms causing impairments to survival and growth or abnormal reproduction and development (Eisler, 1987). In contrast, high molecular weight PAHs (four or more benzene rings) are less acutely toxic at environmental concentrations but can be carcinogenic and mutagenic in higher level organisms (CEPA, 1994, Eisler, 1987). For example, exposure to high molecular weight PAHs is associated with carcinogenesis and immunotoxicity in flatfish from polluted harbours in Puget Sound, WA (Baumann, 1989; Myers et al., 1990). Consequently, thirteen PAHs are listed on the Priority Substances List (i.e., Track 2) administered under CEPA (CEPA, 1994). In addition, PAH emissions from Soderberg smelting are being targeted under the UNEP Protocol on Long-Range Transboundary Air Pollution (UNECE, 1998).

For marine systems, the fate of PAH compounds depends on their degree of hydrophobicity (i.e., K_{ow}). In general, high molecular weight PAHs will associate with organic carbon in bottom sediments or suspended sediment (Mackay et al., 1999), where they are then available for uptake and trophic transfer by marine invertebrates. In temperate marine ecosystems such as Kitimat Arm, BC, this uptake may be important for Dungeness crab which feed directly at many levels of the benthic food web (Stevens et al., 1982).

An important factor that could modulate PAH accumulation in marine organisms is metabolism and potential metabolite elimination. Several reviews describe how many fish and invertebrate species can rapidly metabolize PAHs resulting in low body burdens of parent compounds (James, 1989 and Varanasi et al., 1989a; Livingstone, 1991; Meador et al., 1995). If metabolic rates are high enough, PAHs in food resources of Dungeness crab may be reduced in concentration or biotransformed to metabolic products with a different affinity for trophic transfer. Furthermore, parent PAHs that do accumulate in Dungeness crab from water and dietary sources are likely to undergo biotransformation, reducing body burdens of parent compounds for this higher trophic level receptor.

1.3 RATIONALE AND PURPOSE

Traditionally, biotransformation in aquatic species has been regarded as a mitigating factor for PAH toxicokinetics as it often leads to extremely low or undetectable tissue concentrations of parent PAHs. In many cases, *low concentration* is assumed to be synonymous with *low dose* with the implicit assumption of a lower likelihood of harmful effects. However, metabolic pathways for parent PAHs create reactive metabolic intermediates that are more toxic than the parent compounds. These metabolites are associated with hepatic disease, tumour formation and biochemical stress in fish and invertebrates (Baumann, 1989, Fossi et al., 1997). In addition, mesocosm studies with fish and invertebrates indicate dietary uptake of metabolites, potentially resulting in trophic transfer of biotransformed compounds rather than elimination from the food web (Kane-Driscoll and McElroy, 1997). PAH metabolism is also the mechanism of carcinogenesis in mammals, and thus the presence of parent PAHs and metabolites in seafood has the potential to cause impacts to human health. Figure 1-1 depicts a conceptual diagram of the general rationale for this study.

The methods of ecological and human health risk assessment generally attempt to link the potential exposure and toxicity of a substance in order to develop a risk characterization. The presence of toxic metabolites of PAHs has implications for risk assessment because

Figure 1-1: Conceptual diagram of the processes leading to potential ecological and human health risks from parent PAHs and PAH metabolites.

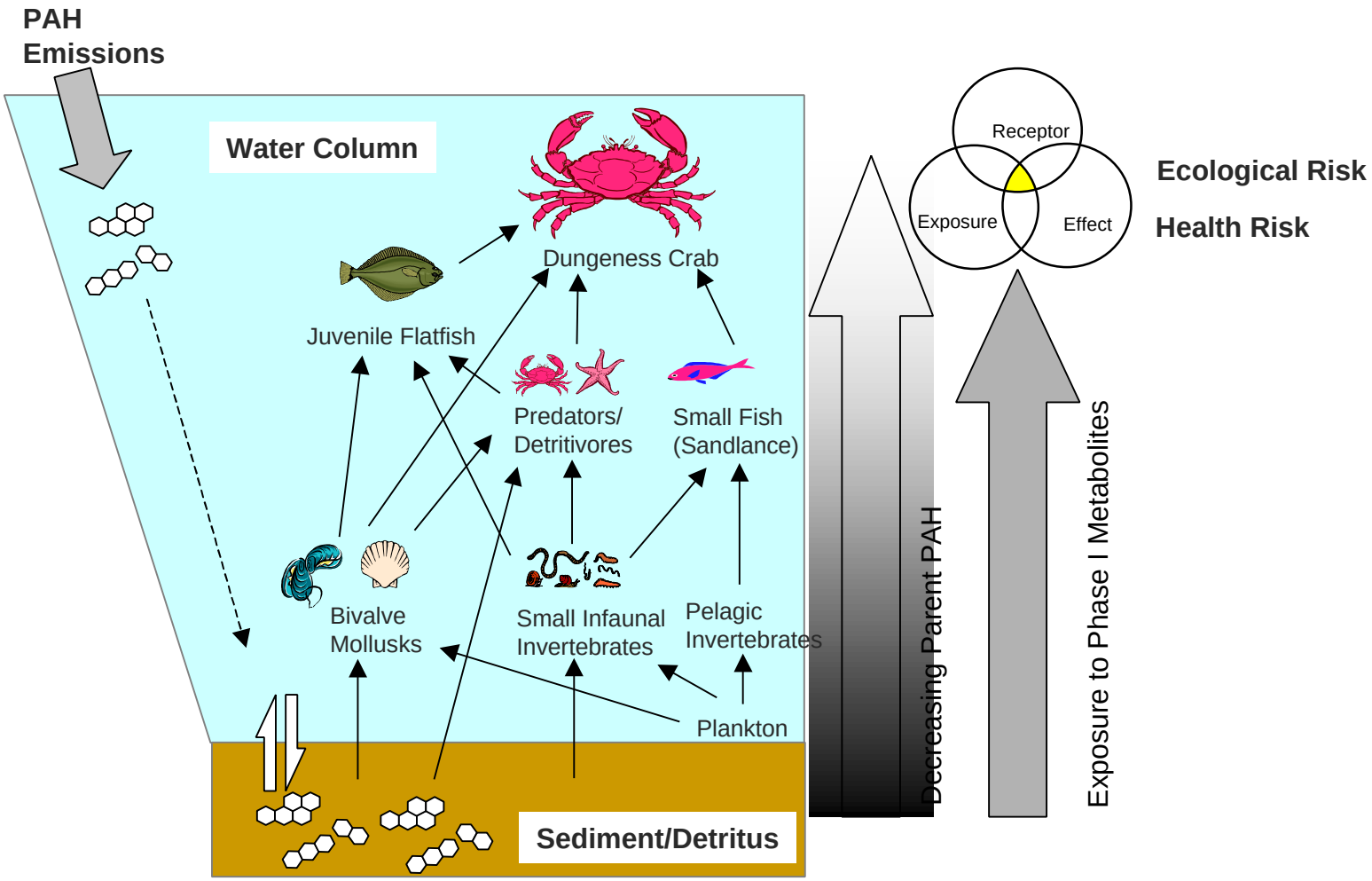

the metabolite-induced effects will be dose-responsive to metabolite residues rather than parent PAH residues. Thus, an assessment strategy for predicting exposure and risks from PAH metabolites is needed for effective management of environmental contamination by PAHs.

In this research project I use environmental modelling to examine the how metabolic transformation of PAH may limit bioaccumulation but also lead to a potential for ecological and health risks in marine organisms and human consumers. Rather than *testing* hypotheses according to traditional scientific methods (i.e., rejection of a null hypothesis lending support to alternative hypotheses), the modelling approach is useful for integrating and refining current knowledge, and generating hypothesis that can be tested in natural systems. The general premises underlying this research include:

1. PAHs in water and sediments will be available for bioaccumulation in marine organisms but food web biomagnification will be prevented by metabolism of parent compound.

2. While metabolism of PAHs in invertebrate and fish species may result in low body burdens of parent PAHs at upper trophic levels such as Dungeness crab, PAH metabolites may be produced as a result of metabolism processes. These metabolites may be available for trophic transfer, leading to potentially significant exposure to upper trophic levels.

3. Since many PAH metabolites are potent toxicants and carcinogens, the formation and accumulation of significant amounts of PAH metabolites in benthic organisms may cause unacceptable ecological risks to benthic organisms or health risks to human consumers of seafood.

To date, there have been no attempts at modelling PAH bioaccumulation with methods which account for the mass balance of PAH metabolites in addition to parent PAHs. The primary goal of this research is to develop a modelling tool for the assessment of the bioaccumulation and resultant exposure of marine organisms to parent PAHs and PAH metabolites.

1.4 DESCRIPTION OF KITIMAT ARM

Kitimat Arm is located at the northeastern extent of Douglas Channel on the northwest coast of British Columbia, Canada (see Figure 1-2). Kitimaat Village, located on the eastern shore of Kitimat Arm, is the home of the Haisla people. They have traditionally inhabited Kitimat Arm and some 13,000 square kilometres of Douglas Channel and the surrounding coastline (Kitamaat Village Council, 2003). The Haisla have a cultural tradition of hunting, gathering and fishing in marine environment of Kitimat Arm and surrounding lands (Kitamaat Village Council, 2003). Consequently, industrial impacts to Kitimat Arm may not only harm the marine ecosystem but also affect traditional ways of life.

The Alcan Kitimat Works Smelter and the town of Kitimat have been located at the head of Kitimat Arm since the 1950s. The Alcan Kitimat Works Smelter is a large point source of PAH to Kitimat Arm, and sediment cores indicate a significant increase of PAH contamination in Kitimat Arm and Douglas Channel since establishment of the smelter (Cretney et al., 1983). The Kitimat Works Smelter contributes approximately $500 million annually to the Canadian economy and Kitimat is one of the busiest ports on Canada's West Coast. (Mining Association of BC, 2003). Despite the industrial setting of Kitimat Arm, Douglas Channel is also a popular area for tourism focused on saltwater fishing and water-based recreation (Kitimat Chamber of Commerce, 2003). Thus, consistent with the concept of sustainable development (WCED, 1987), cultural, environmental, economic, and recreational interests are each important considerations for the management of environmental quality in Kitimat Arm.

There have been several studies of the environmental effects of PAHs in Kitimat Arm by industry (EVS, 1997), university researchers (Simpson et al., 1998; Harris, 1999, Eickhoff et al., 2003) and governmental organizations (NOAA, 2000), but, with the exception of Harris (1999), no studies have modelled PAH dynamics in the marine environment using computer simulation.

Figure 1-2: Map depicting the Location of Kitimat, BC with a close-up on Kitimat Arm.

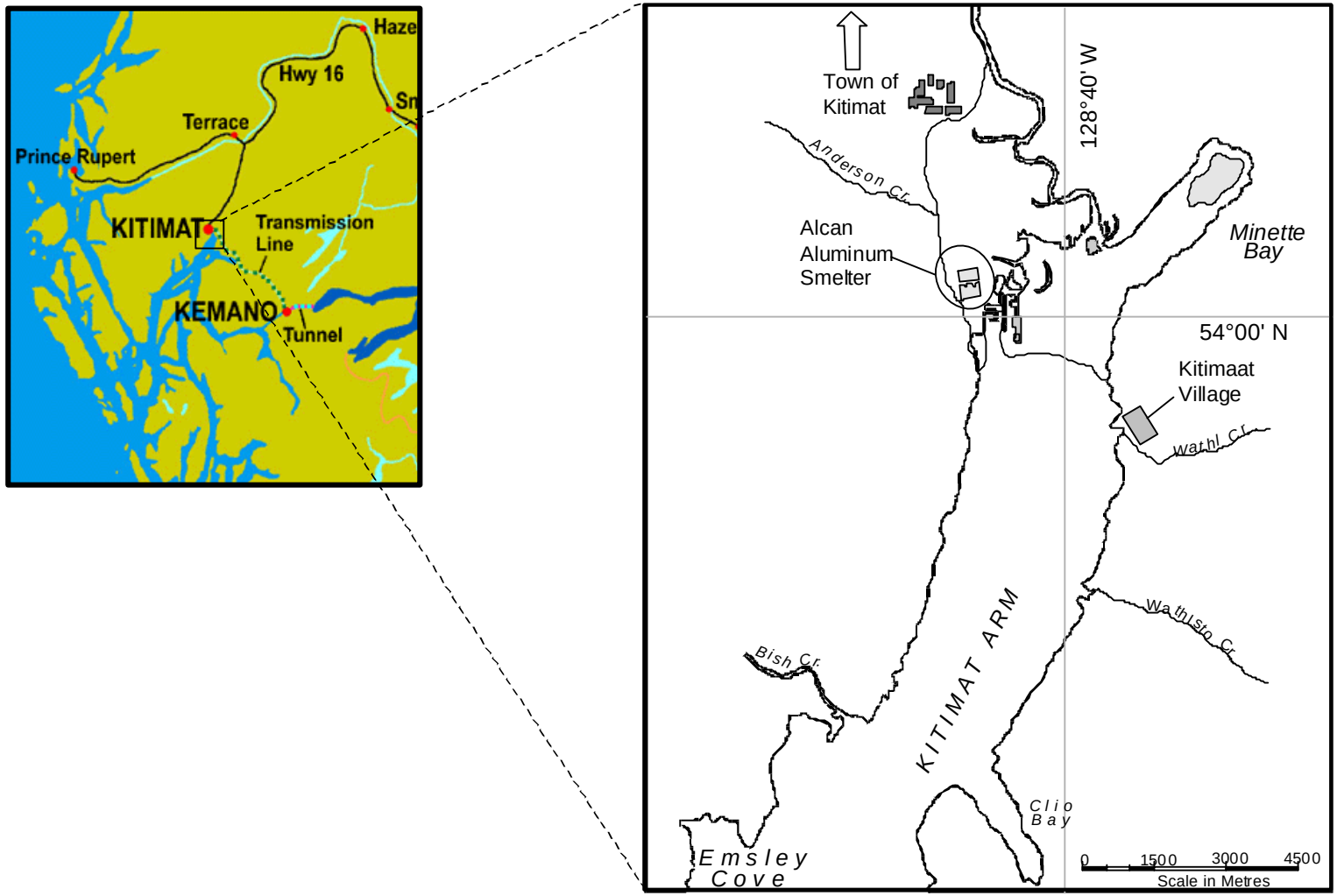

1.5 RESEARCH METHODS

In this study, I apply environmental modelling to examine the processes food-web bioaccumulation and metabolic transformation of PAHs for the temperate marine ecosystem of Kitimat Arm. By modelling biophysical systems, researchers are successful at integrating existing knowledge to learn about system dynamics, examining the significance of physiochemical and biological processes, forecasting system behaviour, and prioritizing research efforts (Jackson et al., 2000). Computer models are currently applied to many problems in environmental toxicology ranging from physiological-based pharmacokinetic models describing toxicokinetic processes at the organism level (e.g., Cahill et al., 2003), to long-range global transport models describing the movement of POPs to polar regions (e.g., Wania and Mackay, 1995). In ecological and human health risk assessment, predictive models play an important role for predicting exposure of bioaccumulative chemicals.

The following research project is divided into four chapters. In Chapter 2, I develop a steady-state food-web bioaccumulation model for a representative benthic food web of coastal British Columbia. The model combines ecological interactions, chemical behaviour and thermodynamic principles to predict food web transfer of PCBs from water and sediment to Dungeness crab. It builds upon models that were developed previously for the Great Lakes (e.g., Gobas, 1993; Morrison et al., 1996; Morrison et al., 1997). The purpose of this chapter is to calibrate and test a bioaccumulation model for non-metabolized substances, which can then be applied to assess PAH bioaccumulation and metabolic transformation. Important sources of data for Chapter 2 include PCB concentrations for various media in Kitimat Arm that were previously collected by Glenn Harris (reported in Harris, 1999), BSAF values for PCBs in False Creek, BC (MacKintosh and Maldonado, *unpublished data*) and PCB BSAF values from the literature (Tracey and Hansen, 1996; Boese et al., 1995; Gunnarson and Skold, 1999)

In Chapter 3, I refine and apply the model to examine how metabolic transformation influences the bioaccumulation of parent PAHs and the mass balance of Phase I PAH

metabolites in benthic organisms. A literature review is presented which forms the basis for determining metabolic rates, characterizing the soot carbon association of pyrogenic PAHs and quantifying the mass balance of PAH metabolites in the bioaccumulation model. By applying the model, the field-measured dynamics of non-metabolized chemicals such as PCBs are compared to the dynamics of PAHs, yielding conclusions regarding PAH biotransformation rates and resulting metabolite body burdens. Important sources of data for Chapter 3 include sediment PAH concentrations and Dungeness crab PAH tissue concentrations for Kitimat Arm that that were previously collected by Glenn Harris (reported in Harris, 1999) and Curtis Eickhoff (reported in Eickhoff et al., 2003), respectively.

Chapter 4 presents the integration of study findings to draw conclusions regarding PAH bioaccumulation and the implications of biotransformation. In this chapter I discuss the ecological significance of predicted tissue residues of parent PAHs and metabolites in benthic organisms. In addition, I explore how PAH metabolism can impact the regulation of PAH residues in harvested organisms. This research integrates the existing knowledge regarding PAH toxicokinetics in marine systems in order to generate recommendations and highlight areas where further research is desirable.

As a result of this research, it is possible to refine the current approach to modelling non-metabolized chemicals and explore the implications of PAH metabolism by benthic organisms. The model development in Chapter 2 highlights the importance of accurately representing dietary transfer efficiencies and organism bioenergetics in bioaccumulation models. Application of the model in Chapter 3 allows for derivation and testing of metabolic rate constants for PAHs. Finally, by conducting sensitivity analysis with the mass balance models for parent PAHs and Phase I PAH metabolites, it is possible to demonstrate both parent PAHs and Phase I metabolites of PAH are expected to undergo trophic dilution (i.e., decrease in concentration through successive trophic levels). These findings have implications for ecological and human health risk assessment.

2 DEVELOPMENT OF A BIOACCUMULATION MODEL FOR PCBS IN A REPRESENTATIVE BENTHIC FOOD WEB FOR THE BC COAST.

2.1 INTRODUCTION

It is generally accepted that the response of an organism to toxicants depends primarily on the internal concentration at the target tissue (McCarty and Mackay, 1993). Substances which are rapidly absorbed and eliminated by organisms are expected to quickly achieve chemical equilibrium between the ambient environment and the organism. For these chemicals, the ambient concentration provides a reasonable approximation of concentrations at internal target tissues. For substances which are eliminated more slowly by organisms, resulting in high levels of accumulation in organisms and potential food web transfer, internal concentrations may reach higher levels than expected at equilibrium with the ambient environment. Chemicals that exhibit this behavior are referred to as "bioaccumulative" (CEPA, 1999; Mackay and Fraser, 2000). It is important to consider bioaccumulation for exposure assessment in ecological risk assessment because it can lead to high internal concentrations at target tissues (i.e., and potential toxic effects), even though ambient concentrations are low. Bioaccumulation is also an important consideration in the protection of human health since these high chemical concentrations can also be present in harvested species.

The simplest model for predicting and assessing bioaccumulation is the equilibrium partitioning model (EQP). It assumes a thermodynamic equilibrium between the organism and relevant exposure media (i.e., water, sediment, porewater). For example, biota-sediment-accumulation factors (BSAFs) for benthic organisms can be calculated according to the following equation (Gobas and Morrison, 2000):

$$BSAF = (C_B/\phi_L) \,/\, (C_S/\phi_{OC}) \qquad [1]$$

Where C_B (g/kg tissue) is the concentration in biota, ϕ_L (%) is the lipid content of the organism, C_S (g/kg sediment) is the bulk sediment concentration and ϕ_{OC} (%) is the organic carbon content of the sediment. The EQP model predicts constant BSAFs, independent of chemical properties, organism characteristics and sediment conditions.

Assuming equal chemical sorptive capacities between lipid and organic carbon, BSAFs of 1 are expected at equilibrium. In addition, given the difference in sorptive capacity between lipid and organic carbon that has been observed (see Seth et al., 1999), BSAF predictions up to approximately 3 are possible if ϕoc is adjusted to account for this difference. Field-measured BSAFs often vary widely from this range and depend on behaviour and feeding mode of benthic organisms (Tracey and Hansen, 1996). Both Tracey and Hansen (1996) and Parkerton (1993) demonstrated that BSAFs for non-metabolized hydrophobic chemicals, such as PCBs, follow a roughly parabolic relationship with log K_{ow}, with a peak between 6 and 7.5, suggesting that chemical accumulation in sediment-coupled organisms is not adequately explained by equilibrium partitioning.

Mechanistic mass-balance models attempt to account for deviations from EQP predictions by deriving mathematical expressions of uptake (absorption from water and diet) and depuration processes (gill elimination, faecal egestion, growth dilution and metabolism) based on organism characteristics and chemical properties. Early mechanistic models were developed to predict bioaccumulation factors (i.e., biota-to-water rather than biota-to-sediment) in pelagic food webs for the Great Lakes. Gobas (1993) and Thomann (1989) each developed bioaccumulation models for simple freshwater food webs using a rate constant approach. While these models accurately represented upper trophic levels (i.e., fish), the assumption of equilibrium in lower trophic levels was less representative of contaminant transfer from sediments to benthic invertebrates. To better characterize accumulation of chemical from water, sediment, and plankton by benthos, Morrison et al., (1996) developed mechanistic equations for benthic invertebrates. An updated model which combined the benthic component of Morrison et al. (1996) with the pelagic food-web component of Gobas (1993) has successfully represented food web bioaccumulation of POPs such as PCBs in several Great Lakes ecosystems (Morrison et al., 1997, Morrison et al., 1999).

Campfens and Mackay (1997) also modelled food web bioaccumulation in Great Lakes systems. Their fugacity approach was algebraically equivalent to the rate constant

approach but allowed for model interpretation based on the thermodynamics of chemical partitioning. Although the Campfens and Mackay (1997) model applied EQP for benthic organisms, it differed from the Gobas (1993) model and the Morrison et al. (1997, 1999) models by using a food web matrix that accounts for the non-linear nature of aquatic food webs. This allows model organisms to feed at all trophic levels including their own, accounting for potential cannibalism within trophic levels and opportunistic feeding on carcasses from higher trophic levels. The assumption of steady state yields a system of equations which can be solved using matrix algebra.

The purpose of this chapter is to develop and calibrate a mechanistic mass balance model of food web bioaccumulation that predicts BSAFs for PCBs in a representative benthic marine ecosystem. With the exception of Connolly (1991), there have been few applications of mechanistic bioaccumulation modelling to marine systems. A calibrated model for non-metabolized chemicals has utility for examining the bioaccumulation and elimination of metabolized chemicals with similar properties, such as PAHs. The model developed here augments previous approaches by incorporating a method for predicting sediment-water disequilibrium, a feeding model based on organisms bioenergetics, and a quantitative digestion model which estimates gastrointestinal magnification factors. Furthermore, the model accounts for food-web complexity by solving the system of model equations using matrix algebra.

The model is developed for Kitimat Arm and False Creek but it is also representative of similar systems along the BC Coast. Dungeness crabs are assumed to feed near the top of the benthic food web due to their life history and importance as a harvested resource. First, I describe the benthic food web and develop model equations for representative functional groups. I then parameterize the model equations for each component of the food web. Finally, the model is calibrated to PCB BSAF data from Kitimat Arm and False Creek, BC.

2.2 MODEL THEORY

2.2.1 Overview of System Ecology and Food Web Structure

Industrial harbours located along the BC Coastline are often receiving waters for POPs such PCBs originating from point industrial sources and atmospheric deposition (Ikonomu et al., 2002). Based on their chemical properties, these chemicals are expected to partition from the water column into organic carbon in bottom sediments, and bioaccumulate in organisms (Mackay et al., 1999). Consequently, benthic organisms which are in close contact with the sediment have potentially significant exposure to these chemicals via water ventilation, sediment ingestion or consumption of prey items.

The Dungeness crab (*Cancer magister*) is a common macroinvertebrate species in BC that is harvested in commercial, recreational and First Nations fisheries. They are large bottom scavengers that inhabit soft-bottom, sediment-dominated areas (Ikonomu et al., 2002). Depending on their size, they feed on infaunal and epifaunal invertebrates, smaller fish such as Pacific sandlance (*Ammodytes hexapterus*) and juvenile flatfish (e.g., *Platichthys stellatus* and *Pleuronectes vetulus*), and, opportunistically, on larger fish carcasses (Stevens et al., 1982). Their presence near the top of the benthic food web means that food web biomagnification plays a potentially significant role in their exposure to bioaccumulative substances.

The trophic levels below Dungeness crab are occupied by a wide range of invertebrates and fish. Pauly et al. (1996) and Oakey and Pauly (1999) have summarized trophic guilds for the Southern BC Shelf, the Georgia Strait, the Alaska Gyre and Prince William Sound, AK. In soft-bottom areas of the BC Coast, these are expected to include (in order of increasing trophic status):

- phytoplankton such as diatoms which absorb chemical from the water column;
- zooplankton such as copepods, daphnids and euphausiids which feed on plankton and detritus;
- small infauna and epifauna such as polychaetes and amphipods, feeding on detritus, phytoplankton and other invertebrates;

- large infauna such as deposit-feeding and filter-feeding clams;
- small fish such as Pacific sandlance which feed on plankton and small benthic invertebrates;
- large epifauna including various shrimps, small crabs, and echinoderms which consume detritus, other invertebrates and occasionally, small fish; and,
- juvenile flatfish such as starry flounder and English sole which feed on a range of smaller benthic fish and invertebrates

In addition to living organisms, the detritus pool provides a critical organic-carbon-based energy source for benthic organisms, especially at lower trophic levels. The general feeding relationships for these trophic guilds are presented in Figure 2-1. Table 2-1 summarizes dietary preference information for Dungeness crab and other benthically-coupled organisms in the Northeast Pacific Ocean (compiled from Stevens et al., 1982; Pauly and Christensen, 1996; Oakey and Pauly, 1999; and Mackintosh, 2002). With increasing trophic level the feeding mode of these trophic guilds generally switches from filter feeding (on phytoplankton and suspended detritus) and deposit feeding (on detritus), to predation and scavenging on smaller invertebrates, fish and fish carcasses.

The close association of benthic organisms with sediments, porewater and the water column indicates potential accumulation of PCBs and dioxins. Furthermore, trophic feeding relationships suggest that dietary exposure is potentially important at higher trophic levels.

2.2.2 Model of Chemical Bioaccumulation

For an individual organism, total bioaccumulation is expected to depend on processes which increase the chemical concentration in the organism (i.e., exposure and uptake) and processes which decrease the chemical concentration in the organism (i.e., removal of chemical from tissues, increase in the mass/volume of tissues, and biotransformation of chemical). The conceptual diagram of these processes is presented in Figure 2-1.

Figure 2-1: Conceptual model of a representative marine benthic food web for the BC Coast, and uptake and depuration processes at the organism level.

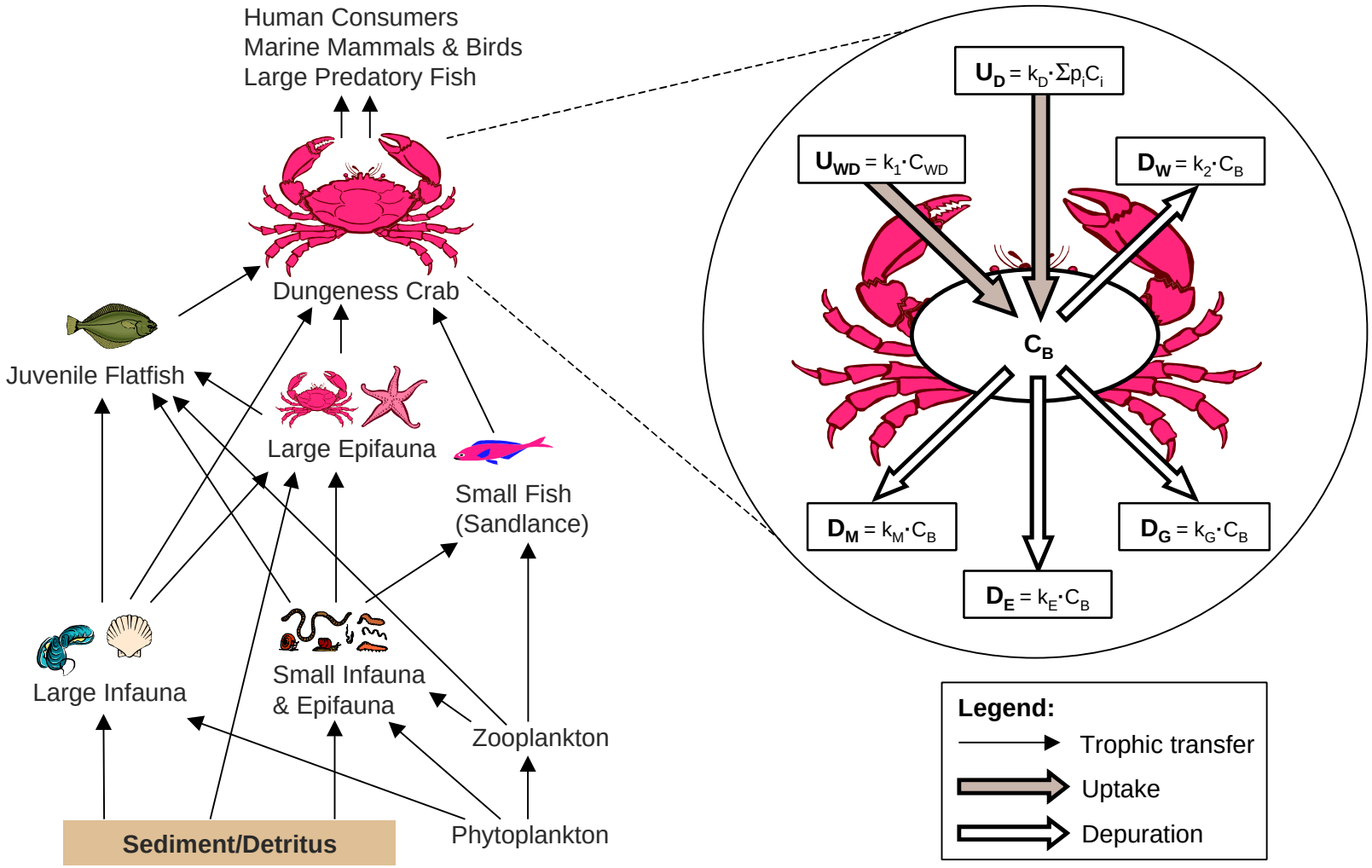

Table 2-1: Summary of dietary composition information for trophic guilds in the benthic food web of the BC Coast.

Predator	Prey Items: Detritus	Phytoplankton	Zooplankton	Large Infauna (e.g., clams)	Small Epifauna (e.g., amphipods)	Small Infauna (e.g., polychaetes)	Large Epifauna (e.g., crustaceans, brittle stars)	Sandlance and Demersal Fish	Juvenile Dungeness Crab	Source
Zooplankton										
microzoop (1.7g/m^2)	25%	75%								Pauly and Christensen (1996)
herbivores (25 g/m^2)	9%	92%								Pauly and Christensen (1996)
omnivores (8 g/m^2)	7%	53%	40%							Pauly and Christensen (1996)
carnivores			100%							Pauly and Christensen (1996)
Small Epifauna and Infauna										
barnacles, mollusks, amphipods	40%	55%			5%					Okey and Pauly (1999)
small benthic crustacean	90%		10%							Pauly and Christensen (1996)
small bivalves/polychaetes <20 m	25%	60%				15%				Okey and Pauly (1999)
small bivalves/polychaetes 20-100m	77%	20%				3%				Okey and Pauly (1999)
polychaetes	100%									Pauly and Christensen (1996)
Large Infauna										
shallow clams	50%	50%								Okey and Pauly (1999)
deep clams	90%	10%								Okey and Pauly (1999)
Large Epifauna										
starfish and crabs					80%	20%				Okey and Pauly (1999)
benthic shrimps	35%				35%	30%				Pauly and Christensen (1996)
benthic crabs	60%			20%			18%	2%		Pauly and Christensen (1996)
Seastars	30%			40%		30%				Pauly and Christensen (1996)
Brittle Stars	80%				18%	2%				Pauly and Christensen (1996)
Planktivorous Forage Fish										
sandlance			93%			7%				Okey and Pauly (1999)
Demersal Fish										
several nearshore species			2%		70%	1%	22%	5%		Okey and Pauly (1999)
Flatfish and skate										Okey and Pauly (1999)
Starry flounder			1%	23%	1%	70%	5%			Mackintosh (2002)
rock sole				5%	22%	67%	4%	2%		Mackintosh (2002)
English sole				22%	7%	45%	24%	2%		Mackintosh (2002)
Dungeness Crab										
unknown life stage	60%			20%			20%			Pauly and Christensen (1996)
juvenile (40-47 mm carapace)				47%		2%	20%	6%	25%	Stevens et al. (1982)
80 mm carapace				16%			30%	44%	10%	Stevens et al. (1982)
120 mm carapace				4%		2%	27%	52%	15%	Stevens et al. (1982)

Bioaccumulation can be described by the following mass balance of uptake and depuration processes:

$$dC_B/dt = U_{WD} + U_D - D_W - D_E - D_G - D_M \quad [2]$$

where dC_B/dt is the rate of change (increase or decrease) of the concentration in the organism (g/kg/day), U_W represents the uptake of dissolved chemical from water and porewater (g/kg/day), U_D represents the uptake of chemical from diet (g/kg/day), D_W is the depuration via elimination to water (g/kg/day), D_E is the depuration via faecal egestion (g/kg/day), D_G is the depuration via growth dilution (g/kg/day) and D_M is the depuration via metabolism (g/kg/day; Morrison et al., 1996). For chemicals that are non-metabolized, or metabolized very slowly relative to other elimination processes, D_M is often assumed to equal zero. Because phytoplankton lack a digestive system, U_D and D_E are not included in the mass balance for this organism.

Figure 2-1 demonstrates how each uptake process can be represented as the product of a 1st-order rate constant and the concentration in the uptake medium (i.e., water or food). Likewise, each depuration process can also be represented as the product of a 1st-order rate constant and the concentration in the organism. Substitution of these rate constants into Equation 2 yields:

$$dC_B/dt = k_1 \cdot C_{WD} + k_D \cdot \Sigma p_i C_i - (k_2 + k_E + k_G + k_M) \cdot C_B \quad [3]$$

where k_1 is the rate constant for uptake from water at respiratory surfaces; C_{WD} is the concentration of chemical dissolved in water (g/kg); k_D is the rate constant for uptake from the diet via gastrointestinal magnification, $\Sigma p_i C_i$ is the weighted average concentration (g/kg) of chemical in food (i.e., C_i weighted by the proportion of that prey item in the diet, p_i); and k_2, k_E, k_G and k_M are rate constants for chemical elimination via gill excretion, faecal egestion, growth dilution and metabolism, respectively (Gobas, 1993). Under steady state conditions where $dC_B/dt = 0$, Equation 3 rearranges to:

$$C_B = \frac{k_1 \cdot C_{WD} + k_D \cdot \Sigma p_i C_i}{k_2 + k_E + k_M + k_G} \quad [4]$$

where C_B is the steady-state concentration in the organism (g/kg). This equation can be applied to estimate C_B for all animals in the benthic food web which are in direct contact with overlying water and porewater and feed at one or more trophic levels.

Phytoplankton lack a digestive system and are composed of primarily of organic carbon and water rather than lipid and water. At steady state, the concentration of chemical in phytoplankton can be approximated as:

$$C_{PHYT} = \frac{k_{1phyt} \cdot C_{WD}}{k_{2phyt} + k_G + k_M} \qquad [5]$$

Where k_{1phyt} and k_{2phyt} are rate constants for uptake and elimination to water, k_G represents the growth in phytoplankton biomass (i.e., both cell size and number rather than only the size of individual cells) and k_M represents chemical biotransformation. Note that phytoplankton are assumed to lack the ability to metabolize many xenobiotic substances resulting in k_M often being zero. For low K_{ow} chemicals with relatively fast kinetics, Equation 5 approximates equilibrium with the water column, whereas, for high K_{ow} chemicals it predicts a steady state concentration below that at equilibrium because of the effect of growth dilution.

A steady-state approach is used because the model is intended to predict bioaccumulation in the benthic food web over long-term exposure. Wania and Mackay (1999) propose that the assumption of steady-state is often valid for mass balance models of the fate and bioaccumulation of POPs. The average chemical concentrations in water and sediments are expected to remain constant or change slowly over time, relative to food web bioaccumulation processes. Thus, individual organisms are expected to have enough *time* to reach steady-state with chemical concentrations in exposure media. The steady-state assumption also simplifies model expressions, allowing for easier interpretation of model results.

Respiratory Uptake (k_1)

Uptake of chemical across respiratory surfaces (i.e., the gills, or dermis for organisms without gills) is expected to occur via diffusion (Gobas, 1993). Thus, k_1 (L water/kg body

weight/day) depends on both the volume of water flowing across respiratory surfaces, normalized to the size of the organism, and the transfer efficiency such that:

$$k_1 = E_w \cdot G_w / V_B \qquad [6]$$

Where E_w is the uptake efficiency of chemical at gill surfaces (%), G_w is the water ventilation rate (L/day) and V_B is the organism size (kg). Gobas and Mackay (1987) derived the following empirical relationship for E_w:

$$E_w = 1 / (1.85+(155/K_{ow})) \qquad [7]$$

For lower K_{ow} substances, E_w is expected to involve diffusion via both aqueous and lipid phases, increasing with increasing hydrophobicity (Gobas and Mackay, 1987). At higher K_{ow}, overall uptake kinetics are limited primarily by diffusion in water phases, resulting in a constant E_w that is independent of chemical hydrophobicity. G_w can be estimated using allometric relationships for fish or species-specific O_2 consumption data for invertebrates according to the following equation:

$$G_w = O_R \cdot V_B / DO \qquad [8]$$

Where O_R is the O_2 consumption rate (g O_2/kg body weight/day) and DO is the dissolved oxygen concentration in the water (g O_2/L). While Equation 8 could underestimate G_w somewhat if the oxygen uptake efficiency is less 100%, it was considered a reasonably accurate estimate of G_w for invertebrates. V_B can be estimated from literature or site-specific data.

Uptake by Phytoplankton (k_{1phyt})

Chemical uptake in phytoplankton is expected to occur via diffusion from the water column into the sorbing matrix of phytoplankton. Thus, k_{1phyt} (kg water/kg biomass/day) behaves similarly to E_w, with diffusion limited by both aqueous and sorbing phases at low K_{ow} and diffusion limited primarily by the aqueous phase at higher K_{ow}. k_{1phyt} can be estimated by fitting the following expression to literature data:

$$k_{1phyt} = \phi_P \cdot 1/(\alpha + \beta/K_{ow}) \qquad [9]$$

Where ϕ_P is equivalent content of phytoplankton combining lipid and organic carbon, and α and β are empirical constants. ϕ_P is calculated as:

$$\phi_P = \phi_{OC,P} + \phi_{L,P}/0.35 \qquad [10]$$

Where $\phi_{L,P}$ is the lipid fraction in phytoplankton and $\phi_{OC,P}$ is the organic carbon fraction in plankton. The constant, 0.35, is included to represent the higher sorptive capacities lipid relative to OC. Skoglund and Swackhamer (1999) found that sorption into organic carbon predicted the accumulation of PCBs by phytoplankton more accurately than sorption into lipid. The small lipid fraction in phytoplankton (approximately 0.4% compared to approximately 6% organic carbon) is also expected to accumulate chemical, but with a higher sorptive capacity than organic carbon. Therefore, the sorbing matrix for phytoplankton was assumed to include organic carbon and lipid matter.

Dietary Uptake (k_D)

Uptake via the diet depends on the amount of food consumed per day, normalized to the size of the organism and the efficiency of uptake from the food. Thus, k_D (kg food/kg body weight/day) can be expressed as:

$$k_D = E_d \cdot G_d/V_B \qquad [11]$$

Where E_d is the uptake efficiency of chemical from food (proportion) and G_d is the food consumption rate (kg/day). Gut absorption of chemical is expected to be a process of desorption from food and diffusion from digestive fluids across intestinal membranes. Desorption from food depends on surface area of the digested food which is related to the digestive capabilities of the organism. Diffusion into the intestinal wall is controlled by the conductivities of the water and lipid phases for chemical transport (Gobas et al., 1988). E_d represents the combined desorption and diffusion processes. Gobas et al. (1988) proposed the following relationship for E_d:

$$E_d = 1/(A \cdot K_{ow} + B) \qquad [12]$$

where A and B are empirical constants. There is a high degree of variability in the data for E_d causing high uncertainty in the values for A and B. This study applied a calibration method to assess values for A and B. In general, E_d is expected to increase in higher

organisms that have longer gut residence times (i.e., longer times for desorption and diffusion to occur), complex guts with higher surface areas (i.e., increasing the surface areas for chemical diffusion) and digestive systems that are more effective at breaking down the gut contents (i.e., thereby increasing the surface area for chemical desorption).

Connolly (1991) described the following simple model for linking growth, respiration and the energy density of food to the size-normalized food consumption rate (G_d/V_B):

$$G_d/V_B = (\lambda_i/\lambda_j)\cdot(k_R+k_G)/A_F \quad [13]$$

Where (λ_i/λ_j) is the ratio between the energy density of the organism (i) and the food (j), k_R is the respiration rate (1/day), k_G is the growth rate (1/day), and A_F is the overall food assimilation efficiency. In general, growth and respiration (k_R+k_G) depend on organism size and determine the energy usage rate of the organism. These parameters refer to either the proportion of tissue equivalents create per day (k_G) or the proportion of tissue equivalents metabolized (k_R) to produce energy per day. The food consumption rate needed to meet the energy requirement for these processes then depends on the ratio of energy densities between the organism and its food (λ_i/λ_j) and the ability of the organism to assimilate energy from its food (A_F).

$\lambda_{i,}/\lambda_j$ can be estimated by comparing the energy content of lipid, NLOM and OC in organism tissues and the diet. In salmonids, the caloric contents of fat, carbohydrate, and protein are approximately 8 kcal/g, 4.1 kcal/g, and 4.8 kcal/g, respectively (Brett, 1995). Based on this information, a factor of approximately 0.6 can be used to represent the difference in energy density between lipid and organic matter. Thus, $\lambda_{i,}/\lambda_j$ in terms of lipid energy equivalents is calculated as:

$$\lambda_{i,}/\lambda_j = (\phi_{L,B} + 0.6\cdot\phi_{NLOM,B}) / (\phi_{L,D} + 0.6\cdot\phi_{OC,D} + 0.6\cdot\phi_{NLOM,D}) \quad [14]$$

Where $\phi_{L,B}$ and $\phi_{NLOM,B}$ are respective fractions of lipid and NLOM in organism tissues and $\phi_{L,D}$ $\phi_{OC,D}$ $\phi_{NLOM,D}$ are respective fractions of lipid, sediment and phytoplankton OC, and NLOM in the food (note that $\phi_{OC,D}$ only pertains to organisms feeding on detritus or phytoplankton).

A_F is calculated as the weighted average of $\phi_{L,D}$ $\phi_{OC,D}$ $\phi_{NLOM,D}$ and the respective absorption efficiencies for these food constituents (α_L, α_{OC}, α_{NLOM}) according to the following equation:

$$A_F = (\phi_{L,D} \cdot \alpha_L) + (\phi_{OC,D} \cdot \alpha_{OC}) + (\phi_{NLOM,D} \cdot \alpha_{NLOM}) \qquad [15]$$

k_R and k_G can be estimated based on organism-specific data and allometric relationships from literature sources.

Elimination to Water (k_2 and k_{2phyt})

Elimination at respiratory surfaces (or through direct contact for phytoplankton) is also assumed to occur via diffusion, but at a slower rate due to the diffusive resistance that water poses to hydrophobic chemicals. This *preference* of the chemical for lipid is characterized by the theoretical bioconcentration factor or BCF (Gobas, 1993). Thus k_2 (1/day) and k_{2phyt} (1/day) can be represented as:

$$k_2 = k_1 / BCF \qquad [16]$$

$$k_{2phyt} = k_{1phyt} / BCF \qquad [17]$$

The BCF is calculated as:

$$BCF = (\phi_{L,B} + 0.35 \cdot \phi_{OC,B} + 0.035 \cdot \phi_{NLOM,B}) \cdot K_{ow} \qquad [18]$$

Where $\phi_{OC,B}$ refers to the OC content of organism tissues and is only applicable for phytoplankton (i.e., since the tissues of other organisms in the model generally do not contain OC), and the constants 0.35, and 0.035 are included to represent the sorptive capacities of sediment OC and NLOM relative to lipid (see Seth et al., 1999 and Gobas et al., 1999).

Faecal Egestion (k_E)

Elimination of chemical via faecal egestion (k_E; 1/day) can be characterized as a function of the rate of chemical excretion to the gut and the rate of faecal excretion from the gut, such that:

$$k_E = G_f \cdot E_d / V_B \cdot K_{BF} \qquad [19]$$

Where G_f is the food intake rate (kg/day), E_d is the uptake efficiency (as above) and K_{BF} is the biota-to-faeces partitioning coefficient (unitless). Under steady state conditions, G_f is estimated as a constant proportion of the food consumption rate G_d. This proportion will depend on the digestion and absorption efficiencies for the various components in the diet such that:

$$G_f/G_d = (1-\alpha_L)\cdot\phi_{L,D} + (1-\alpha_{OC})\cdot\phi_{OC,D} + (1-\alpha_{NLOM})\cdot\phi_{NLOM,D} + (1-\alpha_W)\cdot\phi_{W,D} + (1-\alpha_I))\cdot\phi_{I,D} \quad [20]$$

Where $\phi_{W,D}$ and $\phi_{I,D}$ are respective dietary fractions of water and inorganic material, and α_W and α_I are respective absorption efficiencies for these constituents (other parameters defined above). Again, $\phi_{OC,D}$ only pertains to organisms feeding on detritus or phytoplankton.

During digestion lipid, OC, and NLOM are removed from gut contents, decreasing the amount of sorptive matrix (lipid, OC and NLOM) present in the faeces and resultant fugacity capacity. Consequently, a thermodynamic gradient is created which opposes excretion of chemical to the faeces. This gradient is the primary cause of food chain biomagnification and is represented by the gastrointestinal magnification factor (i.e., K_{BF}). K_{BF} can be estimated by relating the composition of organism tissues and the faeces where:

$$K_{BF} = \frac{Z_L\cdot(\phi_{L,B} + 0.035\cdot\phi_{NLOM,B})}{Z_L\cdot(\phi_{L,F} + 0.35\cdot\phi_{OC,F} + 0.035\cdot\phi_{NLOM,F})} \quad [21]$$

Where the Z_L is the fugacity capacity of lipid and the constants 0.35 and 0.035 represent the fugacity capacities of sediment OC and NLOM relative to lipid. Z_L, which depends on chemical K_{ow}, cancels out in Equation 21, meaning that K_{BF} is the same for all chemicals (i.e., regardless of chemical hydrophobicity) and only a function of the change in gut content composition during digestion. Note that Z values for water and inorganic matter are assumed to be sufficiently small relative to Z_L that they can be omitted from Equation 21. $\phi_{L,F}$, $\phi_{OC,F}$, and $\phi_{NLOM,F}$ represent the fractions of lipid, OC and NLOM in the faeces and are related to diet composition and food absorption efficiencies by:

$$\phi_{L,F} = (1-\alpha_L)\cdot\phi_{L,D} / (G_f/G_d) \quad [22]$$

$$\phi_{OC,F} = (1-\alpha_{OC})\cdot\phi_{OC,D} / (G_f/G_d) \quad [23]$$

$$\phi_{NLOM,F} = (1-\alpha_{NLOM})\cdot\phi_{NLOM,D} / (G_f/G_d) \quad [24]$$

Note that $\phi_{OC,F}$ refers to the fraction of sediment or phytoplankton OC remaining in the faeces while $\phi_{L,F}$ and $\phi_{NLOM,F}$ refer to the respective fractions of biota lipid and NLOM remaining in the faeces.

Growth Dilution (k_G)

Growth is expected to be organism-specific, varying with body size and activity level. As an organism grows, its mass and volume increase, with a diluting effect on chemical concentration. In the absence of species-specific data, k_G can also be estimated using allometric relationships (Gobas, 1993). For phytoplankton, k_G represents growth in biomass and can be estimated from studies of aquatic systems with similar characteristics to the one being modelled.

Elimination Via Metabolism (k_M)

When chemical substrate concentrations are low, relative to maximal enzyme activities, metabolism can be represented as a first-order rate constant where the amount of chemical biotransformed per day depends only on chemical concentration. For many bioaccumulative chemicals, metabolic rates are sufficiently small relative to other elimination processes that k_M can be assumed to equal zero. This is generally the case for PCBs.

Matrix Solution

Early food web bioaccumulation models were solved in a mathematically-simple, unidirectional fashion where an organism at a particular trophic level only consumed organism at lower trophic levels. However, feeding relationships in ecological systems are often complex, with organisms potentially feeding within their trophic level (i.e., cannibalism) or opportunistically at higher trophic levels (i.e., scavenging on carcasses). This may be especially important for a marine benthic food web with high proportions of scavengers and detritivores. For example, Stevens et al. (1982) found rates of cannibalism ranging from 10 to 25% in Dungeness crab.

Under the assumption of steady state, food web complexity can be accounted for by representing bioaccumulation as a system of equations (i.e., one for each organism in the food web) and solving using matrix algebra (Campfens and Mackay, 1997; Sharpe and Mackay, 2000). To convert to matrix form, let *n* equal the number of trophic guilds feeding in the food web. Rearranging Equation 4 to separate the terms representing accumulation from water, detritus and phytoplankton (i.e., phases with *known* concentrations that can be determined independent of the food web model), from the terms representing accumulation from food web sources (i.e., predicted by the food web model) yields the following expression:

$$\underbrace{\frac{k_1 \cdot C_{WD} + k_D \cdot (p_{phyt} \cdot C_{phyt} + p_{det} \cdot C_{det})}{k_2 + k_E + k_G + k_M}}_{\text{Term 1}} = \underbrace{C_{B,i} - \frac{k_D \cdot \Sigma\, p_i C_{B,i}}{k_2 + k_E + k_G + k_M}}_{\text{Term 2}} \quad [25]$$

Where $C_{B,i}$ is the chemical concentration in a given trophic guild, *i*, p_{phyt} and p_{det} are the respective proportions of phytoplankton and detritus in the diet, C_{phyt} and C_{det} are the chemical concentrations in these prey items, and $\Sigma p_i C_{B,i}$ refers only to prey items feeding in the food web.

Figure 2-2 displays the matrix representation of Equation 25. Term 1 represents the bioaccumulation of chemical from non-food-web sources. Phytoplankton is classified as non-food web because this organism accumulates chemical only from the water and does not feed in the food web. Term 1 is expressed as the product of a 3 x *n* coefficient matrix for accumulation from non-food-web sources (A_{NFW}), and a 3 x 1 vector (C_{NFW}) representing the concentrations in water, detritus and phytoplankton. $A_{NFW} \cdot C_{NFW}$ can be solved for each *i* yielding a known solution vector (NFW).

Term 2 represents bioaccumulation of chemical from food-web sources and can be represented as $A_{FW} \cdot C_{FW}$. C_{FW} is a 1 x *n* vector of unknown quantity which represents the concentration in each trophic guild, *i*. A_{FW} is an *n* x *n* coefficient matrix representing the

Figure 2-2: Matrix representation of the system of model equations.

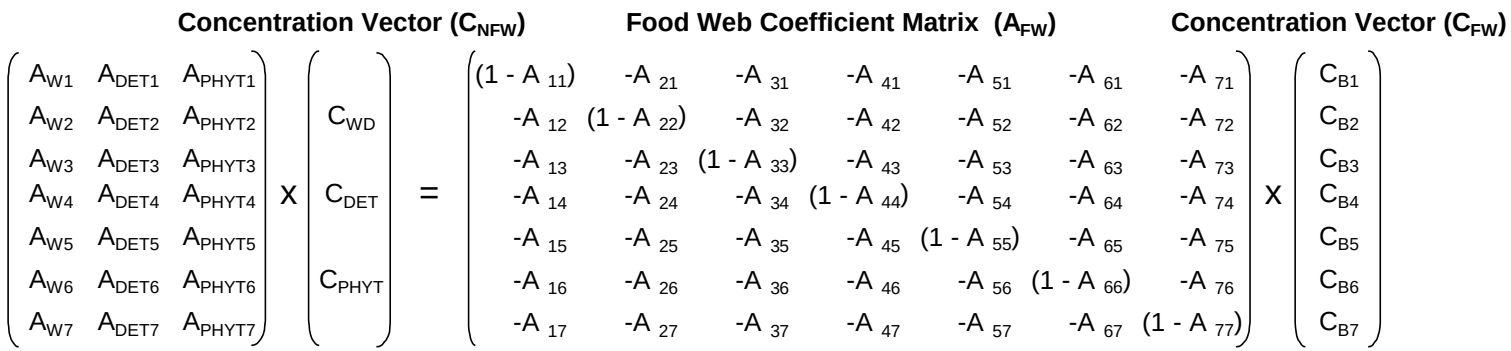

$$\begin{pmatrix} A_{W1} & A_{DET1} & A_{PHYT1} \\ A_{W2} & A_{DET2} & A_{PHYT2} \\ A_{W3} & A_{DET3} & A_{PHYT3} \\ A_{W4} & A_{DET4} & A_{PHYT4} \\ A_{W5} & A_{DET5} & A_{PHYT5} \\ A_{W6} & A_{DET6} & A_{PHYT6} \\ A_{W7} & A_{DET7} & A_{PHYT7} \end{pmatrix} \times \begin{pmatrix} \\ C_{WD} \\ \\ C_{DET} \\ \\ C_{PHYT} \\ \end{pmatrix} = \begin{pmatrix} (1 - A_{11}) & -A_{21} & -A_{31} & -A_{41} & -A_{51} & -A_{61} & -A_{71} \\ -A_{12} & (1 - A_{22}) & -A_{32} & -A_{42} & -A_{52} & -A_{62} & -A_{72} \\ -A_{13} & -A_{23} & (1 - A_{33}) & -A_{43} & -A_{53} & -A_{63} & -A_{73} \\ -A_{14} & -A_{24} & -A_{34} & (1 - A_{44}) & -A_{54} & -A_{64} & -A_{74} \\ -A_{15} & -A_{25} & -A_{35} & -A_{45} & (1 - A_{55}) & -A_{65} & -A_{75} \\ -A_{16} & -A_{26} & -A_{36} & -A_{46} & -A_{56} & (1 - A_{66}) & -A_{76} \\ -A_{17} & -A_{27} & -A_{37} & -A_{47} & -A_{57} & -A_{67} & (1 - A_{77}) \end{pmatrix} \times \begin{pmatrix} C_{B1} \\ C_{B2} \\ C_{B3} \\ C_{B4} \\ C_{B5} \\ C_{B6} \\ C_{B7} \end{pmatrix}$$

Legend:

A_{ji} - accumulation of chemical from trophic guild *j* by trophic guild *i*

C_{Bi} - concentration of chemical in trophic guild *i* *(unknown)*

A_{Wi} - accumulation from water by trophic guild *i*

A_{DETi} - accumulation from detritus by trophic guild *i*

A_{PHYTi} - accumulation from phytoplankton by trophic guild *i*

C_{WD} - concentration of chemical dissolved in water (*known*)

C_{DET} - concentration of chemical dissolved in detritus (*known*)

C_{PHYT} - concentration of chemical in phytoplankton (*known*)

Trophic Guilds:

1 - zooplankton
2 - small infauna and epifauna
3 - large infauna
4 - small fish (Pacific sandlance)
5 - large epifauna
6 - juvenile flatfish
7 - Dungeness crab

accumulation of chemical in *i* from each trophic guild including *i*. Thus, converted to matrix form, Equation 25 is:

$$NFW = A_{FW} \cdot C_{FW} \qquad [26]$$

Equation 26 can be solved for C_{FW} by computing the product of NFW and the inverse of A_{FW}, a mathematical operation which is greatly simplified through the use of a spreadsheet program such as Microsoft Excel.

2.2.3 Model of Sediment-Water Disequilibrium

In the absence of measured concentrations, both overlying water and sediment porewater are often assumed to be in equilibrium with bottom sediments (e.g., Di Toro et al., 1991). Gobas and Maclean (2003) observed that for many aquatic systems, dissolved water concentrations in overlying water are often much lower than predicted by equilibrium partitioning, with the magnitude of disequilibrium increasing at lower K_{ow}. They hypothesized that the phenomenon could be explained by an increase in chemical fugacity during the process of sediment diagenesis. Based on their study, the authors derived the following model for estimating the steady state disequilibrium between sediment and overlying water:

$$DF_{ss} = Q_{poc}/(Q_{ss} \cdot \phi_{ssoc}) \cdot Z_{poc}/Z_{ssoc} \cdot f_p/f_w \qquad [27]$$

where DF_{SS} is the disequilibrium factor; Q_{poc} is the phytoplankton primary productivity in terms of organic carbon (kg carbon/m^2/day), Q_{ss} is the sediment deposition rate (kg/m2/day), ϕ_{ssoc} is the organic carbon content of suspended sediment (%); Z_{poc}/Z_{ssoc} is the ratio of the fugacity capacities for plankton organic carbon and sediment organic carbon (equal to approximately 3; Gobas and Maclean, 2003); and f_p/f_w represents the disequilibrium between phytoplankton and water at steady state, which can be determined by comparing C_{phyt} from Equation 5 with the theoretical maximum value under equilibrium conditions. Once DF_{ss} is estimated, the following equation can be used to calculate the dissolved concentration in overlying water:

$$C_{wd} = C_{S,OC} / (K_{ow} \cdot 0.35 \cdot DF_{ss}) \qquad [28]$$

Where C_{wd} is the dissolved water concentration (g/kg) and $C_{S,OC}$ is the organic-carbon-normalized sediment concentration (g/kg OC).

2.3 METHODS

2.3.1 Overview

The model was applied to estimate the BSAFs of PCBs in the benthic food webs of Kitimat Arm and False Creek, BC. Application to Kitimat Arm allowed for evaluation of model performance in predicting the bioaccumulation of four PCB congeners in the top level trophic guild, Dungeness crab, so that the model could then be applied to examining PAH metabolism in Kitimat Arm. The model was also applied to False Creek where a more complete set of PCB data for sediments and biota allowed evaluation of model performance in multiple trophic levels and for a larger set of PCB congeners. By applying the model to both systems it was possible to ensure that Kitimat Arm was accurately represented for the next phase of the study (i.e., PAH bioaccumulation and metabolism in Kitimat Arm), and that model performance was reasonable for lower trophic levels.

The general approach to model application involved site-specific parameterization, model calibration to determine the parameter set that resulted in the best representation of Dungeness crab BSAFs in both systems, and model performance evaluation for trophic guilds in each system. The following sections describe the BSAF data for each system, the model parameterization for each system, model calibration methods, and the approach to model performance evaluation.

2.3.2 BSAF Data for PCBs

Kitimat Arm

BSAFs for PCBs in Dungeness crab from Kitimat Arm were determined from data presented in Harris (1999). Harris (1999) collected sediment and crab PCB data for Kitimat Arm and calculated seasonal and site-specific estimates of BSAFs. To obtain a data set of BSAFs for the current study which uses a steady state model that characterizes time-independent (i.e., non-seasonal) conditions, the raw data for crab and sediment

concentrations were re-analyzed. For each site, the averages of organic carbon-normalized PCB concentrations in sediment from 1995 and 1996 were assumed to represent the average exposure to Dungeness crab at that site. A distribution of observed BSAFs for each PCB congener was then obtained by dividing lipid normalized tissue concentrations for individual crabs by their corresponding organic-carbon-normalized sediment concentrations.

Year-to-year variation in PCB measurements was assumed to be related to differences in sampling location, rather than actual changes in environmental conditions in Kitimat Arm. Dungeness crabs are highly mobile, and individuals captured in at a specific site are expected to have been moving and foraging throughout a larger area. Thus, the variability in observed BSAFs will reflect the variability in behaviour and exposure by individual crabs. This data analysis method was assumed to account for this variability. Observed BSAFs were log-transformed prior to calculating descriptive statistics. Environmental concentration data and ratios are typically expected to follow log-normal distributions. BSAFs for PCBs in Dungeness crab from Kitimat Arm are summarized in Table 2-2.

Although there were no site-specific data for PCB BSAFs in large epifauna or large infauna from Kitimat Arm, it was possible to compare model predictions for these trophic guilds to literature-reported BSAFs. Boese et al. (1995) reported BSAFs for several PCB congeners in *Macoma nasuta* which were measured in laboratory mesocosms. The sediment organic carbon content in this laboratory study (~1.3%) matched that in Kitimat Arm. Gunnarson and Skold (1999) reported PCB concentrations in brittle stars (*Aphiura filiformis and A. chiajei*) and corresponding sediments from the Baltic Sea. Sediments from the offshore site in this study contained 1.8% organic carbon, roughly corresponding to Kitimat Arm. The BSAFs from these studies are presented in Tables 2-3 and 2-4. Predictions for large infauna were compared to BSAFs for *Macoma nasuta* whereas predictions for large epifauna were compared to BSAFs for brittle stars. While these data may not represent the exact conditions along the BC Coast, they were

Table 2-2: Summary of observed log BSAFs for PCBs in Dungeness crab from Kitimat Arm. Table headings include minimum (min) and maximum (max) values, the mean, and standard deviation (SD). Source: Harris (1999)

	Observed log BSAFs				
Chemical	**n**	**min**	**max**	**mean**	**SD**
PCB-66	15	1.04	2.18	1.59	0.38
PCB-118	15	-0.95	1.92	0.52	1.14
PCB-105	15	-1.53	1.81	1.17	0.81
PCB-156	8	0.24	0.91	0.58	0.22

Table 2-3: Average BSAFs and BSAF standard errors (SE) for PCBs in *Macoma nasuta* from the study by Boese et al. (1995) and calculated BSAFs.

	PCB-18	**PCB-52**	**PCB-101**	**PCB-128**	**PCB-138**	**PCB-153**	**PCB-194**
BSAF	0.44	2.34	3.42	2.31	2.54	2.66	0.72
SE	0.19	0.3	0.3	0.32	0.28	0.33	0.12
log BSAF	-0.357	0.369	0.534	0.364	0.405	0.425	-0.143

Table 2-4: Organic-carbon-normalized sediment concentrations ($C_{s,oc}$) and lipid-normalized tissue concentrations of PCBs in brittle stars (*Aphiura filiformis and A. chiajei*) from the study by Gunnarson and Skold (1999), and calculated BSAFs. Sediments at nearshore collection sites contained 3.24% organic carbon while sediments at offshore collection sites sediments contained 1.6% organic carbon.

	PCB-28	**PCB-101**	**PCB-118**	**PCB-138**	**PCB-153**	**PCB-180**
Near Shore						
$C_{s,oc}$ (ng/g OC)	5.2	24.4	26.9	52.5	43.2	21.3
Aphiura filiformis (ng/g lipid)	31.1	80.7	93.0	296.4	301.1	168.9
BSAF	5.9	3.3	3.5	5.6	7.0	7.9
log BSAF	**0.77**	**0.52**	**0.54**	**0.75**	**0.84**	**0.90**
Offshore						
C_{soc} (ng/g OC)	14.4	16.0	20.7	30.3	24.5	8.0
A. filiformis (ng/g lipid)	17.2	39.9	17.8	38.0	42.7	12.5
BSAF	2.2	5.5	0.9	1.8	2.3	2.4
log BSAF	0.4	0.7	0.0	0.3	0.4	0.4
A chiajei (ng/g lipid)	32.3	88.5	19.2	55.4	56.9	19.2
BSAF	2.2	5.5	0.9	1.8	2.3	2.4
log BSAF	**0.35**	**0.74**	**-0.034**	**0.26**	**0.37**	**0.38**

considered useful for making order-of-magnitude estimates of expected BSAFs and examining overall trends.

False Creek

PCB BSAF data for multiple organisms and PCB congeners in False Creek were provided by Mackintosh and Maldonado (*unpublished data*). The researchers in this study measured PCB concentrations in several fish and invertebrate species and provided average log BSAFs for several PCB congeners and organisms. The Dungeness crab analyzed in this study were generally of a smaller size (mean weight 220 g) than those analyzed in Kitimat Arm (mean weight 800 g). The False Creek flatfish composite was comprised of intermediate-sized English sole and starry flounder (approximately 15 cm in length) while the minnow composite was comprised of several small-sized species/life stages including sticklebacks, sculpins, perch, trout, greenling and flounder. The BSAFs from this study are presented in Table 2-5.

While there were no site-specific data for PCB BSAFs in large epifauna in False Creek, Gunnarson and Skold (1999) reported PCB concentrations in brittle stars (*Aphiura filiformis and A. chiajei*) and corresponding sediments from the Baltic Sea. Sediments from the nearshore site in this study contained 3.24% organic carbon, roughly corresponding to False Creek. Model predictions for large infauna in False Creek were compared to observed BSAFs in brittle star from the nearshore site. While these data may not represent the exact conditions along the BC Coast, they were considered useful for making order-of-magnitude estimates of observed BSAFs and examining overall trends.

2.3.3 Model Parameterization

Chemical Properties for PCBs

Chemical properties are presented in Table 2-6. For co-eluting PCB congener groups, the geometric mean of congener K_{ow} values (i.e., mean log K_{ow}) was assumed to represent the group K_{ow}. The K_{ow} for each chemical/chemical group was adjusted according to the method described in Xie et al. (1997) to account for the “salting-out” effect in saltwater.

Table 2-5: Log BSAFs and log standard deviation (SD) for PCBs in marine biota from False Creek. Data were collected and analyzed by Mackintosh and Maldonado (*unpublished data*). Numbers in table headings refer to PCB congeners and co-eluting congener groups.

Common Name	16/32	47/75/48	73/52	101/90	99	110	149	118
Manila Clams								
BSAF	-1.09	-0.54	-0.81	-0.80	-0.67	-0.90	-0.83	-0.71
SD	0.24	0.31	0.29	0.26	0.21	0.27	0.34	0.27
Geoduck Clams								
BSAF	-0.73	-0.32	-0.44	-0.42	-0.40	-0.50	-0.47	-0.32
SD	0.38	0.50	0.44	0.49	0.43	0.53	0.60	0.48
Dungeness Crab								
BSAF	-0.30	0.54	0.41	0.53	0.61	0.33	0.42	0.66
SD	0.54	0.60	0.61	0.53	0.51	0.52	0.58	0.49
Minnow Composite								
BSAF	-0.93	-0.24	-0.10	0.14	0.30	-0.07	-0.10	0.40
SD	0.43	0.65	0.62	0.66	0.57	0.65	0.70	0.55
Flatfish Composite								
BSAF	-0.10	0.58	0.57	0.73	0.73	0.67	0.51	0.72
SD	0.24	0.24	0.26	0.19	0.25	0.36	0.37	0.29

Common Name	132/153	160/163/ 164/138	177	187/182	200/204	180	203/196	194
Manila Clams								
BSAF	-0.55	-0.71	-0.89	-0.75	-0.86	-0.93	-1.00	-1.10
SD	0.29	0.27	0.30	0.33	0.34	0.39	0.32	0.32
Geoduck Clams								
BSAF	-0.32	-0.47	-0.60	-0.56	-0.56	-0.84	-1.02	-1.37
SD	0.49	0.51	0.47	0.50	0.52	0.41	0.52	0.46
Dungeness Crab								
BSAF	0.68	0.54	0.19	0.39	0.10	0.14	-0.20	-0.18
SD	0.48	0.51	0.52	0.51	0.51	0.55	0.64	0.65
Minnow Composite								
BSAF	0.49	0.31	-0.10	0.12	-0.07	-0.01	-0.25	-0.35
SD	0.63	0.63	0.64	0.64	0.69	0.63	0.68	0.63
Flatfish Composite								
BSAF	0.88	0.70	0.29	0.61	0.50	0.49	0.40	0.27
SD	0.35	0.21	0.45	0.65	0.49	0.46	0.47	0.42

Table 2-6: Log K_{ow}, molar volume and saltwater-adjusted log K_{ow} for PCBs and co-eluting congener groups. log Kow values based Hawker and Connell (1988), molar volumes based on Mackay et al., (1999), log K_{ow} adjusted for saltwater using the method described by Xie et al. (1997).

Chemical Name	Log K_{ow}	Molar Volume (cm^3/mol)	Adjusted Log K_{ow}
PCB-16/32	5.30	247.3	5.52
PCB-18	5.24	247.3	5.46
PCB-28	5.67	247.3	5.89
PCB-47/75/48	5.89	268.2	6.13
PCB-52	5.84	268.2	6.08
PCB-66	6.20	268.2	6.44
PCB-73/52	5.94	268.2	6.18
PCB-99	6.39	289.1	6.65
PCB-101	6.38	289.1	6.64
PCB-101/90	6.37	289.1	6.63
PCB-105	6.65	289.1	6.91
PCB-110	6.48	289.1	6.74
PCB-118	6.74	289.1	7.00
PCB-128	6.74	310	7.02
PCB-132/153	6.75	310	7.02
PCB-138	6.83	310	7.11
PCB-149	6.67	310	6.95
PCB-153	6.92	310	7.20
PCB-156	7.18	310	7.46
PCB-160/163/164/138	6.94	310	7.30
PCB-177	7.08	330.9	7.38
PCB-180	7.38	330.9	7.66
PCB-187/182	7.18	330.9	7.53
PCB-194	7.80	351.8	8.12
PCB-200/204	7.28	351.8	7.61
PCB-203/196	7.65	351.8	7.97

Briefly, the adjusted K_{ow} is related to the freshwater value ($K_{ow,F}$) and the Le Bas molar volume (V) according to the following relationship:

$$K_{ow} = K_{ow,F} \cdot 10^{0.0009 \cdot V} \qquad [29]$$

Organism Size and Tissue Composition

Table 2-7 summarizes organism size (V_B) and tissue composition ($\phi_{L,B}$, $\phi_{OC,B}$, $\phi_{NLOM,B}$, ϕW_B) for each trophic guild. Lipid contents for all trophic guilds except phytoplankton were estimated based on data for North Pacific fish and invertebrates reported in Higgs et al. (1995), Payne et al. (1999) and Iverson et al. (2002) and Harris (1999). The lipid andorganic carbon content of phytoplankton was based on data reported in Skoglund and Swackhamer (1999). The water content of all organisms was assumed to be 80% with non-lipid organic matter making up the remaining fraction.

Rate Constants for Phytoplankton

The model for k_{1phyt} was parameterized to fit observed uptake rates in phytoplankton. Skoglund et al., (1996) found an average logk_{1phyt} of 5.21 for PCBs (log K_{ow} ranging from 5.2 to 8.2) in four freshwater phytoplankton species. Values of $5x10^{-7}$ for α and $1x10^{-3}$ for β yielded a maximum log k_{1phyt} of 5.15, providing reasonable agreement with the observed data. Figure 2-3 depicts the relationship of k_{1phyt} and k_{2phyt} with K_{ow}. k_G in phytoplankton was set at 0.52/day based on the production:biomass ratio of 190/year for Northeast Pacific phytoplankton reported by Oakey and Pauley (1999).

Water Ventilation Rates

G_w for each trophic guild was calculated using either species-specific information or general allometric equations (refer to Table 2-8). Arnot (2003) provides an allometric equation for estimating G_w in fish. This equations was applied to the representative fish groups in the model (small fish and juvenile flatfish). Given the differences between invertebrates and fish in activity level, it was assumed that this equation did not accurately represent invertebrates species. Instead, values for G_w were estimated from oxygen consumption rates or ventilation rates measured in laboratory studies using Equation 8 (Lasker, 1962; Kristensen, 1989; Marsden, 1999; Brown and Terwilliger, 1999). The equation for E_w described by Gobas (1993) was applied for all trophic guilds.

Table 2-7: Organism size (V_B) and tissue composition for phytoplankton and trophic guilds. $\phi_{L,B}$ – lipid content, $\phi_{OC,B}$–organic carbon content, $\phi_{NLOM,B}$–non-lipid organic matter content, $\phi_{W,B}$–water content,)

Trophic Guild	**V_B**	$f_{L,B}$	$f_{OC,B}$	$f_{NLOM,B}$	$f_{W,B}$
phytoplankton	-	0.4%	6%	13.6%	80%
zooplankton	1 mg	3.5%	0%	16.5%	80%
small infauna and epifauna	0.5 g	1.5%	0%	18.5%	80%
large infauna	5 g	1%	0%	19%	80%
small fish	5 g	3%	0%	17%	80%
large epifauna	5 g	2%	0%	18%	80%
juvenile flatfish	75 g	1.5%	0%	18.5%	80%
Dungeness crab	0.8 kg (Kitimat Arm) 0.22 kg (False Creek)	3%	0%	17%	80%

Figure 2-3: Relationship between k_{1phyt} (—) and k_{2phyt} (---) and log K_{ow} for phytoplankton.

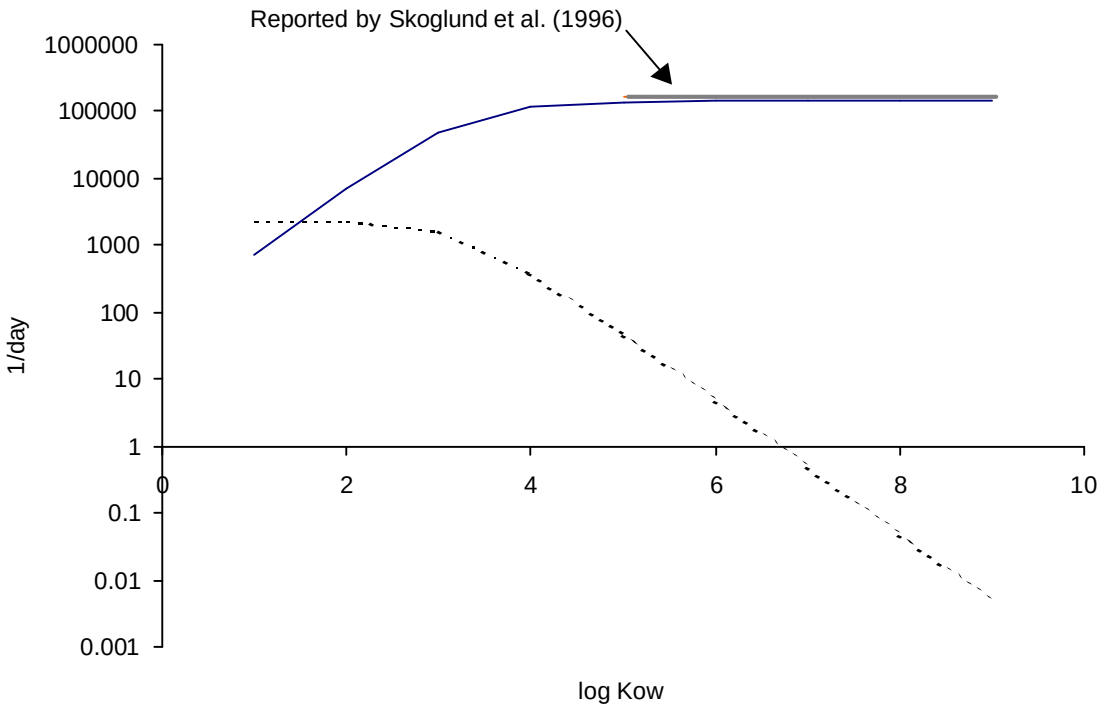

Table 2-8: Estimation of water ventilation rates (G_W) for trophic guilds in the benthic food web.

Trophic Guild	G_w (L/day)	Estimation Method
zooplankton	0.017	Estimated using Equation 8 based on oxygen consumption of 1.47 µL/mg/h in euphausiids (Lasker, 1962); assuming 75% O_2 saturation
small infauna and epifauna	0.198	Estimated using Equation 8 based on oxygen consumption of 7.72 µmol/g/h in polychaetes Kristensen (1989); assuming 75% O_2 saturation
large infauna	21.77	$G_w = 24 \cdot (0.1 \cdot (V_B \cdot 1000)^{1.37})$ (based on allometric relationship in Marsden, 1999)
small fish	5.96	$G_w = (1400 \cdot V_B^{0.65})/DO$ (allometric relationship from Arnot, 2003)
large epifauna	2.29	Estimated using Equation 8 based on oxygen consumption of 0.2 ml O_2/g/h in juvenile Dungeness crab (between 1st and 5th instar; Brown and Terwilliger, 1999); assuming 75% O_2 saturation.
juvenile flatfish	34.7	$G_w = (1400 \cdot V_B^{0.65})/DO$ (allometric relationship from Arnot, 2003)
Dungeness crab	135.2 (Kitimat Arm) 37.2 (False Creek)	Estimated using Equation 8 based on oxygen consumption of 55 mmol O_2/kg/min adult Dungeness crab (McDonald et al., 1980)). Assuming 75% O_2 saturation.

Table 2-9: Absorption efficiencies for lipid (α_L), organic carbon (α_{OC}), non-lipid organic matter (α_{NLOM}) and water (α_W), and the combined food assimilation efficiency (A_F) for trophic guilds.

Trophic Guild	a_L	a_{OC}	a_{NLOM}	a_W	A_F
zooplankton	0.80	0.60	0.60	0.80	0.61
small infauna and epifauna	0.80	0.60	0.60	0.80	0.61
large infauna	0.80	0.60	0.60	0.80	0.61
small fish	0.92	0.80	0.80	0.80	0.82
large epifauna	0.92	0.80	0.80	0.80	0.81
juvenile flatfish	0.92	0.80	0.80	0.80	0.81
Dungeness crab	0.92	0.80	0.80	0.80	0.81

Food Absorption Efficiencies

Table 2-9 displays absorption efficiencies for the tissue and dietary constituents listed in Table 2-7. Nichols et al. (2001) found a dietary uptake efficiency for lipid of 91% in rainbow trout; this value was applied to upper trophic guilds in the digestion model. Given the more simple digestive systems of lower trophic guilds α_L was set at 80% for these organisms. Absorption efficiencies for organic carbon and non-lipid organic matter were set lower to reflect the lower digestibility and nutritional value of these components. In marine organisms, the diet is the primary absorption route for water. Therefore, α_W was set at 80%. For each trophic guild, the overall food assimilation efficiency for each organism (A_F) was determined as the sum of products of the proportion and absorption efficiency of each dietary constituent. Connolly (1991) reviewed A_F in marine organisms and reported values of near 0.8 for carnivores, 0.3-0.6 for detritivores and as low as 0.3 for herbivores. The calculated values for A_F were within these reported ranges.

Respiration and Growth Rates

k_R for each trophic guild was estimated using the equation described by Thomann et al. (1992). Growth rates for fish were estimated using the allometric relationship described by Gobas (1993). For Dungeness crab, the growth rates in Kitimat Arm and False Creek matched the size-specific rates quoted in Harris (1991). Growth rates reported by Connolly (1991) of 0.007/day in polychaetes and 0.008/day in clams (both derived from field-observed relationships) were applied for small infaunal and epifaunal invertebrates and large infauna, respectively. Harris (1991) reported that juvenile Dungeness crabs grow from a size of approximately 1 g to over 500 g in their second year of life, representing a linear growth rate of approximately 0.003/day. This rate was applied to the large epifauna trophic guild which contains small crustaceans such as juvenile Dungeness crab. Lasker (1966) reported linear growth in euphausiids consistent with a k_G of 0.02/day.

Chemical Uptake Efficiency

Figure 2-4 summarizes laboratory measurements of chemical uptake efficiency (E_d) for several chemicals in both fish and invertebrate species. Based on an earlier subset of these measurements, Gobas et al. (1988) used non-linear regression to parameterize the

Figure 2-4: Dietary uptake efficiencies (E_d) for hydrophobic chemicals measured in fish (◇) and invertebrates (△) and the relationship determined by Gobas et al. (1988;—). Data for fish compiled from Fisk et al. (1998), Gobas et al. (1988), and Gobas et al. (1993a). Data for invertebrates represent median values from Wang and Fisher (1999).

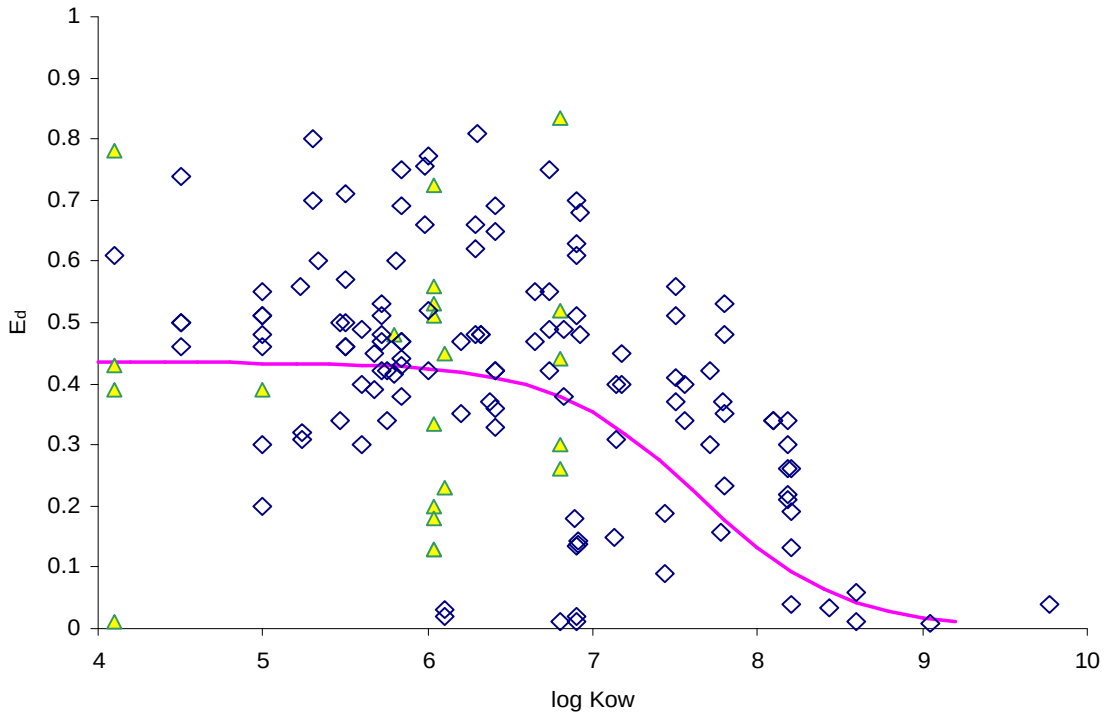

E_d equation such that A = 5.3?10^{-8} and B = 2.3. While this E_d relationship could potentially represent the natural case, the chemical absorption efficiency data are highly variable and uncertainty exists as to whether experiments with primarily freshwater fish species also apply to marine invertebrates. In addition, laboratory studies with spiked food may not accurately represent natural conditions. Therefore, the relationship between E_d and K_{ow} was not specified *a priori*. Rather, the E_d relationship was varied as part of model calibration.

Food Web Structure

The feeding matrix for the BSAF model is provided in Table 2-10. The diet composition for trophic guilds was estimated from the dietary fractions presented in Table 2-1. For zooplankton, the weighted-average proportion of each food item was calculated from the relative biomass of microzooplankton, herbivores, omnivores and carnivores (refer to Table 2-1). For False Creek, feeding preferences for small infauna and epifauna, and large infauna, were based on the "shallow" class (refer to Table 2-1) whereas for Kitimat Arm they were based on the "deep" class (refer to Table 2-1), in order to account for differences in depth between the systems. Small fish were represented by Pacific sandlance, an important prey species for benthic predators. Diet composition for Dungeness crabs in Kitimat Arm corresponded to the data reported by Stevens et al. (1982) for crabs with a 120 mm carapace (refer to Table 2-1). To reflect the smaller size of False Creek Dungeness crab, diet composition there was based on the average of the 80mm carapace and 120 mm carapace data reported by Stevens et al. (1982; refer to Table 2-1). Because of their close association with sediments when feeding, incidental sediment ingestion was assumed to comprise a small dietary proportion for upper trophic guilds (small forage fish, juvenile flatfish and Dungeness crab).

Ecosystem Properties

Ecosystem properties for Kitimat Arm and False Creek are summarized in Table 2-11. Estimates of sediment deposition (Q_{ss}), water temperature (T_w) and the organic carbon fractions of suspended sediment (ϕ_{ssoc}) and bottom sediment (ϕ_{oc}) were based on the study of Kitimat Arm by Harris (1999). Dissolved oxygen (DO) was estimated from the

Table 2-10: Feeding matrix for trophic guilds in the food web BSAF model.

	Prey Item								
Trophic Guild	**Detritus**	**Phytoplankton**	**Zooplankton**	**Small Infauna and Epifauna**	**Large Infauna**	**Large Epifauna**	**Small Fish**	**Juvenile Flatfish**	**Dungeness Crab**
Zooplankton	8.7%	79.5%	11.8%	0.0%	0.0%	0.0%	0.0%	0.0%	0.0%
Small Infauna and Epifauna (Kitimat Arm)	83.4%	10.0%	2.0%	4.6%	0.0%	0.0%	0.0%	0.0%	0.0%
Small Infauna and Epifauna (False Creek)	58.0%	34.0%	5.0%	3.0%	0.0%	0.0%	0.0%	0.0%	0.0%
Large Infauna (Kitimat Arm)	90.0%	10.0%	0.0%	0.0%	0.0%	0.0%	0.0%	0.0%	0.0%
Large Infauna (False Creek)	50.0%	50.0%	0.0%	0.0%	0.0%	0.0%	0.0%	0.0%	0.0%
Small Fish	5.0%	0.0%	90.0%	5.0%	0.0%	0.0%	0.0%	0.0%	0.0%
Large Epifauna	34.2%	0.0%	0.0%	36.2%	17.8%	10.5%	0.7%	0.7%	0.0%
Juvenile Flatfish	10.0%	0.0%	0.5%	52%	22%	15%	0.0%	0.0%	0.0%
Dungeness Crab (Kitimat Arm))	5.0%	0.0%	0.0%	2.0%	4.0%	35.0%	34.0%	15.0%	5.0%
Dungeness Crab (False Creek)	5.0%	0.0%	0.0%	2.0%	30.0%	35.0%	20.0%	5.0%	2.5%

Table 2-11: Ecosystem parameters including primary productivity (Q_{poc}), sediment deposition rate (Q_{ss}), organic carbon fraction of suspended sediment (ϕ_{oc}), organic carbon fraction of bottom sediment (ϕ_{oc}), dissolved oxygen in seawater (DO) and average water temperature (T_w).

Parameter	Description	Value	Source
Q_{poc}	phytoplankton primary productivity (kgC/m^2/day)	0.00033 (Kitimat Arm)	Estimated from data quoted in Pauly and Kristensen (1996) and Oakey and Pauly (1999)
		0.00095 (False Creek)	
Q_{ss}	sediment deposition rate (kg/m^2/day)	0.0047	Harris (1999)
ϕ_{ssoc}	organic carbon fraction of suspended sediment	1.4% (Kitimat Arm)	Harris (1999)
		2.8% (False Creek)	assumed
ϕ_{oc}	organic carbon fraction of bottom sediments	1.3% (Kitimat Arm)	Harris (1999)
		2.8% (False Creek)	Mackintosh (2002)
DO	dissolved oxygen in seawater (mg/L)	7.5	BCMELP (1997), assuming 75% saturation
T_W	average water temperature (^{o}C)	8.75	Average of values quoted by Harris (1999)

temperature- and salinity-dependent values quoted in BCMELP (1997), while the sorptive capacity of OC, relative to lipid, was based on the study by Seth et al. (1999). The sorptive capacity of non-lipid-organic matter is expected to be lower than that of lipid; therefore a factor of 0.035 was applied based on the findings of Gobas et al. (1999). The organic carbon content of detritus was assumed to equal that of suspended sediment.

Estimates of phytoplankton primary productivity (Q_{poc}) in coastal areas of the Northeast Pacific Ocean include a range from 120 to 345 gC/m^2/year for the Georgia Strait, BC, (quoted by Pauly and Kristensen, 1996) and a value of 114 gC/m^2/year for Port Valdez, AK (quoted by Oakey and Pauly, 1999). Kitimat Arm has a similar physical setting to Port Valdez (i.e., both are narrow inlets with significant river inputs of freshwater and silt) but is situated at a lower latitude where primary productivity may be higher. Therefore, primary productivity for Kitimat Arm was set at 120 gC/m^2/year (0.00033 kgC/m^2/day).

For predicting BSAFs in False Creek, both the organic carbon content of sediment particles and the primary productivity were adjusted to reflect the different conditions there. Mackintosh (2002) found that False Creek bottom sediments contained 2.8% organic carbon. The organic carbon content of suspended sediment was also set at this value. The higher organic carbon in False Creek suggests higher overall productivity than Kitimat Arm, which is likely due to the lower latitude and higher nutrient inputs from anthropogenic sources. Thus, primary productivity was set at 345 gC/m^2/year (0.00095 kgC/m^2/day), the highest value found for the Georgia Strait, which is located nearby.

Measured concentrations of PCBs dissolved in overlying water were not available for Kitimat Arm or False Creek. Therefore, dissolved overlying water concentrations were calculated using Equation 28. Figure 2-5 depicts the relationship of DF_{ss} with K_{ow} that is predicted by the model, in Kitimat Arm and False Creek. Sediment porewater was assumed to be in equilibrium with bottom sediments (i.e., calculated using EQP). Because they inhabit the sediment surface, benthic organisms are potentially exposed to a combination of overlying water and sediment porewater. Sediment porewater is often low

Figure 2-5: Relationship between predicted sediment-water disequilibrium (DF_{ss}) and log K_{ow} for overlying water in Kitimat Arm (—) and False Creek (---).

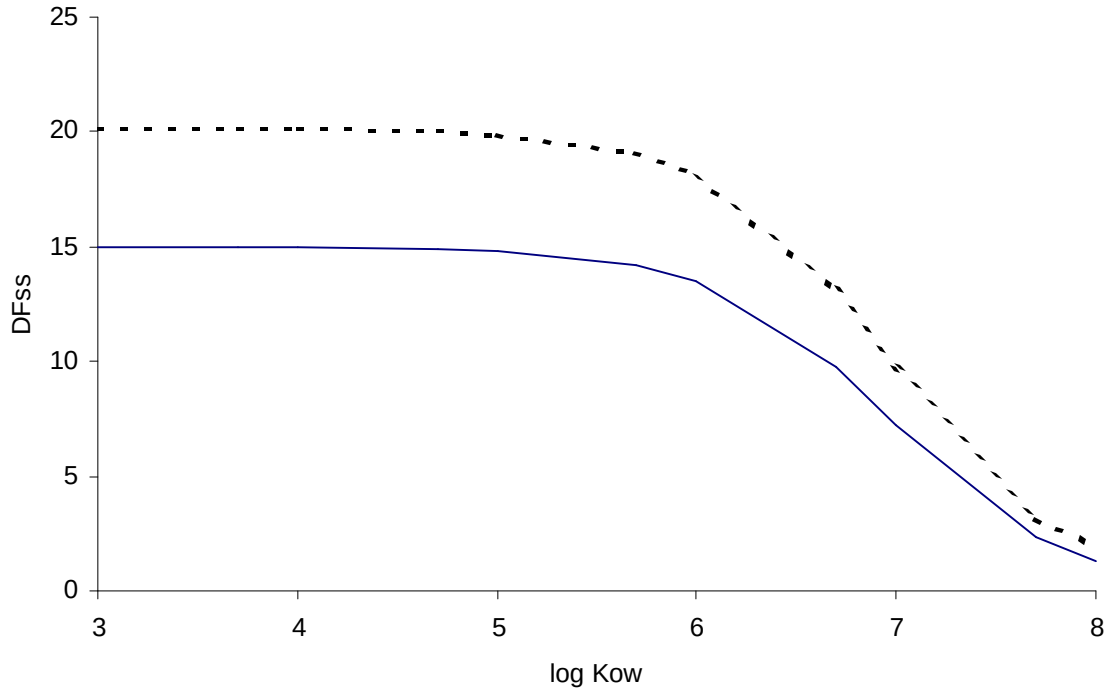

in oxygen meaning that benthic organisms are generally reliant on overlying water for respiration. Infaunal invertebrates (e.g., polychaetes and bivalves) are expected to pump overlying water into their burrows as a source of both oxygen and food (Aller, 1983; Winsor, 1990). In addition, the expected disequilibrium in overlying water may also be present in porewater from the sediment surface, resulting in a depth gradient from overlying water concentrations to porewater concentrations. Given this uncertainty, the relative proportions of overlying water and porewater were not specific *a priori*, but were evaluated further during model calibration.

2.3.4 Model Calibration

The purpose of this phase was to calibrate the model so that it accurately represented sediment-to-biota transfer for both Kitimat Arm and False Creek. Model calibration involves sensitivity analysis to obtain the set of conditions that (i) provide an accurate representation of the system being modelled and (ii) are scientifically defensible based on mechanistic considerations and empirical data. (Jackson et al. 2000; Connolly, 1991). The two model parameters with the highest uncertainty were E_d and the proportion of sediment porewater ventilated by benthic organisms. Sensitivity analysis was conducted for these parameters to determine the parameter set that resulted in the best representation of BSAF for PCBs in Dungeness crab, in both Kitimat Arm and False Creek.

E_d

Model calibration for E_d involved systematically changing the values for A and B in Equation 12 (repeated below) to test varying forms of the relationship for E_d:

$$E_d = 1/(A \cdot K_{ow} + B)$$

As an initial set of conditions, the values for A and B proposed by Gobas et al. (1988) were chosen to represent E_d for upper trophic guilds (Dungeness crab, fish and large epifauna). Lower trophic guilds (large infauna, small infauna and epifauna, and zooplankton) were assumed to have a lower E_d than upper trophic guilds because they feed primarily on organic carbon (i.e., with a lower digestibility than lipid) and have lesser developed digestive systems (i.e., with a lower gut surface area and lower food residence times). These characteristics are expected to lessen the surface area and time

for diffusion of chemical from food into the organism, reducing chemical transfer efficiency. E_d was set lower for these trophic guilds by increasing A and B by 25% over the values for higher trophic guilds and varying them in proportion to A and B for upper trophic guilds. The proportion of porewater ventilated by benthic organisms was set at 5% based on the concurrent sensitivity analysis for this parameter (discussed below).

Two quantitative criteria were used to evaluate how well the model represented BSAFs for PCBs in Dungeness crab with the different values for A and B: a modified sum-of-squares criterion (SSQ/n) and model bias (MB). The modified sum-of-squares criterion (SSQ/n) was calculated from the deviation between the predicted and average observed BSAF for each PCB congener. SSQ was calculated as:

$$SSQ = \sum_{i=1}^{n} (BSAF_{p,i} - BSAF_{o,i})^2 \qquad [30]$$

Where $BSAF_{p,i}$ is the model predicted BSAF for congener *i*, $BSAF_{o,i}$ is the observed average BSAF for PCB congener *i*, and *n* is the number of PCB congeners. SSQ/n is then calculated by dividing SSQ by *n*.

SSQ/n was used to select a range of values for A and B that resulted in reasonably accurate representations of Dungeness crab BSAFs for both systems. Because the False Creek data set was based on more PCB congeners, SSQ for each data set was normalized to the sample size (i.e., SSQ/n, where n = the number of chemicals) in order to prevent a bias towards the False Creek system. Parameter combinations which resulted in low results for SSQ/n were then further evaluated based on MB in order to finalize the calibration.

MB for each chemical in a given trophic guild can be determined by comparing predicted and observed BSAFs according to the following equation:

$$\log MB = \left(\sum_{i=1}^{n} \log \frac{BSAF_p}{BSAF_{o,i}} \right) / n \qquad [31]$$

Where $BSAF_p$ is the model-predicted BSAF for the chemical, $BSAF_{o,i}$ is an observed BSAF for the chemical, and n is the number of BSAF observations for the chemical. Expressing logMB in arithmetic form yields the model bias (MB). MB>1 indicates overprediction and MB<1 indicates underprediction, for each specific trophic guild and chemical. For example, MB=0.5 indicates *underprediction* by a factor of 2 whereas MB=2 indicates *overprediction* by a factor 2. Thus, an observed range in MB of 0.5 to 2 (i.e., for several chemicals in a specific trophic guild) indicates that model predictions are within a factor of 2 of observed values, for all chemicals. As part of the calibration process, the range in MB for Dungeness crab (i.e., for all chemicals) was examined. The final values of A and B were selected by considering both SSQ/n and the range in MB for Dungeness crab, along with a visual evaluation of the representation of the overall trend in observed BSAFs. While SSQ/n resulted in the best "fit" to the data, it did not result in the best balance of underprediction and overprediction for the model. Hence, inclusion of MB ensured that the model was a reasonably accurate fit to the data but also was not overly biased toward overprediction or underprediction.

Proportion of Porewater in Ventilated Water

Sensitivity analysis for the proportion of porewater in ventilated water involved systemically varying this parameter from 0% to 20%. Model calibration for this parameter was less rigorous, and a final value was chosen based on a visual evaluation of the fit to observed data.

2.3.5 Model Performance Evaluation

MB was the primary criterion for evaluating the performance of the model for predicting the BSAFs of PCBs in trophic guilds from Kitimat Arm and False Creek. By plotting MB vs. log K_{ow} for a given trophic guild, it is possible detect systematic bias, if any, and evaluate model performance at representing BSAFs over a range of chemicals with varying hydrophobicity. For each trophic guild, the average model bias (MB_{avg}), based on the pooled values of MB for all chemicals, can also be calculated according to the following formula:

$$\log MB_{avg} = \left(\sum_{j=1}^{n} \log MB_j \right) / n \qquad [32]$$

where *n* is the number of chemicals with observed BSAFs for a given trophic guild. This statistic is interpreted the same as MB and provides a general indication of overprediction or underprediction for a trophic guild, independent of chemical K_{ow}. For example, MB_{avg}=2 indicates that, on average, independent of chemical log K_{ow}, model predictions are two times higher than observed values.

By considering both MB vs. log K_{ow} and MB_{avg} it is possible to determine the overall performance of the model. A slope of zero for MB vs. log K_{ow} (i.e., no incremental change in MB for an increase or decrease in log K_{ow}) and MB_{avg} of 1 (i.e., roughly equal distribution of MB about 1) indicates a very accurate representation of the observed BSAFs. Deviations from these values indicate some systematic bias, either dependent on, or independent of log K_{ow}.

2.4 RESULTS AND DISCUSSION

2.4.1 Model Calibration

Dietary Uptake Efficiency

As demonstrated by Figure 2-4, the empirical data for E_d are highly variable and a range of values for A and B in the empirical model for E_d may represent the *true* condition for each organism. With the Gobas et al. (1988) parameters the predicted log BSAFs for Dungeness crab were biased toward overprediction above log K_{ow} of approximately 6.5.

Figure 2-6 presents SSQ/n for a range of values of A and B. The lowest SSQ/n was obtained for values of A ranging from approximately $2.5x10^{-7}$ to $3.25x10^{-7}$, depending on the value for B. These parameter ranges were further evaluated considering both model bias and the subjective *fit* to the observed BSAFs in Kitimat Arm and False Creek. Model bias ranges for representative parameter combinations are presented in Table 2-12. Based on this final evaluation, the following equations were selected to represent Ed for trophic guilds in the BSAF model:

Dungeness crab, juvenile flatfish, small fish and large epifauna:

$$E_d = 1/(2.6x10^{-7} \cdot K_{ow} + 2.0) \qquad [33]$$

Large infauna, small infauna and epifauna, zooplankton:

$$E_d = 1/(3.25x10^{-7} \cdot K_{ow} + 2.5) \qquad [34]$$

Although other combinations produced slightly smaller SSQ/n and ranges in MB, these other combinations did not match the general trend in observed BSAFs with K_{ow} as well as the selected values.

Figures 2-7 and 2-8 compare model predictions with representative parameter pairs to observed BSAFs for Kitimat Arm and False Creek. In general, alternative parameter pairs (i.e., other than the chosen values) resulted in either systematic overprediction or underprediction across all chemicals, or good model performance in one system but poor performance in the other. For example, with $A=2 \cdot 10^{-7}$ and B=1.7, BSAFs appeared to be overpredicted in both system. As another example, the parameter group of $A=2 \cdot 10^{-7}$ and B=2.2, provided a more accurate representation of the observed BSAFs for False Creek, but model predictions for Kitimat Arm exhibited a systematic bias from underprediction to overprediction as log K_{ow} increased.

With the exception of juvenile flatfish, the final E_d relationship obtained in this sensitivity analysis resulted in relatively accurate prediction of BSAFs for the trophic guilds below Dungeness crab (see Model Performance, below). For juvenile flatfish, BSAFs appear to be underpredicted at higher K_{ow}, suggesting that, for this trophic guild, the decline in E_d may occur at higher K_{ow} than in marine invertebrates or smaller forage fish.

Figure 2-9 depicts the E_d/K_{ow} relationship for upper trophic guilds and lower trophic guilds determined here, along with the relationship proposed by Gobas et al. (1988). The model calibration suggests that the estimated E_d is consistent with experimental data up to log K_{ow} of 6.0 but declines more rapidly than experimental values above this threshold. A similar result was obtained by Connolly (1991) when calibrating a model for PCB BSAFs in the benthic food web of New Bedford Harbour, USA. In addition, the E_d

Figure 2-6: E_d sensitivity analysis results – SSQ/n for various combinations of A and B. SSQ/n, A and B are defined in the text.

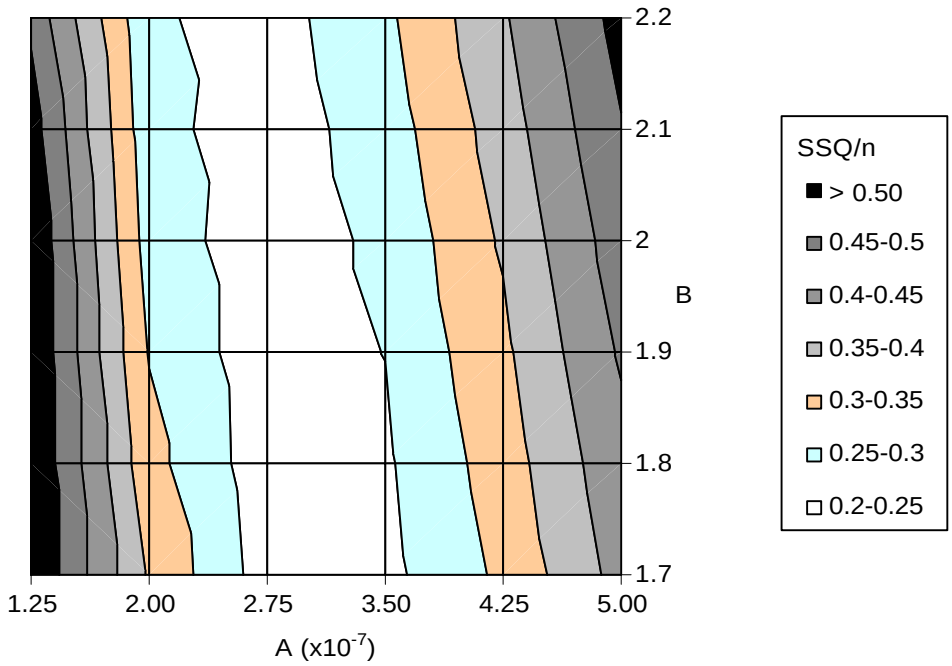

Table 2-12: E_d sensitivity analysis results – MB and SSQ/n for selected combinations of A and B. SSQ/n and MB are defined in the text. Bold/shaded numbers indicate chosen values.

A	B	Range in MB		SSQ/n
		Kitimat Arm	False Creek	
$2.25x10^{-7}$	2.1	0.29 – 4.00	0.36 – 3.81	0.236
$2.25x10^{-7}$	2.2	0.26 – 3.75	0.36 – 3.56	0.233
$2.5x10^{-7}$	1.9	0.33 – 3.87	0.32 – 3.99	0.228
$2.5x10^{-7}$	2	0.30 – 3.63	0.32 – 3.71	0.224
$2.5x10^{-7}$	2.1	0.27 – 3.42	0.32 – 3.47	0.223
$2.6x10^{-7}$	**2**	**0.29 – 3.42**	**0.30 – 3.57**	**0.220**
$2.75x10^{-7}$	1.8	0.34 – 3.52	0.28 – 3.88	0.221
$2.75x10^{-7}$	1.9	0.31 – 3.32	0.28 – 3.62	0.218
$2.75x10^{-7}$	2	0.28 – 3.13	0.28 – 3.38	0.219
$3x10^{-7}$	1.8	0.32 – 3.04	0.26 – 3.53	0.218
$3x10^{-7}$	1.9	0.29 – 2.87	0.26 – 3.3	0.220
$3x10^{-7}$	1.8	0.30 – 2.64	0.23 – 3.22	0.226

Figure 2-7: Comparison of E_d sensitivity analysis results to observed (▲) and mean observed (◇) BSAFs for PCBs in Dungeness crab from Kitimat Arm. Lines represent model results with various combinations of A and B (see Legend). Error bars represent 1 standard deviation.

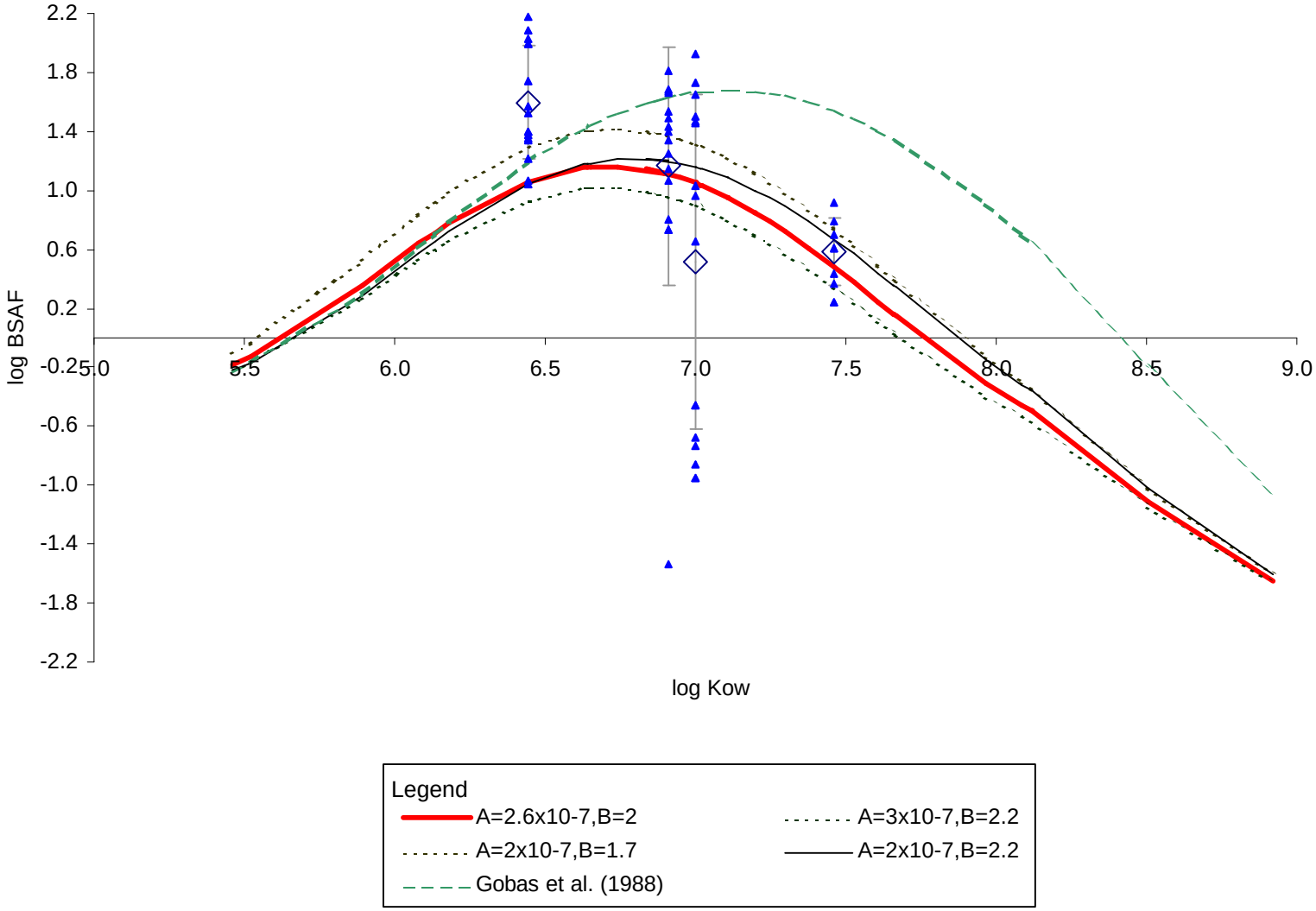

Figure 2-8: Comparison of E_d sensitivity analysis results to mean observed BSAFs (□) for PCBs in Dungeness crab from False Creek. Lines represent model results with various combinations of A and B (see Legend). Error bars not included for clarity.

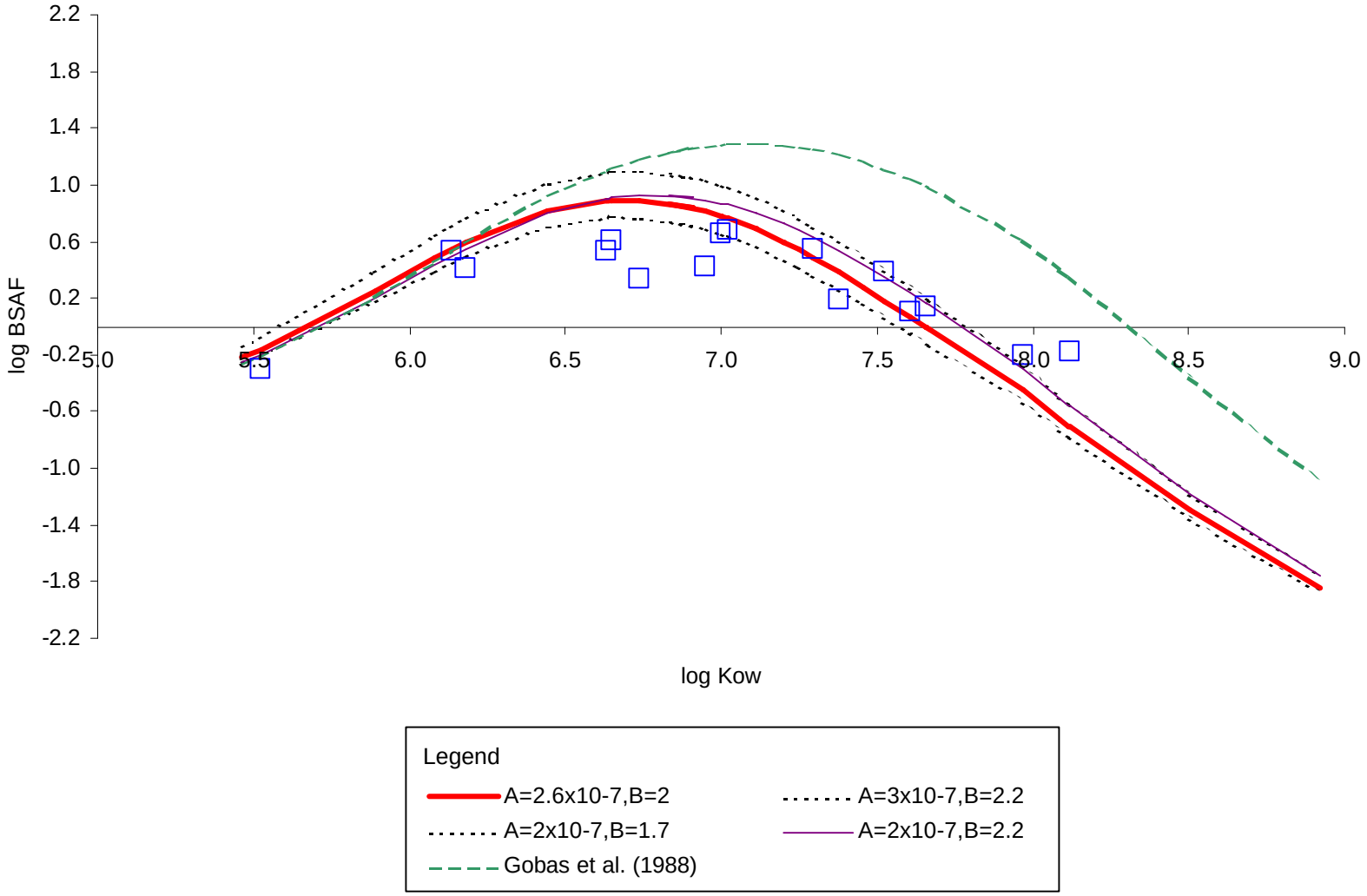

Figure 2-9: Comparison of the calibrated E_d relationship for upper trophic guilds (—) and lower trophic guilds (– –) to observed data for invertebrates (△) and fish (◇), and the E_d relationship reported by Gobas et al. (1988; —).

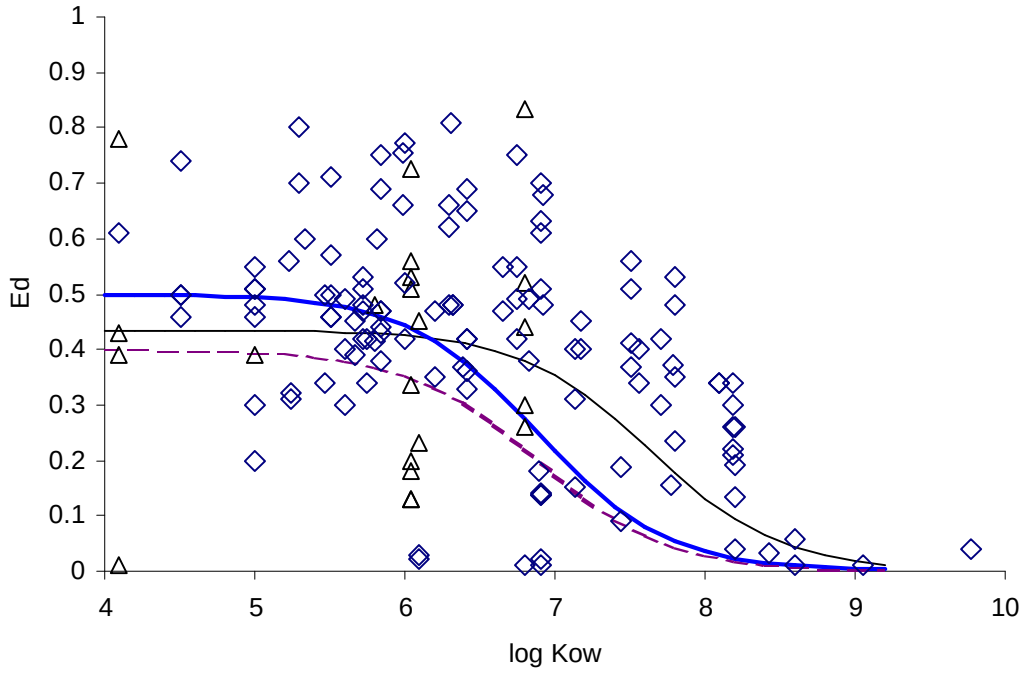

relationship determined here is similar to calibration results for a new bioaccumulation model for the Great Lakes (Arnot, 2003). Laboratory studies can potentially overestimate dietary absorption in natural diets because the spiking process may not accurately represent the sorption of hydrophobic substances into stable lipid or organic carbon compartments, especially at higher K_{ow}. Based on this discussion, the results obtained in this model calibration are deemed to accurately predict dietary uptake in benthic organisms.

Proportion of Porewater in Ventilated Water

Figures 2-10 and 2-11 depict the range of model predictions determined by sensitivity analysis for the proportion of porewater ventilated by benthic organisms. For both systems, model predictions did not appear to be highly sensitive to the porewater proportion. The results of the sensitivity analysis for each system appeared to be contradictory with a value of 0% resulting in the best model fit for False Creek and higher values (e.g., up to 20%) resulting the in the best model fit for Kitimat Arm. Consequently, an intermediate value of 5% was chosen to represent both systems.

This low porewater exposure for benthic organisms is supported by literature studies. Kaag et al. (1996) compared contaminant accumulation in *Arenicola marina* (a deep deposit feeding worm), *Macoma balthica* (a facultative deposit feeding bivalve) and *Mytilus edulis* (a filter feeding bivalve) and hypothesized that uptake was primarily from sediment particles or overlying water. Aller (1983) reported that the lugworm lines its burrow with mucus and ventilates overlying water, limiting exposure to porewater. Finally, Winsor et al. (1990) reported that porewater comprises only 4% of the water ventilated by *Macoma nasuta*, a deposit-feeding clam.

It is also hypothesized that the disequilibrium in overlying water may persist in surface sediments with a gradient of low to high concentration with increasing depth. This would cause sediment porewater concentrations near the sediment-water interface to be lower than those predicted by equilibrium partitioning. Thus, the low porewater exposure indicated by model calibration appears to be reasonable.

Figure 2-10: Comparison of sensitivity analysis results for % porewater to observed (▲) and mean observed (◇) BSAFs for PCBs in Dungeness crab from Kitimat Arm. Lines represent model results for 0% (—), 5% (—), and 20% (---) porewater, respectively. Error bars represent 1 standard deviation.

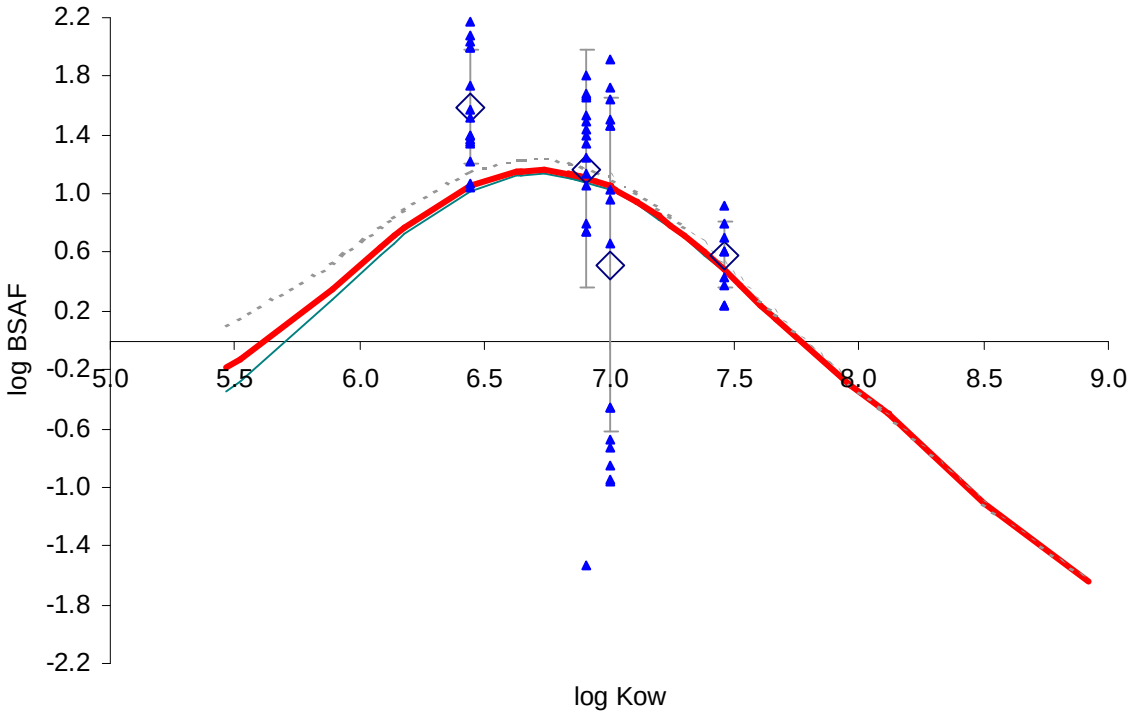

Figure 2-11: Comparison of sensitivity analysis results for % porewater to mean observed BSAFs (□) for PCBs in Dungeness crab from False Creek. Lines represent model results for 0% (—), 5% (—), and 20% (---) porewater, respectively. Error bars not included for clarity.

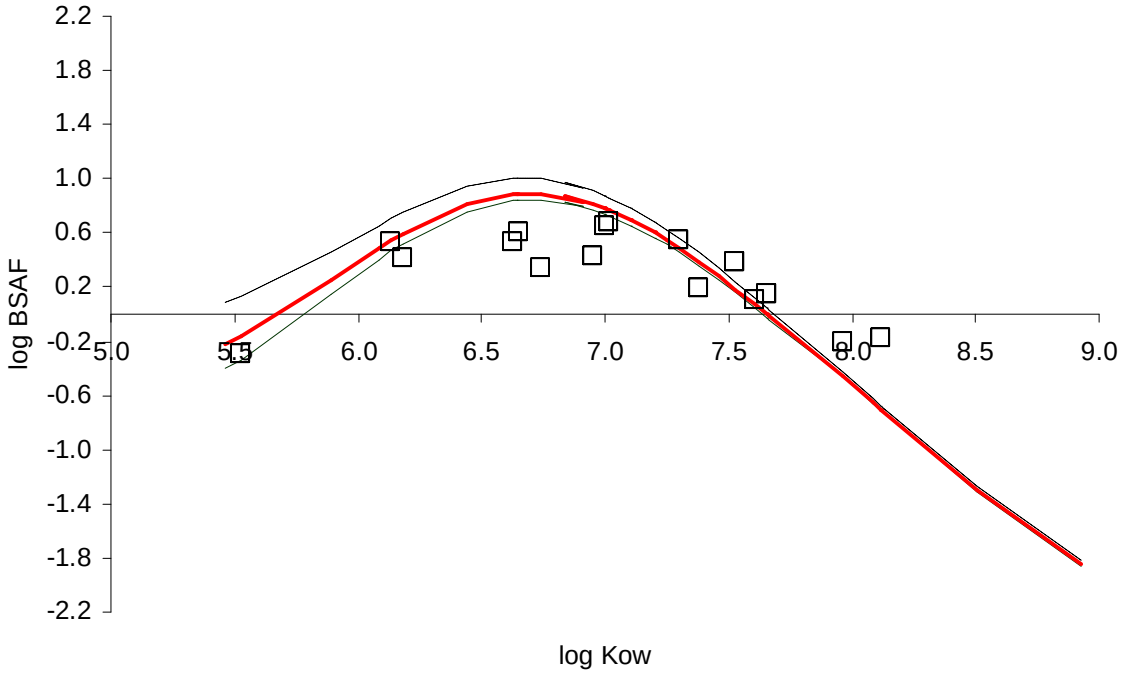

2.4.2 Model Performance Evaluation

Dungeness Crab

Figures 2-12 and 2-13 present the respective comparisons between predicted and observed BSAFs for Dungeness crab in Kitimat Arm and False Creek. For Kitimat Arm, predicted BSAFs were within one standard deviation of observed values for PCB-105, PCB-118 and PCB-156. For PCB-66 the model prediction is within the range of observed BSAFs but generally appears to underpredict the BSAF for this congener. The cause of this apparent underprediction is uncertain since the model predictions for other congeners appear to accurately represent observed data for Kitimat Arm and False Creek. For False Creek, the model predictions appear to mimic the general trend of observed log BSAFs with log K_{ow}, with some over-prediction in the middle of the range.

MB results for Kitimat Arm and False Creek are plotted vs. log K_{ow} in Figure 2-14. MB ranged from 0.29 to 3.42 in Kitimat Arm indicating BSAF prediction within a factor of 3.5. For False Creek, MB ranged from 0.30 to 3.58 and model predictions were within a factor of approximately 3 for all but one PCB congener. MB_{avg} for both systems combined was 0.98 suggesting that while there is some observed underprediction and overprediction, on average, the model predictions match observed data. Figures 2-12 and 2-13 demonstrate that model predictions are in general agreement with the trend in observed BSAFs. Based on these results, it can be concluded that the calibrated model provides reasonable representations of PCB bioaccumulation by Dungeness crab, in both Kitimat Arm and False Creek.

False Creek Fish

Figure 2-15 depicts the comparison of predicted and observed BSAFs for fish in False Creek. While the model predictions for small fish appear to match the BSAFs for the minnow composite, predictions for juvenile sole are lower than observed BSAFs for the flatfish composite, especially at higher K_{ow}.

Model bias results for False Creek fish is summarized in Figure 2-16. MB for juvenile flatfish ranged from 0.20 to 1.10 (i.e., prediction within a factor of five) with an average

Figure 2-12: Comparison of model-predicted BSAFs (—) to observed (▲) and mean observed (◇) BSAFs for PCBs in Dungeness crab from Kitimat Arm. Error bars represent 1 standard deviation.

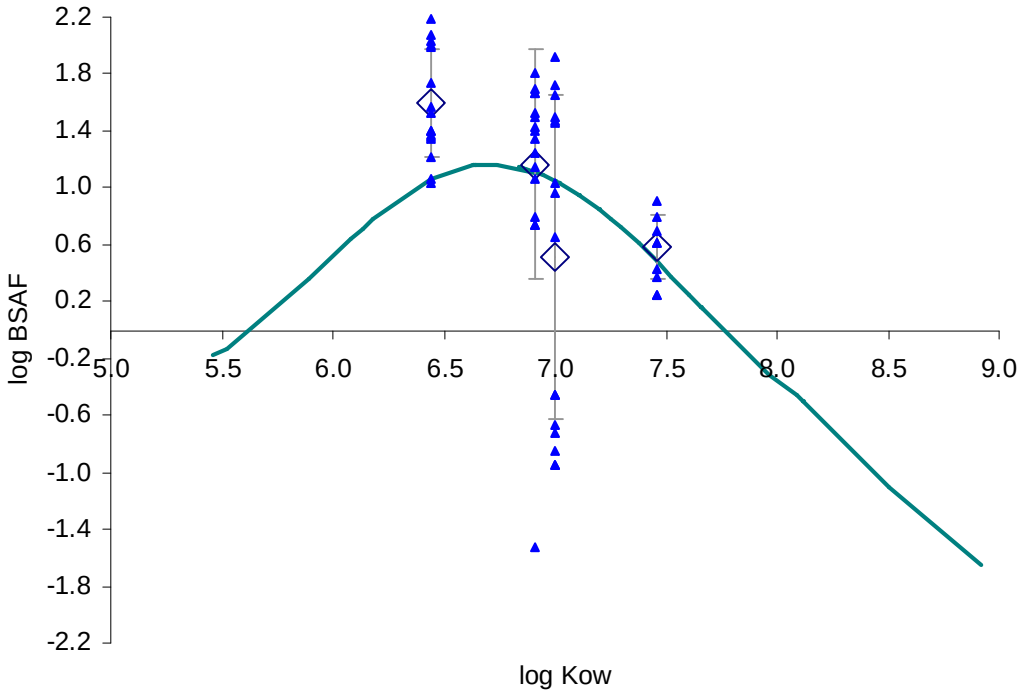

Figure 2-13: PCBs in Dungeness crab from False Creek – comparison of predicted BSAFs to mean observed BSAFs (□). Error bars represent 1 standard deviation.

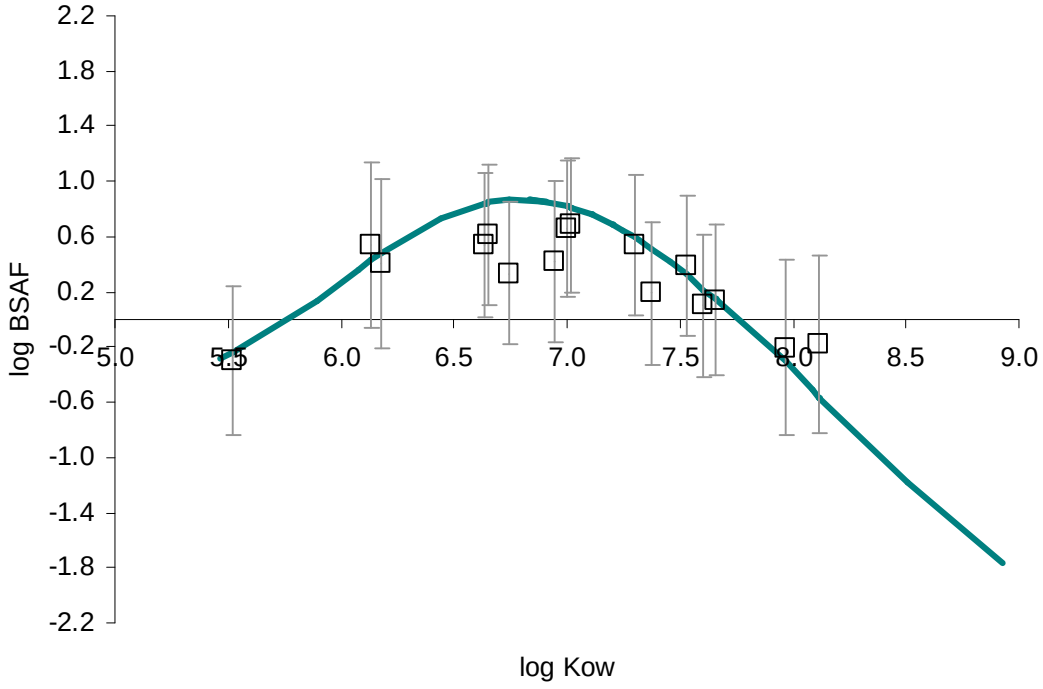

Figure 2-14: Model bias **(**MB) vs. log K_{ow} for Dungeness crab in Kitimat Arm (◇) and False Creek (□).Upper and lower dashed lines indicate MB of 4 and 0.25, respectively. MB results between the dashed lines indicate BSAF predictions within a factor of 4 of observed average BSAFs.

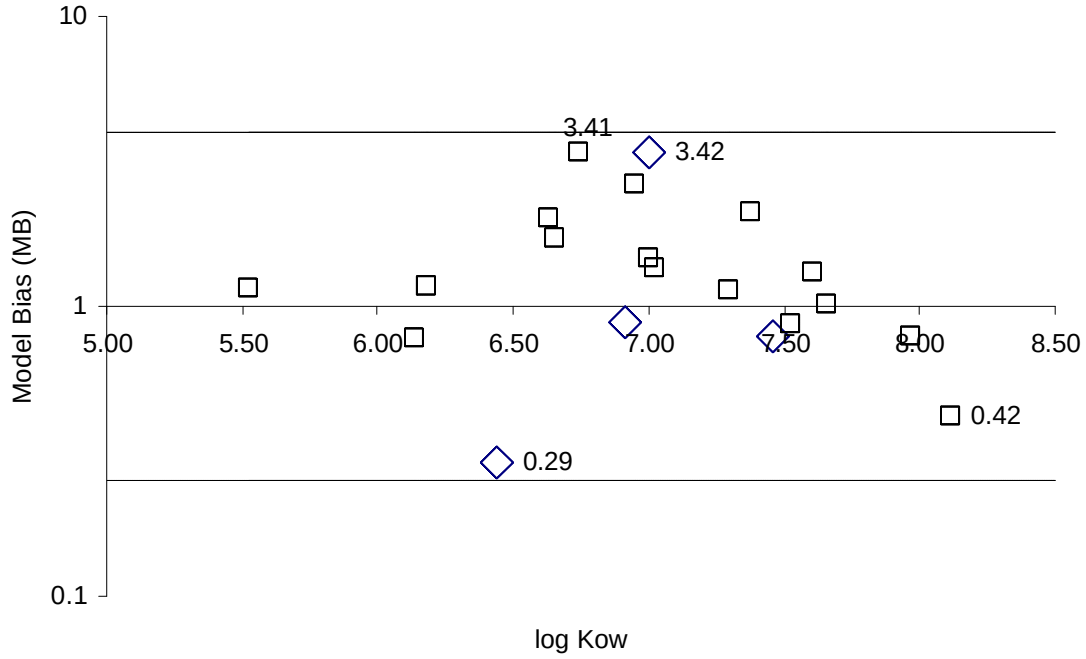

Figure 2-15: PCBs in fish species in False Creek – comparison of model-predicted BSAFs for juvenile flatfish (—) and small fish (---) to observed BSAFs for juvenile flatfish (□) and small fish (◇).

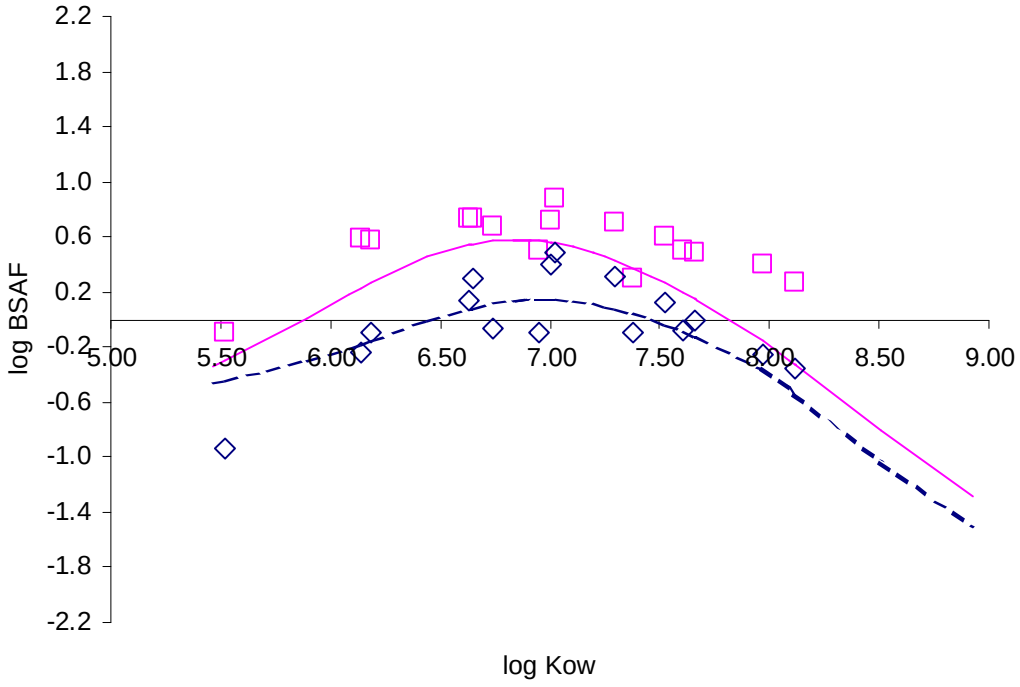

Figure 2-16: Model bias **(**MB) vs. log K_{ow} for juvenile flatfish (□) and small fish (◇) in False reek. Upper and lower dashed lines indicate MB of 4 and 0.25, respectively.

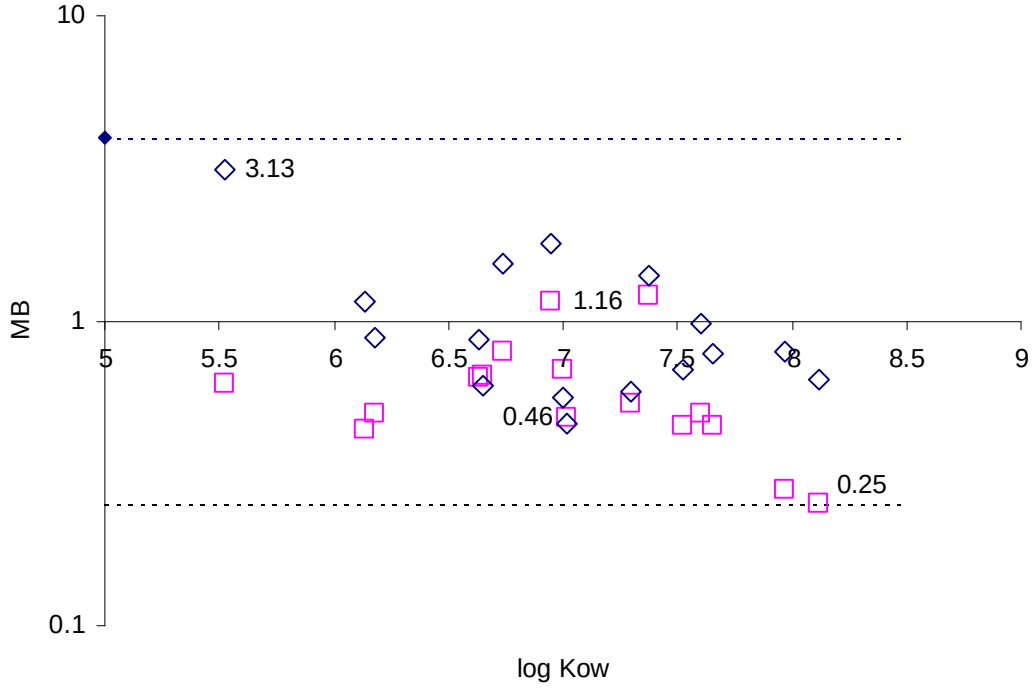

model bias (MB_{avg}) of 0.52 confirming the under-prediction described above. It is possible that the calibrated E_d relationship determined here may not accurately represent juvenile flatfish, due to a more developed digestive system in flatfish, relative to other trophic guilds, which could increase chemical absorption. This would cause BSAFs for higher K_{ow} PCBs to be underpredicted if the "true" E_d relationship for flatfish exhibits a less pronounced decline with increasing K_{ow}. While a higher proportion of ventilated porewater would increase predicted BSAFs for lower K_{ow} PCBs (i.e., below log K_{ow} of approximately 6.5), it is not expected to improve model performance above this value, where model BSAFs show incrementally more underprediction with an increase in log K_{ow}. Notwithstanding, this underprediction for juvenile flatfish does not have a large impact on the accuracy of model predictions for Dungeness crab because of the relatively low proportion of flatfish in the diet of this trophic guild.

For small fish, MB ranged from 0.43 to 3.3 indicating prediction of BSAFs within a factor of 3.3. MB_{avg} in small fish was 0.87 indicating a generally accurate representation of small forage fish in False Creek.

Large Epifauna

Predicted BSAFs for large epifauna were compared to observed BSAFs for brittle stars (*Aphiura filiformis and A. chiajei*) in the Baltic Sea (based on data presented in Gunnarsson and Skold, 1999; refer to Figure 2-17). While the model predictions are not directly applicable to the Baltic Sea, comparison to these data provides a "ballpark" indication of prediction accuracy.

In the Gunnarson and Skold study, sediments from coastal areas contained 3.24% organic carbon, roughly corresponding to that in False Creek, while offshore sediments contained 1.88% organic carbon, roughly corresponding to that in to Kitimat Arm.

In general, predicted BSAFs were within the range of those observed for brittle stars. MB ranged from 0.14 to 8.6 and MB_{avg} was 1.55, indicating some overprediction (refer to Figure 2-18). The larger range in MB, relative to fish and Dungeness crab is likely due to differing site-specific conditions for Baltic Sea brittle stars compared to Kitimat Arm and

Figure 2-17: PCBs in large epifauna –comparisons of model-predicted BSAFs for Kitimat Arm (—) and False Creek (---) to observed BSAFs for brittle stars from offshore (□) and coastal (◇) areas of the Baltic Sea. Observed BSAFs for offshore specimens correspond to Kitimat Arm whereas observed BSAFs for coastal specimens correspond to False Creek. Data source: Gunnarsson and Skold (1999)

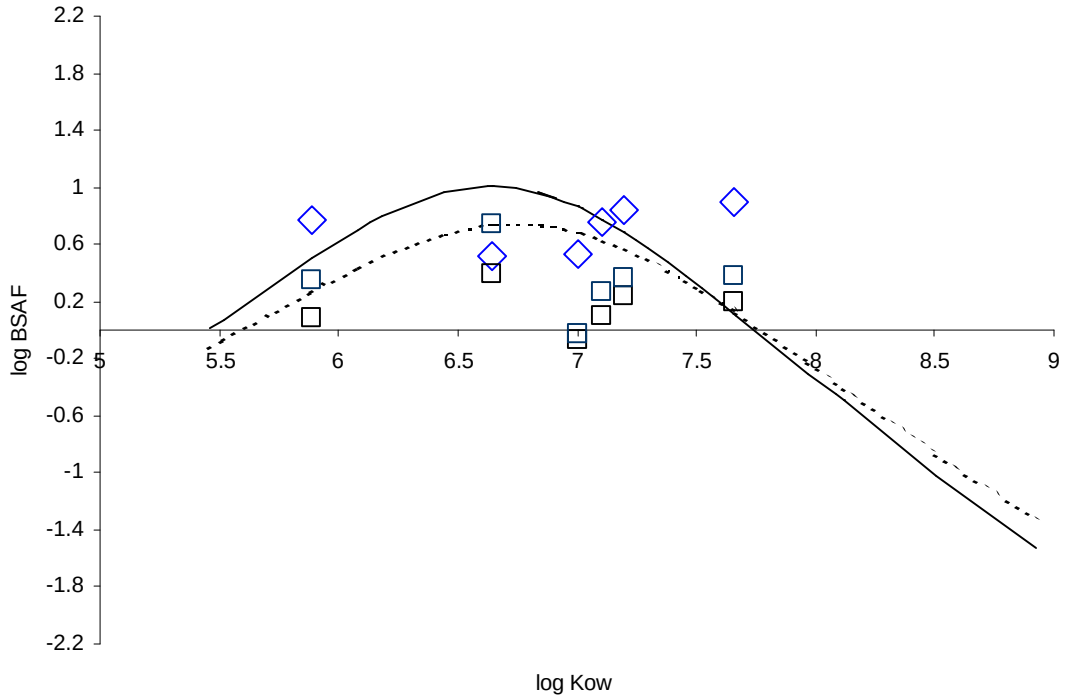

Figure 2-18: Model bias for large epifauna in Kitimat Arm (□) and False Creek (◇).

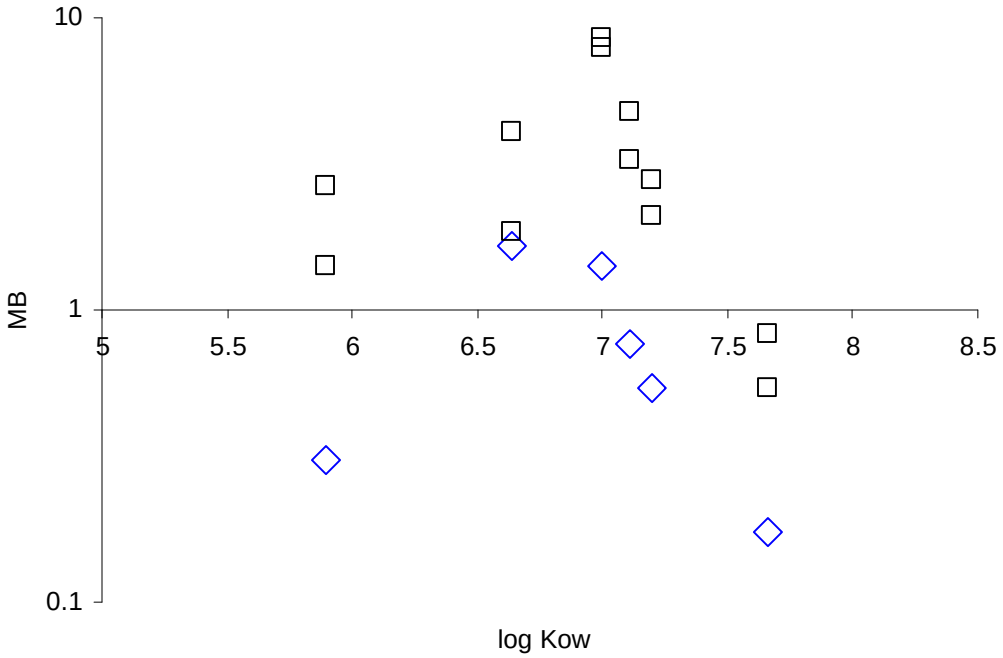

False Creek. Despite this larger range, the model predictions were considered to be reasonable for this trophic guild especially since it is meant to represent several organisms, and higher trophic levels will consume a variety of large epifauna, averaging out the uncertainty in predictions.

Large Infauna

Predicted BSAFs for large infauna in False Creek were compared to observed site-specific BSAFs for Manila clams and geoduck clams. Both are filter feeders, consuming a combination of phytoplankton and detritus. Kitimat Arm predictions were compared to data reported by Boese et al. (1995) for BSAFs in *Macoma nasuta*, a sediment-dwelling deposit feeder (refer to Figure 2-19). Predicted BSAFs for both False Creek and Kitimat Arm were intermediate between those observed for Manila clam and geoduck clam in False Creek, and *Macoma nasuta* in the study by Boese et al. (1995). Note that BSAFs predicted in False Creek were lower than those predicted in Kitimat Arm due to differences in sediment organic carbon content and a higher proportion of phytoplankton in the diet of large infauna.

The large infauna trophic guild in the model is intended represent a "composite" of both filter feeders and deposit feeders. Because of phytoplankton uptake kinetics and the expected sediment-water disequilibrium in aquatic systems, deposit feeders (i.e., consuming primarily sediment rather than phytoplankton) are expected to have higher dietary exposure to PCBs, potentially resulting in higher BSAFs than for filter feeders consuming primarily phytoplankton. Therefore, the model predictions that are intermediate between observed BSAFs for deposit feeders and filter feeders provide a reasonably accurate representation of this trophic guild, especially since Dungeness crab are likely to feed on a combination of deposit feeding and filter feeding bivalve mollusks.

MB for large infauna ranged from 0.39 to 7.6 (refer to Figure 2-20) indicating that model predictions were generally within an order of magnitude of observed values. MB_{avg} of 2.5 suggested over-prediction for large infauna. However, the calculation of MB_{avg} does not account for differences in sample size between organisms. Therefore, the larger data sets

Figure 2-19: PCBs in large infauna - comparison of model-predicted BSAFs for Kitimat Arm to laboratory-observed BSAFs for *Macoma nasuta* (◇; data from Boese et al., 1995) and comparison of model-predicted BSAFs for False Creek to observed BSAFs for Manila clams (△) and geoduck clams (□) from False Creek.

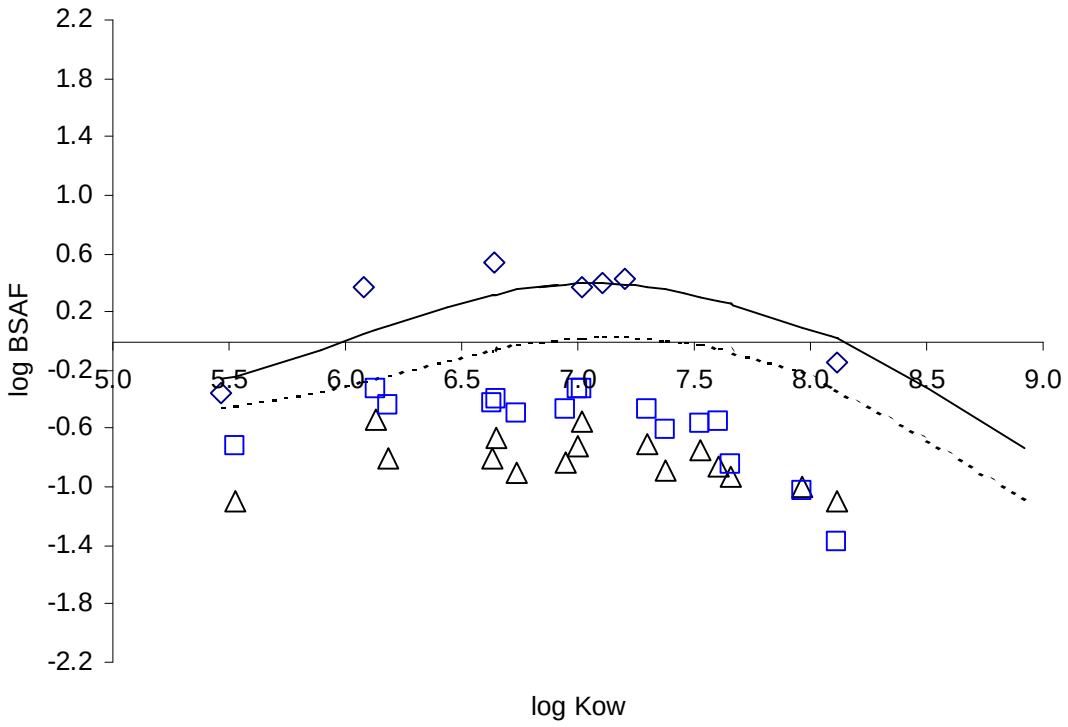

Figure 2-20: Model bias for large infauna in Kitimat Arm (◇, corresponding to *Macoma nasuta*; Boese et al., 1995) and False Creek (△, corresponding to Manila clams, □, corresponding to geoduck clams; Mackintosh and Maldonado, unpublished data).

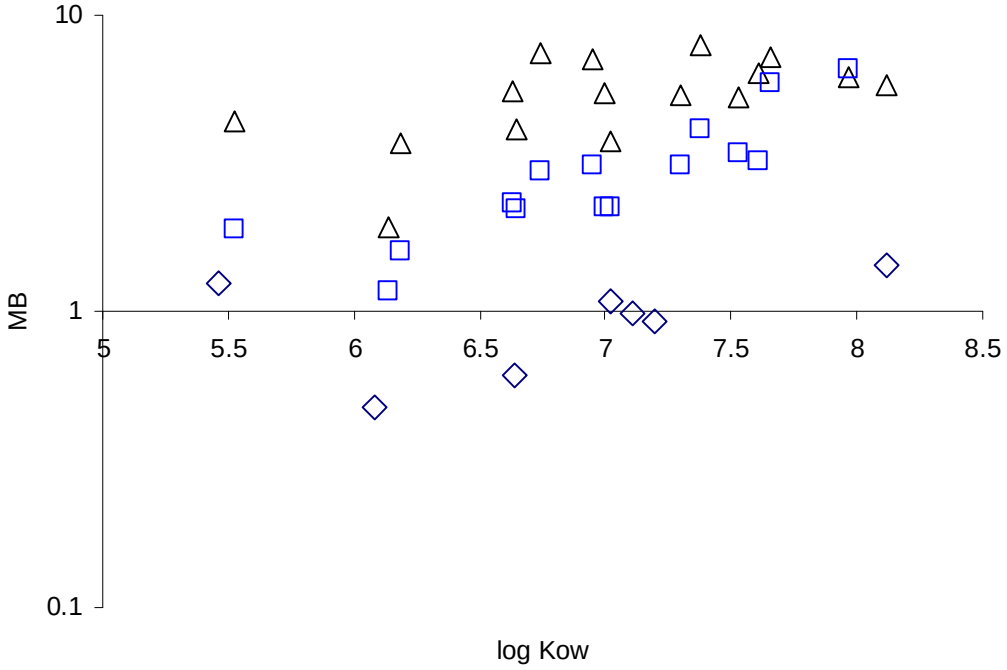

for Manila clam and geoduck clam, which are both filter feeders with BSAFs overpredicted by the model, may have caused MB_{avg} to be overestimated.

Small Infauna and Epifauna

BSAFs for small infauna and epifauna have not been determined in Kitimat Arm or False Creek. As a result, it was not possible to directly compare model predictions to observed data for this trophic guild. Tracey and Hansen (1996) compiled literature data for PCB BSAFs in benthic invertebrates. They found a median BSAF of 2.36 for the estuarine amphipod, *Hyallela azteca* and a range in median BSAFs of 1.37 to 3.71 for marine polychaetes. These values were based on a log K_{ow} range from 5.99 to 7.27. The model predicted maximum BSAFs of PCBs in small infauna and epifauna of 7.1 for Kitimat Arm and 3.6 for False Creek at log K_{ow} of 6.5. Thus, it appears that for False Creek BSAF predictions were within the range reported by Tracey and Hansen (1996) but for Kitimat Arm, BSAF predictions were higher than the reported range. In the absence of site specific data for small infauna and epifauna, it was not possible to confirm whether the model actually overpredicted BSAFs in Kitimat Arm. A small overprediction for Kitimat Arm would not have a large impact on BSAF predictions in higher trophic guilds since they feed on a range of lower trophic guilds, decreasing the effect of model uncertainty in any single trophic guild.

Phytoplankton and Zooplankton

There were no data to verify predicted concentrations in phytoplankton and zooplankton. Because of their association with the water column, bioaccumulation factors (BAFs) rather than BSAFs are most relevant for describing chemical accumulation in these organisms. Figure 2-21 presents predicted BAFs for these species. In general, the model predicts equilibrium with the water column for lower K_{ow} substances due to fast uptake and elimination kinetics. At higher K_{ow}, BAFs are lower than equilibrium predictions because slower kinetics increase the relative effect of growth dilution.

Figure 2-21: Comparison of predicted bioaccumulation factors (BAFs) for phytoplankton and zooplankton to the BAF predicted using equilibrium partitioning.

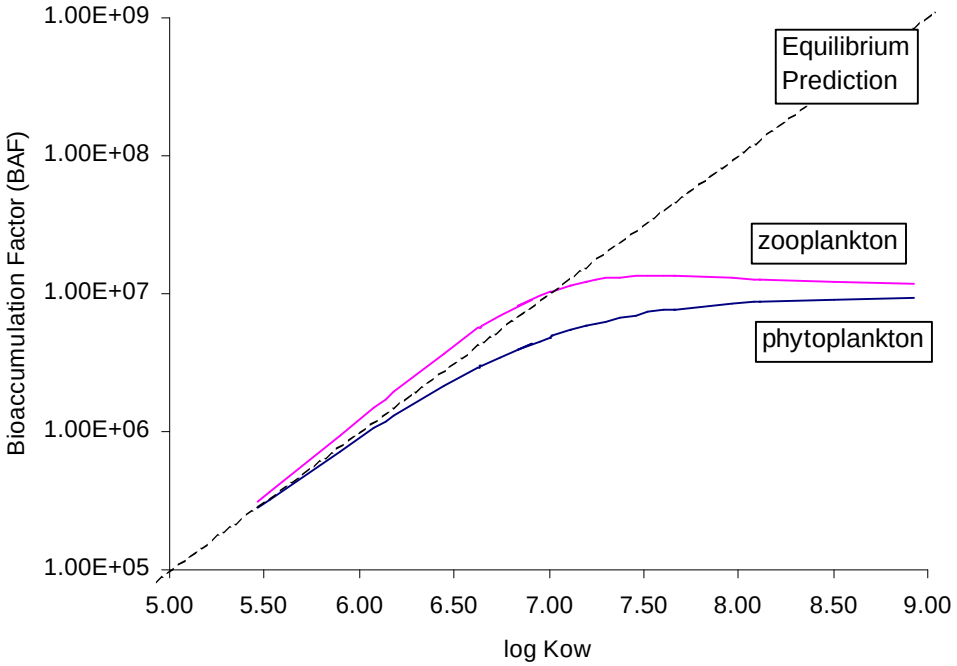

2.5 CONCLUSION

The preceding model development and calibration represents the application of mechanistic bioaccumulation modelling to important marine ecosystems of British Columbia. Testing of the model in two distinct systems lends support to the generality of the model. Further model testing in coastal ecosystems of the Northeast Pacific Ocean would verify its performance. While there are several published studies where researchers have validated the mechanistic approach in freshwater ecosystems (e.g., Gobas, 1993, Morrison et al., 1997, Thomann, 1989) it has had only limited application to marine benthic food webs (e.g., Connolly, 1991; Linkov et al., 2002). In addition, there are few, if any, published bioaccumulation models for ecosystems of the Northeast Pacific Ocean. The calibrated model provides a reasonably accurate representation of PCB bioaccumulation in benthic organisms with model-predicted BSAFs within a factor of four of observed values for Dungeness crab, the upper trophic-level receptor of interest.

The current model for predicting bioaccumulation in aquatic systems augments past modelling approaches (e.g., Thomann, 1989; Gobas, 1993 and Morrison et al., 1996; Morrison et al., 1997) by including additional mechanistic components that better represent processes at the organism and ecosystem level. The matrix approach to modelling steady state bioaccumulation is consistent with a currently proposed standardized methodology for food web modelling (Sharpe and Mackay 2002) It distinguishes between chemical accumulation from water, sediments and primary producers, and chemical accumulation due to predator-prey interactions, and also accounts for cannibalism within trophic levels. Thus, aggregation of species at lower trophic levels is possible, reducing the quantity of detailed species information and computational intensity that is necessary for representing each species individually.

One of the most significant obstacles to assessing bioaccumulation is the estimation of dissolved water concentrations of potentially bioaccumulative chemicals. The approach used here addresses this critical data gap by applying the sediment diagenesis model proposed by Gobas and Maclean (2003). The data inputs necessary for applying this model in two coastal ecosystems of BC were readily available from literature sources and

site-specific research of Kitimat Arm by Harris (1999). While Gobas and Maclean (2003) validated their model for large lake ecosystems, further research is necessary to validate this model in marine systems. Nevertheless, this approach is considered an improvement over the equilibrium partitioning model given the sediment-water disequilibrium that is observed in many systems.

The model developed here also includes revised methods for characterizing feeding and dietary uptake processes at the organism level. Studies by Gobas et al. (1999) and Gobas et al. (1993b) suggest that a thermodynamic gradient caused by digestion is the primary cause of food chain biomagnification. The digestion model uses current knowledge of dietary absorption efficiencies to quantitatively predict biomagnification factors that are specific to the dietary composition and digestive processes of modelled species. This is an improvement over Gobas (1993) who assumed a standard BMF of four for fish. The model calibration results highlight the need for further research in the area of dietary uptake efficiency. The calibration results suggest that a decline in E_d should occur at a log K_{ow} lower than that observed in laboratory studies with spiked food. This observation is supported by calibration results for bioaccumulation models in other systems. Thus, it is possible that either the current modelling approach needs refinement, or that the methods for measuring E_d do not accurately represent the “natural” situation; these are both potential areas of further study.

The current model applies the equations described by Connolly (1991) to link food quality, food assimilation efficiency and organism bioenergetics to food intake rates. To my knowledge, the Connolly (1991) equations have not been applied to derivatives of the Gobas (1993) model, which provided the basis for the model developed here. In higher aquatic trophic levels such as predatory fish, the energetic content of food is expected to remain relatively constant among different systems, and generalizations about feeding rates can be based solely on environmental factors such as temperature. In contrast, food quality for aquatic detritivores is highly dependent on the productivity of the system and resulting organic-carbon content of sediments. In benthic food chains, detritivores provide the initial link between the biotic food web and abiotic sediments. Accurate

representation of the dietary flux for detritivores is therefore essential for developing a model which is applicable in multiple systems with differing productivity. The model performance in both Kitimat Arm and False Creek, demonstrates the ability of the model to respond to differences in detrital organic carbon.

This simple bioenergetic model should be considered a first step to incorporating organism ecology and bioenergetics into bioaccumulation models. Currently, the respiration rate in the feeding submodel (an indication of energy usage) is not directly linked to the oxygen consumption rate in the gill ventilation submodel (also an indication of energy usage for organisms that use primarily aerobic metabolism). Thus, the model could be improved by quantifying the degree of aerobic and anaerobic metabolism in the benthic species, facilitating the development of a bioenergetic model which integrates gill ventilation, feeding rates, and growth based on ecosystem conditions and organism bioenergetics. The compartmentalized approach to bioaccumulation modelling, which has been conducted to date, tends to ignore the interdependence of these processes. While these processes have been studied extensively in numerous aquatic species, to my knowledge there are few simple bioenergetic models with direct, easy application to the practice of bioaccumulation modelling.

The result of adding these mechanistic components is a model that accurately represents BSAFs in two different systems of the BC Coast, without site-specific calibration. The applicability of the model to different systems suggests that ecosystem factors affecting BSAFs are accurately described by the model.

Despite these improvements, it is important to consider the limitations of the modelling approach. Because of the steady-state assumption, the BSAF model does not capture the dynamic nature of natural systems but rather provides an average representation of chemical bioaccumulation. Microscale processes affect chemical concentrations in sediments, and mobile organisms such as fish and crustaceans are expected to have variable exposure as they move and forage throughout their range. Therefore, in natural

systems, BSAFs will vary in time and space according to the habits of organisms and spatial and temporal variability in the abiotic environment.

There is generally higher uncertainty in model predictions at lower trophic levels. Potential causes of this uncertainty include the aggregation of species in lower trophic levels and less knowledge of organism processes in lower trophic levels, requiring more assumptions for model parameters. Thus, conclusions regarding PCB bioaccumulation for these lower levels may have less validity. However, BSAFs predictions for Dungeness crab are still relatively accurate because their consumption of multiple trophic levels and on multiple organisms within a trophic level averages out this uncertainty. Thus, the observed under-prediction and over-prediction for individual species at lower trophic levels does not appear to prevent accurate predictions at higher trophic levels.

An increase in mechanistic components also increases the inputs necessary to parameterize the model. This is the primary limitation of an increase in model complexity. As the number of parameters increase, the potential for error propagation through the model also increases. The digestion and feeding models require accurate estimates of food absorption efficiencies and respiration rates. Where species-specific data do not exist it is necessary to extrapolate from other species, increasing the uncertainty in chosen parameters. In addition, more parameters generally require more time and resources for model development.

Consequently, the detailed approach used here is most appropriate when there is adequate knowledge of the system and organisms being modelled, and the potential benefits of the research offset the large cost of doing so. The development of detailed models is especially important for examining how specific processes, such as the biotransformation of persistent organic pollutants, affect their bioaccumulation.

3 DEVELOPMENT OF A BIOACCUMULATION MODEL FOR PAHS AND PAH METABOLITES IN THE BENTHIC FOOD WEB OF KITIMAT ARM.

3.1 INTRODUCTION

A significant challenge to assessing the ecological and human health risks posed by persistent organic pollutants in marine systems is the quantification of food chain bioaccumulation and resultant ecological effects for chemicals that are metabolized in various ways and at variable rates by marine organisms. Bioaccumulation models such as the one developed in the previous chapter have had success at demonstrating the mechanisms leading to the food web biomagnification of persistent hydrophobic chemicals such as PCBs (e.g., Connolly, 1991, Morrison et al., 1997). For PAHs, an important factor that can modulate bioaccumulation in aquatic organisms is metabolism and subsequent metabolite elimination (James, 1989; Varanasi et al., 1989a; Meador et al., 1995). In addition, there is growing evidence suggesting that pyrogenic PAHs (i.e., those originating from smelting processes) have decreased bioavailability due to slow desorption from, and sequestering in, soot carbon (Gustaffson et al., 1997; Jonker and Koelmans, 2002)

Both of these processes are expected to reduce bioaccumulation and resultant BSAFs for parent PAHs, relative to non-metabolized substances that are not soot-associated. Tracey and Hansen (1996) summarized BSAFs for hydrophobic chemicals and found mean BSAFs of 0.29 for PAHs in benthic invertebrates, as opposed to 2.1 for PCBs in benthic invertebrates and fish, and 2.69 for pesticides in benthic invertebrates in fish. Gewurtz et al. (2000) compared the dynamics of PAHs and PCBs in benthic invertebrates of Lake Erie and found that BSAFs for PAHs were inversely related to K_{ow}, suggesting metabolism at higher K_{ow}. BSAFs for higher K_{ow} PAH congeners were generally one to two orders of magnitude lower than PCB congeners with a similar K_{ow}. Parkerton (1993) compiled BSAF data for several hydrophobic compounds and found a similar decrease in BSAFs with increasing K_{ow}, for high K_{ow} compounds. He also suggested that BSAFs for PAHs in fish have generally not been reported in the literature due to very low bioaccumulation in fish.

Harris (1999) reported BSAFs for PCBs and PAHs in Dungeness crab from Kitimat Arm. Although highly variable, BSAFs for PAHs were approximately 3 to 4 orders of magnitude lower than BSAFs for PCBs, and lower than literature-reported PAH BSAFs. PAHs in Kitimat Arm are smelter-derived and exhibit lower BSAFs relative to PCBs, and relative to PAHs in other literature studies. The lower BSAFs are likely due to a combination of metabolism and low bioavailability.

Lower contaminant bioavailability is expected to reduce organism exposure and bioaccumulation, lowering the potential for ecological and human-health risks. In contrast, metabolism occurs only as an elimination process once a chemical has been absorbed into the organism. Thus, the influx of chemical into the organism, and outflux of chemical and metabolites will affect the likelihood of adverse effects from chemical exposure and the accumulation of parent chemical and metabolites in tissues. While metabolism is an important detoxification and elimination route, metabolic transformation of PAH often creates reactive metabolic intermediates that are more toxic than the parent compounds, causing hepatic disease, carcinogenesis and biochemical stress in fish and invertebrates (Fossi et al., 1997; Baumann, 1989). In addition, studies in laboratory mesocosms indicate that slow elimination and dietary uptake of Phase I PAH metabolites can potentially cause trophic transfer of biotransformed compounds (Kane-Driscoll and McElroy, 1997).

Thus, while PAH metabolism results in lower measured body burdens of parent congeners, it produces the reactive intermediates that cause the toxicity of PAH compounds. Accumulation of metabolites via parent PAH transformation and trophic transfer may result in a potential for a toxic effect that is independent of the body burden of parent chemical in higher trophic level organisms. An understanding of the processes of accumulation and metabolism of PAH in the marine benthic food web is important to more accurately assess ecological and human health risks from PAH-contaminated sediments in Kitimat Arm. The development of a mechanistic model for these processes can serve to integrate the current knowledge of PAH metabolism and highlight important uncertainties. While Van der Linde et al., (2001) examined PAH metabolism using a

bioconcentration model and laboratory data, few studies have quantitatively examined metabolism in natural situations using a food web bioaccumulation model and field data.

In this chapter, I apply the model developed in Chapter 2 to explore how soot association and metabolic transformation affect the bioaccumulation and food web dynamics of seven PAH congeners - phenanthrene, anthracene, pyrene, fluoranthene, chrysene, benz(a)anthracene, and benzo(a)pyrene. First, I develop a conceptual model for organism-level metabolism and develop a metabolism sub-model for each organism. I then parameterize the sub-model equations and discuss important uncertainties regarding the processes of PAH metabolism and elimination. By comparing the field-measured dynamics of PCBs and PAHs in Kitimat Arm, it is possible to evaluate the performance of the model which has been modified to include soot-carbon partitioning and literature derived metabolic rates for PAHs. Once the Phase I metabolic rates are known, the model is useful as an evaluative tool to examine the mass balance of PAH metabolites and explore the implications for ecological and human health risk assessment.

3.2 MODEL THEORY

3.2.1 Overview of Processes Affecting Bioaccumulation of Parent PAHs and PAH Metabolites

PAH Bioavailability

An important factor that may limit the bioavailability of PAHs in Kitimat Arm is their association with smelter-derived soot carbon. PAH compounds and soot carbon are produced simultaneously as byproducts of the high-temperature smelting process, resulting in strong associations (i.e., sorption and encapsulation) between them. Once associated with soot carbon, the smelter-derived PAHs may be less available for equilibrium desorption than PAHs sorbed in amorphous organic carbon, especially at the much lower temperature in the environment, relative to that during pyrogenesis.

Gustaffson et al. (1997) hypothesized that the net effect of this strong association would be an increase in the partitioning coefficient from soot carbon to water, to a level higher than that for octanol to water (i.e., K_{ow}). The higher partition coefficient for PAHs in soot

carbon provides a reasonable approximation of the expected slower desorption behaviour in water because of the strong associations formed at high temperature. Higher partition coefficients for desorption processes will lower the expected dissolved water concentrations, reducing the amount of chemical available for uptake from this medium.

Although there have been no studies of the dietary bioavailability of soot-associated PAH, the uptake of chemical from the soot carbon is expected to be very low, because detritivores are unlikely to digest this matrix in ingested sediments.

These processes affecting the bioavailability of PAHs in water and in the diet have important impacts on the exposure of benthic organisms to PAHs.

PAH Metabolism

Bioaccumulation of hydrophobic chemicals depends on the chemical mass balance that results from uptake and elimination processes, as discussed for PCBs in Chapter 2. Once absorbed, metabolic transformation is the most important route of elimination for most PAH compounds since their chemical properties (i.e., log K_{ow} > 4) cause these compounds to be eliminated slowly through other routes. The mass balance of PAH metabolites is also potentially important because these metabolic products have the potential to cause toxic effects. Figure 3-1 presents a conceptual diagram of the organism-level processes of parent PAH uptake and depuration, and PAH metabolite formation, uptake and depuration.

Figure 3-2 describes how biotransformation of PAH compounds occurs through two primary stages: Phase I (functionalization) and Phase II (conjugation). (Livingstone 1991, Livingstone,1992, James, 1989). Phase I metabolism involves the action of a Cytochrome P-450 mixed function oxidase (MFO). MFO is generally universally distributed among higher organisms (Livingstone 1992) with its activity paralleling the overall metabolic activity of a particular organism. The primary action of Phase I metabolism is the introduction of functional groups (i.e., -OH, -NH2, -COOH) into the PAH compound. For

Figure 3-1: Conceptual diagram of the uptake, production and elimination of parent PAHs and Phase I metabolites of PAH in benthic organisms.

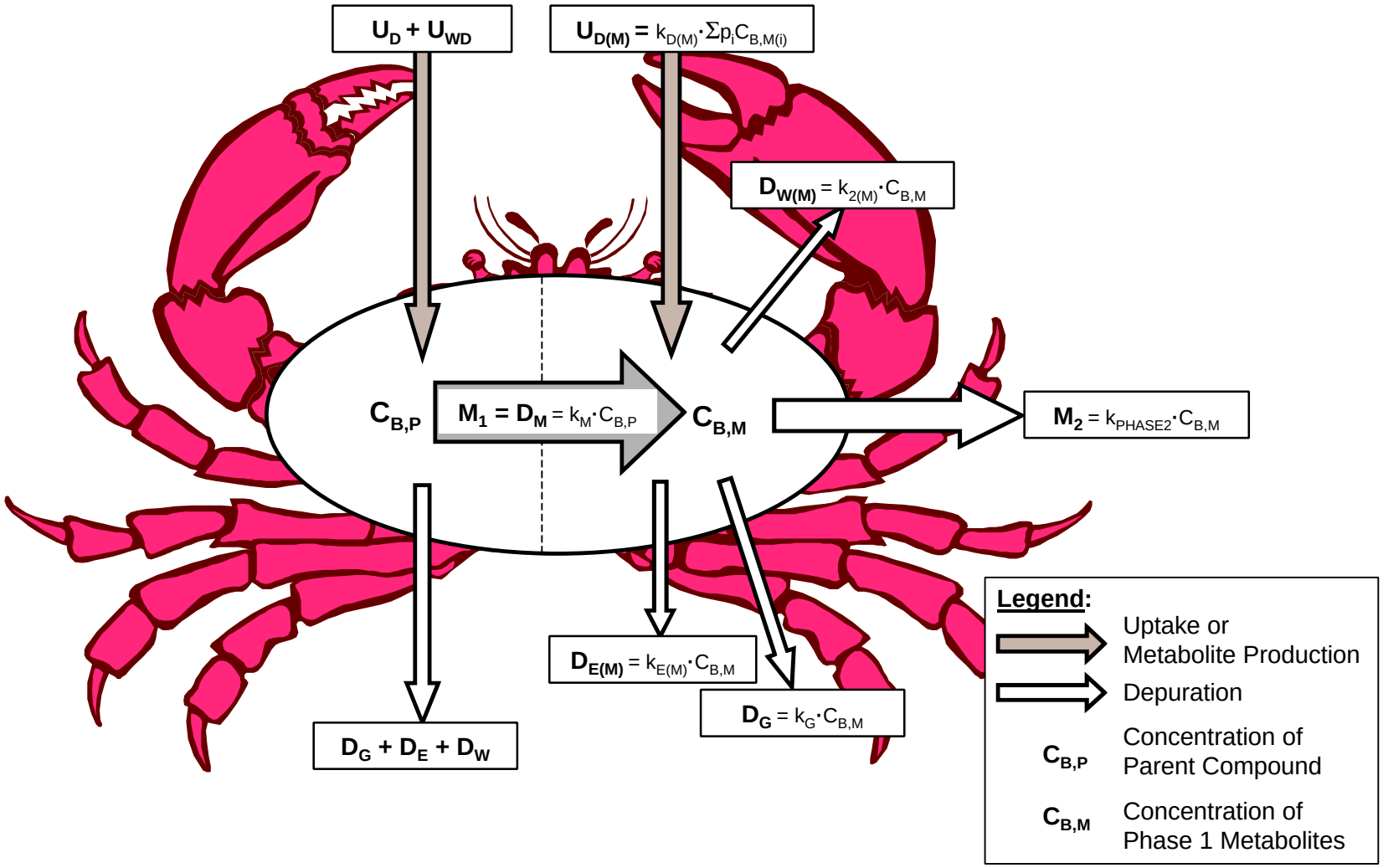

Figure 3-2: Conceptual diagram of the pathways of PAH metabolism and metabolic activation.

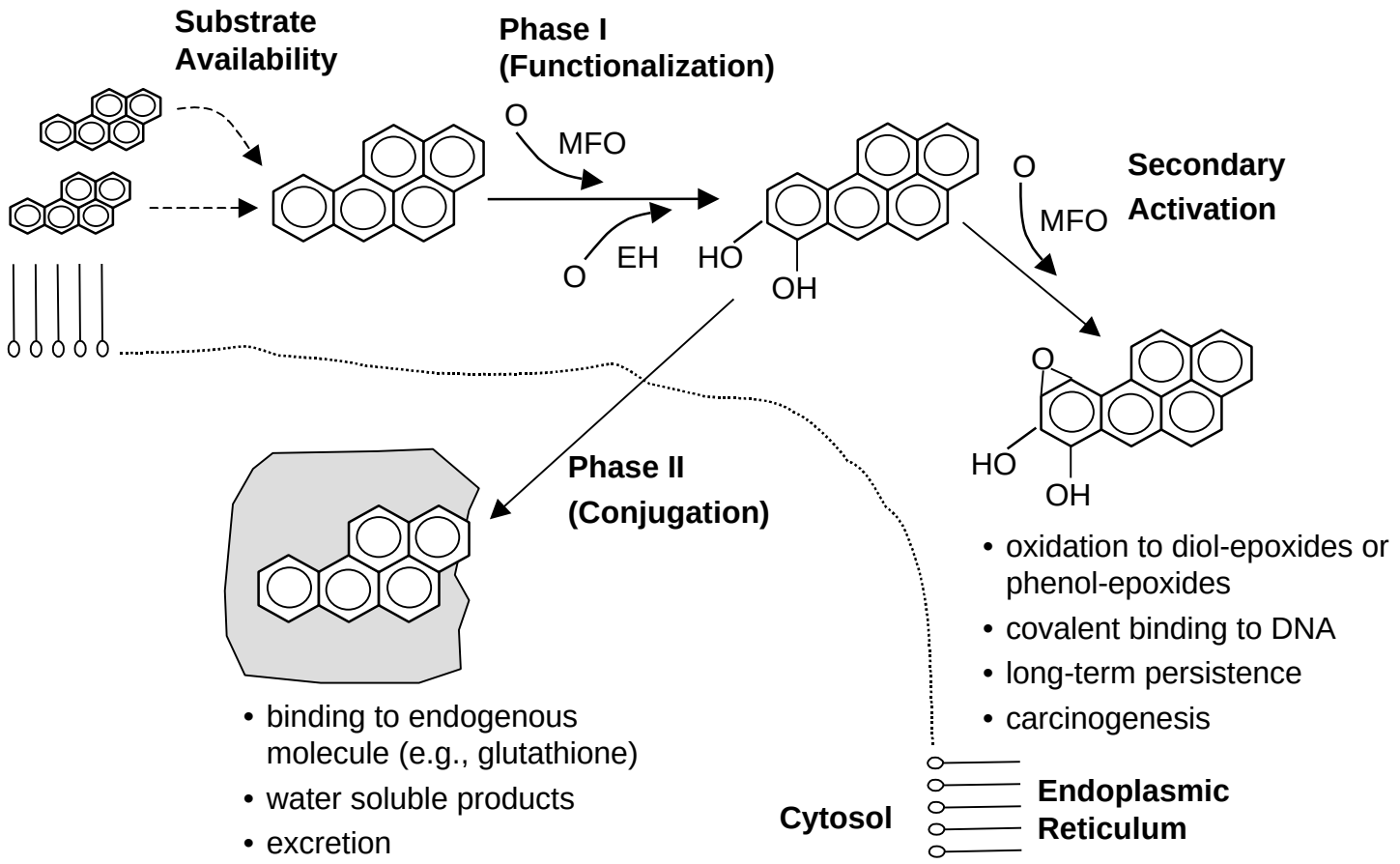

MFO - mixed function oxidase

EH - epoxide hydroxylase

example, two common products of MFO action on benzo(a)pyrene are 3-hydroxy-benzo(a)pyrene (substituted with –OH in the "3" position) and the *proximate carcinogen* trans 7,8 dihydrodiol-benzo(a)pyrene (substituted with –OH in the "7" and "8" position) (Livingstone, 1991). Introduction of the functional group prepares the molecule for conjugation reactions involved in Phase II metabolism.

Alternatively, unstable products of Phase I metabolism may undergo secondary oxidation to diol-epoxides or phenol-oxides, both of which are the ultimate carcinogenic products of PAH metabolism. These electrophilic compounds can potentially form covalent adducts with cellular macromolecules such as DNA, a process that may lead to carcinogenesis (Reichert et al., 1998). Carcinogenesis is the first step in hepatic disease in fish and marine invertebrates, potentially leading to neoplasia, tumours, and ecological impairment (for a review see multiple chapters in Varanasi, 1989).

Phase II metabolism involves the conjugation of the reactive intermediate with endogenous molecules to form water soluble products that are more easily excreted. For example, activated PAH compounds are often conjugated with glutathione via glutathione-S-transferases (Livingstone, 1991). Overall, Phase I metabolism produces most of the carcinogenic metabolic products of PAH whereas Phase II metabolism is the primary detoxification mechanism for PAH compounds. The key factor affecting the likelihood of DNA adduct formation is the relative rates of conjugation by Phase II enzymes and secondary oxidation by MFO (Varanasi et al., 1989a). Thus, if Phase II processes are absent or ineffective, Phase I processes can lead to high body burdens of reactive, Phase I metabolites and a high potential for toxic effects in marine organisms (James, 1989).

An important limiting factor for PAH metabolism may be the potential for high K_{ow} PAHs to partition into a more stable lipid compartment over long term exposures (Boehm and Quinn 1977). Partitioning to the lipid compartment could limit the availability of PAH substrates for Phase I metabolism. Therefore, a more accurate representation of the chain of events in metabolism is: (i) substrate availability, (ii) Phase I metabolism

(addition of a functional group) and (iii) Phase II metabolism (conjugation) (Livingstone 1991). Given that MFO acts on the "bay" region of PAH molecules (McElroy et al. 2000) and that the affinity of MFO for PAH substrates is believed to depend on the presence or absence of this region, Phase I metabolic rates for PAH with similar structures may also be comparable. However, factors affecting the availability of PAHs such as the chemical fugacity (i.e., thermodynamic pressure or escaping tendency) within the lipid compartment may also be a key limiting factor for Phase I metabolism.

Substrate availability may have larger relative effect in more developed organisms with high metabolic capacity, because lack of available PAH substrates limit the rate of PAH biotransformation by the MFO system. Limitation of substrate availability would have a normalizing effect on realized rates of metabolism, reducing the range of in vivo PAH biotransformation rates between organism with high and low activities of metabolizing enzymes.

Trophic Transfer of PAH Metabolites

In two recent reviews of PAH biotransformation in marine invertebrates, Meador et al. (1995) and Livingstone (1991) both suggest that the elimination rate of polar metabolites of PAH compounds will be slower than the rate for parent compounds. Potential explanations for slower elimination include covalent binding to cellular macromolecules or a decreased ability of conjugated polar compounds to diffuse through lipid membranes. In addition, Meador et al. (1995) suggests that the primary elimination route for PAH metabolites is via excretion to bile or excretion through the kidneys and this is generally made possible by Phase II conjugation. Thus, Phase II metabolism is the key process for initiating metabolite elimination.

Kane-Driscoll and McElroy (1997) examined elimination of benzo(a)pyrene and metabolites in two species of marine polychaete, *Marenzellaria viridis* and *Nereis diversicolor.* The results of this study showed that aqueous (i.e., conjugated) and residual (i.e. covalently bound) metabolites were eliminated very slowly by these species. For polar metabolites (i.e., from Phase I reactions), *M. viridis* showed very little elimination whereas in *N. diversicolor,* polar metabolites were eliminated at a rate similar to that of

parent compound. The authors concluded that slow elimination of PAH metabolites may result in higher steady state body burdens along with a higher potential for trophic transfer.

McElroy et al., (1991) conducted both oral and intramuscular exposures of winter flounder to parent benzo(a)pyrene and metabolite mixtures produced by polychaete worms, and benzo(a)pyrene-7,8 –dihydrodiol (a proximate carcinogen of benzo(a)pyrene). The results of this study indicated that the measured uptake of Phase I metabolites from a dietary source was lower than that of parent benzo(a)pyrene and may have been reduced by rapid conjugation reactions (i.e., detoxification) during absorption. Normalization of DNA adduct formation to the dose reaching target organs indicated that metabolites were equally active as parent compound. Thus, the authors concluded that benzo(a)pyrene metabolites were also able to enter metabolic cycles and initiate carcinogenesis in winter flounder.

While there is some uncertainty in the factors affecting absorption and elimination of PAH metabolites, trophic transfer of metabolites is a potentially important process for PAHs. Therefore, marine food web models for PAH should also account for the mass balance of metabolites within organisms and potential metabolite transfer among trophic levels. Although metabolism will reduce the concentration of parent compound in prey items, it may not reduce the total load of PAH + metabolites. Given that metabolites initiate carcinogenesis in marine organisms, it is possible that the potential for a toxic effect transfers through successive trophic levels, even if parent compound does not. The model development and application that follows is intended to evaluate this possibility.

3.2.2 Model of Parent PAH Bioaccumulation

Bioaccumulation of parent PAH compounds in individual organisms is expected to follow a process similar to PCBs, as described by the following general equation:

$$C_{B,P} = \frac{k_1 \cdot C_{WD} + k_D \cdot \Sigma p_i C_i}{k_2 + k_E + k_M + k_G} \qquad [35]$$

Where $C_{B,P}$ (g/kg) is the concentration of the parent PAH congener in the organism (other terms are defined in Chapter 2). Because PAHs are metabolized by marine organism, k_M plays a significant role in elimination of parent PAHs, resulting in lower steady state body burdens of parent chemical relative to non-metabolized chemicals with similar properties. For PAHs, k_M is assumed to represent the Phase I metabolic pathway only. Thus, biotransformation and the resultant reduction in the concentration of parent PAHs is dependent only on the rate of Phase I metabolism, and is independent of Phase II conjugation or secondary activation.

3.2.3 Mass Balance Model for Phase I Metabolites of PAH

Given that Phase I metabolites are implicated in carcinogenesis, characterizing the mass balance of Phase I metabolites is useful for assessing the risk of metabolite-induced toxic effects. Total accumulation of Phase I metabolites will depend on processes which increase the metabolite concentration in the organism (metabolism of parent compound and dietary uptake) and processes which decrease the chemical concentration in the organism (i.e., excretion of chemical from tissues, increase in the mass/volume of tissues, and Phase II conjugation of metabolites; refer to Figure 3-1). Thus, the mass balance of Phase I metabolites can be represented as:

$$dC_{B,M}/dt = M_1 + U_{D(M)} - D_{W(M)} - D_{E(M)} - D_G - M_2 \qquad [36]$$

where $dC_{B,M}/dt$ is the rate of change (increase or decrease) of the Phase I metabolite concentration in the organism (g/kg/day), M_1 represents the Phase I production of metabolites via biotransformation of parent chemical (g/kg/day) and is equal to D_M in Equation 2; $U_{D(M)}$ represents the uptake of Phase I metabolites from the diet (g/kg/day), $D_{W(M)}$ is the elimination of Phase I metabolites to water (g/kg/day), $D_{E(M)}$ is the elimination of Phase I metabolites via fecal egestion (g/kg/day), D_G is the depuration via growth dilution (g/kg/day) and M_2 is the elimination of Phase I metabolites via Phase II conjugation (g/kg/day). Conjugation changes the nature of metabolites so that they will no longer react to form DNA adducts, assuming that de-conjugation and re-entry into Phase I pathways is negligible. Thus, Phase II metabolism was assumed to represent elimination of potentially toxic Phase I metabolite.

Figure 3-1 demonstrates how metabolite accumulation and elimination processes can be represented as the product of a 1st-order rate constants and the concentrations in relevant media. Under steady state conditions where $dC_{B,M}/dt = 0$, and with substitution of the terms from Figure 3-1, Equation 36 rearranges to:

$$C_{B,M} = \frac{k_M \cdot C_{B,P} + k_{D(M)} \cdot \Sigma p_i C_i}{k_{2(M)} + k_{E(M)} + k_{phase2} + k_G} \qquad [37]$$

where $C_{B,M}$ (g/kg) is the steady-state concentration of Phase I metabolites in the organism, k_M is the rate constant for Phase I metabolism; $C_{B,M}$ is the concentration of parent chemical in the organism (g/kg); $k_{D(M)}$ is the rate constant for uptake of Phase I metabolites from the diet, $\Sigma p_i C_i$ represents the weighted average concentration of Phase I metabolites in food (i.e., C_i weighted by the proportion of that prey item in the diet, p_i); and $k_{2(M)}$, $k_{E(M)}$, k_{phase2} and k_G are rate constants for metabolite elimination via gill excretion, faecal egestion, Phase II conjugation and growth dilution, respectively. Equation 37 is analogous to Equation 4 except that metabolic production of Phase I metabolites ($k_M \cdot C_{B,P}$) replaces the term for uptake from water.

Again, a steady state approach is employed based on the discussion in Chapter 2. Metabolism of PAH and PAH metabolites will cause faster elimination of these chemicals, decreasing the time needed to achieve steady state. Hence, the steady state assumption is appropriate for PAHs in the same fashion as that for PCBs.

As with the food web bioaccumulation of PCBs and parent PAHs, the steady state dynamics of Phase I metabolites can be represented as a system of equations, with one equation for each trophic guild in the food web. These equations can then be rearranged to matrix form and solved according to the method described in Chapter 2.

Phase I Metabolism (k_M)

A 1st-order rate constant is used to characterize metabolism of parent PAHs resulting in production of Phase I metabolites. k_M in Equation 37 is equal to k_M in Equation 4 since they both refer to the conversion of parent chemical to metabolites.

Enzyme catalyzed reactions in organisms are often described by Michaelis-Menten kinetics with maximum rate constants for metabolite production occurring at low substrate concentrations but a saturation effect decreasing the rate constants at higher substrate concentrations. For PAH, substrate availability (i.e., of parent chemical) is expected to be rate limiting for *in vivo* biotransformation rather than the enzyme concentration in the *in vitro* situation (De Maagd et al. 1998a). At environmental doses, PAHs are expected to be present at much lower concentrations than endogenous molecules that are metabolized by MFO. In addition, the lipophilic nature of parent PAHs means that diffusion from lipid may further limit substrate availability. Therefore, a 1st-order rate constant, where the metabolic rate is a linear function of the parent PAH concentration, is assumed to adequately represent biotransformation of PAH at environmental doses.

Dietary Uptake ($k_{D(M)}$)

Phase I metabolites are expected to be available for dietary uptake as prey are digested. Therefore, $k_{D(M)}$ can be characterized by as a 1st-order rate constant similar to that for other hydrophobic chemicals such as PCBs.

A few authors (Livingstone, 1991; Meador et al., 1995) have suggested that polar PAH metabolites may exhibit slower diffusion from water into lipid, resulting in lower dietary uptake efficiencies (E_d) for these chemicals. In contrast, the addition of hydroxyl groups in Phase I metabolism lowers metabolite K_{ow}, and is expected to facilitate faster diffusion out of the gut contents into the gastrointestinal juices. The lipid-to-water desorption process is expected to be the rate limiting step for E_d, resulting in lower E_d as K_{ow} increases because higher K_{ow} substances exhibit slower diffusion into aqueous phases (Gobas et al., 1988). Thus, the calibrated E_d-K_{ow} relationship from Chapter 2 was assumed to also apply to Phase I metabolites of PAHs.

Elimination to Water ($k_{2(M)}$)

Metabolite elimination to water is assumed to occur via diffusion, similar to the parent chemical, and is represented by a 1st-order rate constant. However, the BCF is expected to change because of the lower K_{ow} of PAH metabolites. Gobas (1987) describes how E_w involves diffusion via both aqueous and lipid phases. At log K_{ow} greater than approximately 3, E_w is limited by resistance in water phases and remains constant with K_{ow}. Below this threshold, limitation by the lipid phase becomes more significant, lowering E_w. Assuming that resistance at the water-lipid interface is negligible, the lower K_{ow} of Phase I PAH metabolites will result in an E_w that is either equal to (if metabolite log K_{ow} is still above 3), or lower than that for parent compound (if metabolite log K_{ow} is below 3).

Faecal Egestion ($k_{E(M)}$)

Faecal egestion for Phase I metabolites is expected to occur via a similar process to parent compounds with $k_{E(M)}$ depending on G_f, E_d and K_{BF}. Note that E_d and K_{BF} are expected to be different for metabolites relative to parent compounds as a result of the lower metabolite K_{ow}.

Phase II Metabolism (k_{phase2})

As with Phase I metabolism, Phase II metabolism is also described by a 1st-order rate constant. Enzyme activities for Phase II reactions are generally higher than for Phase I reactions. These faster rates should keep substrate concentrations (i.e., of Phase I metabolites) at levels below which enzyme saturation begins to occur. Therefore, a 1st-order rate constant provides an accurate representation of the rate of Phase II metabolism under these conditions.

k_{phase2} is treated as an elimination term for the metabolite mass balance because Phase II metabolism converts the metabolites to non-toxic conjugates. Thus, k_{phase2} represents a reduction in the body burden of the toxic Phase I metabolites which are of interest for ecological risk assessment.

Growth Dilution (k_G)

The process of growth dilution is independent of the chemical species because it represents a volume increase rather than chemical removal or transformation. Therefore, k_G for PAH metabolites is the same as k_G for parent compound and other chemicals.

3.2.4 Soot Carbon Partitioning and Bioavailability

Sediment/Water Disequilibrium

When soot carbon is not present in sediments, the steady-state sediment-to-water distribution coefficient (K_d) for overlying water can be represented through a rearrangement of Equation 28 as:

$$K_d = C_s/C_{wd} = K_{ow} \cdot 0.35 \cdot \phi_{oc} \cdot DF_{ss} \qquad [38]$$

Where K_d is the sediment-to-water distribution coefficient (unitless), C_s is the chemical concentration in bottom sediments or suspended sediments (g/kg), C_{wd} is the dissolved chemical concentration in water (g/kg), ϕ_{oc} is the fraction of organic carbon in bottom sediments or suspended sediments and DF_{ss} is the sediment-water disequilibrium factor (unitless, described in Chapter 2). Likewise, for sediment porewater which is assumed to be in equilibrium with bottom sediments DF_{ss} is omitted such that:

$$K_d = C_s/C_{wd} = K_{ow} \cdot 0.35 \cdot \phi_{oc} \qquad [39]$$

These equations represent either steady state partitioning (i.e., accounting for plankton dynamics) or equilibrium partitioning to organic carbon in bottom sediments. In order to account for the stronger binding of pyrogenic PAHs within soot carbon, Gustaffson et al. (1997) proposed that a second term, representing soot carbon partitioning, be added resulting in the following equation for the case of equilibrium partitioning:

$$K_d = C_s/C_{wd} = K_{ow} \cdot 0.35 \cdot \phi_{oc} + K_{sc} \cdot \phi_{sc} \qquad [40]$$

Where ϕ_{sc} is the fraction of soot carbon in bottom sediments or suspended sediments. For overlying water where the steady-state disequilibrium factor is applied to account for plankton dynamics, K_d is then calculated as:

$$K_d = C_s/C_{wd} = K_{ow} \cdot 0.35 \cdot \phi_{oc} \cdot DFss + K_{sc} \cdot \phi_{sc} \qquad [41]$$

Equations 40 and 41 can be rearranged (i.e., to obtain $C_{wd}=C_s/K_d$) to estimate the concentrations of chemical in sediment porewater and overlying water, respectively.

Dietary Bioavailability

Given the expected association of PAHs with both organic carbon and soot carbon in Kitimat Arm sediments, it is also reasonable to expect that the dietary bioavailability of PAHs may be decreased due to sequestering in soot carbon. As sediment is digested by detritivores, organic carbon in broken down and absorbed, resulting in uptake of chemical from the organic carbon matrix. Conversely, soot carbon is not expected to be broken down and absorbed from the food resulting in minimal uptake of chemical from this matrix. Therefore, only the fraction of chemical associated with organic carbon was assumed to be bioavailable. The fraction of chemical associated with soot carbon (F_{sc}) was calculated using mass balance principles, assuming that partitioning of the chemical between soot carbon and organic carbon is dependent on K_{sc}, K_{ow}, ϕ_{sc}, ϕ_{oc}, such that:

$$F_{sc} = \frac{1}{1 + (K_{ow} \cdot 0.35/K_{sc}) \cdot (\phi_{oc}/\phi_{sc})} \qquad [42]$$

The remainder represented the fraction of chemical associated with organic carbon and bioavailable in the diet.

3.3 METHODS

3.3.1 Overview

The model was applied to predict food web bioaccumulation of PAHs in Kitimat Arm, BC. As described in Chapter 2, the calibrated model for Kitimat Arm provides a reasonable representation of PCB BSAFs for Dungeness crab in this system. Application of the PCB-BSAF model to PAHs involved adding additional model components to account for both the lower bioavailability of soot-associated PAH and the metabolism of PAH. By making broad estimates of k_M, derived from literature studies, and evaluating these estimates through model performance analysis, it was possible to characterize a mass balance of parent PAHs and Phase I metabolites. Because the initial model

development was based on PCBs with log K_{ow} greater than 5.24, model application was limited to PAH congeners with log K_{ow} near to this range (i.e., log K_{ow} 4.6 or greater).

The general approach to model analysis for parent PAHs and Phase I PAH metabolites involved site-specific parameterization followed by sensitivity analysis and evaluation of model predictions and results. For parent PAHs, the availability of BSAF data allowed for model performance evaluation. For Phase I metabolites of PAH, concentration data were not available for Dungeness crab in Kitimat Arm. Therefore, an evaluative analysis of model predictions was conducted. It was also possible to calculate chemical fluxes for both parent PAHs and Phase I metabolites.

3.3.2 BSAF Data for PAHs

BSAFs for PCBs and PAH in Dungeness crab were determined from data presented in studies by Harris (1999) and Eickhoff et al. (2003). Harris (1999) collected sediment and crab PCB data and sediment PAH data for Kitimat Arm whereas Eickhoff et al. (2003) collected crab PAH data for Kitimat Arm. The sampling locations of Harris (1999) and Eickhoff et al. (2003) corresponded with three areas of Kitimat Arm: the inner harbour and portion of Kitimat Arm, Kitimaat Village and the middle portion of Kitimat Arm, and the outer portion of Kitimat Arm.

Harris (1999) reported seasonal and area-specific estimates of BSAFs for PCBs and PAHs in Dungeness crab from Kitimat Arm. In order to obtain a data set of BSAFs for the current study which uses a steady state model that characterizes time-independent (i.e., non-seasonal) conditions, the raw data for crab and sediment concentrations were re-analyzed. For each box, the averages of OC-normalized sediment PCB and PAH concentrations from 1995 and 1996 were assumed to represent the average exposure to Dungeness crab within that box. A distribution of observed BSAFs for each PCB and PAH congener was then obtained by dividing lipid normalized tissue concentrations for individual crabs by their corresponding average sediment-OC concentrations. Given that PAH emission rates during the 1990s have remained relatively constant, variations in the BSAFs were assumed to be related to differences in sampling location, rather than actual

changes in environmental conditions in Kitimat Arm. Dungeness crabs are highly mobile, and individuals captured within a certain area are expected to have been moving and foraging throughout a large area of Kitimat Arm. Hence, the variability in observed BSAFs will reflect the variability in behaviour and exposure by individual crabs. This data analysis method was assumed to account for this variability.

Observed BSAFs were log-transformed prior to calculating descriptive statistics. Environmental concentration data and ratios are typically expected to follow log-normal distributions. Average log BSAFs and standard deviations were calculated for the log-transformed data sets. These statistics are presented in Table 3-1 and summarized in Figure 3-3.

3.3.3 Model Parameterization

Chemical Properties of PAHs and Phase I Metabolites of PAH

To account for different partitioning behaviour in saltwater, the K_{ow} of each chemical was adjusted according to the method described in Xie et al. (1997; refer to Equation 29). K_{ow}, adjusted K_{ow} and the Le Bas molar volume for PAHs are presented in Table 3-2.

The products of Phase I metabolism PAH are primarily phenols or diols of the parent molecule (i.e., substituted with one or two hydroxyl groups; James, 1989; Livingstone 1991) but more highly substituted molecules are also possible. While K_{ow} values for PAH metabolites have not been determined, Bodor and Buchwald (1997) propose a simple method for estimating the K_{ow} of substituted organic compounds. According to their model, substitution of an aromatic ring with a simple oxygen containing group (e.g., -OH, -O-) results in a reduction of log K_{ow} by 0.723, per added functional group. Thus, on average (i.e., assuming that a Phase I metabolite substituted with two oxygen-containing groups represents the average case), a Phase I metabolite should have a log K_{ow} that is $2 \cdot 0.723 = 1.44$ lower than the log K_{ow} of the parent compound. The log K_{ow} values obtained for Phase I metabolites using this method are summarized in Table 3-2.

Ksc:

Studies by Gustaffson et al (1997) and Jonker and Koelmans (2002) indicate that partitioning to, and sequestration within soot carbon has a significant impact on the bioavailability of pyrogenic PAHs. Gustaffson (1997) proposed that partitioning coefficients for soot carbon-to-water (K_{sc}) could be approximated by studies of the partitioning between activated carbon and water. Jonker and Koelmans (2002) conducted experiments to determine K_{sc} for various types of carbon including coal soot, wood soot, coal and charcoal. Figure 3-4 summarizes the values for K_{sc} that were experimentally estimated in each of these studies for various PAH compounds, in relation to K_{ow}.

Using linear regression on the combined data set, I determined the following empirical relationship between log K_{sc} and log K_{ow} (coefficients ± one standard error):

$$\log K_{sc} = 0.68 \pm 0.09 \cdot (\log K_{ow}) + 3.43 \pm 0.49 \qquad [43]$$

$$r^2 = 0.49$$

The higher partition coefficient for PAHs in soot carbon provides a reasonable approximation of the expected slower desorption behaviour because of the strong associations formed at high temperature. Equation 43 was considered a simple, reasonably accurate approximation of soot carbon partition coefficients for PAHs in Kitimat Arm.

k_M and k_{phase2}:

The primary gap in knowledge for modelling PAH bioaccumulation is the rates of Phase I metabolism of parent chemicals and Phase II metabolism of reactive metabolites. k_M is often set to zero for non-metabolized chemicals such as PCBs. Because PAHs are metabolized extensively by many marine organisms, estimates of k_M are necessary for accurate model prediction of BSAFs.

For aquatic organisms, rates of metabolism of PAH generally increase with increasing level of organization. James (1989), Buhler and Williams (1989), Foureman (1989) and

Table 3-1: Observed log BSAFs for PAHs in Dungeness crab from Kitimat Arm. Table headings include number of observations (n), minimum (min), maximum (max), mean observed BSAF (mean) and standard deviation (SD).

Chemical	Observed Log BSAFs				
	n	min	max	mean	SD
Phenanthrene	117	-5.30	-1.26	-3.47	1.09
Anthracene	117	-4.31	-0.66	-2.76	0.68
Fluoranthene	117	-4.90	-1.27	-3.43	0.53
Pyrene	117	-4.95	-1.49	-3.61	0.48
Benz(a)anthracene	117	-6.25	-1.75	-3.99	0.71
Chrysene	117	-5.54	-1.10	-3.61	0.69
Benzo(a)pyrene	117	-6.20	-2.69	-4.24	0.84

Figure 3-3: Average observed BSAFs for PCBs (◇) and PAHs (□) in Dungeness crab from Kitimat Arm, BC. Error bars represent 1 standard deviation. 66–PCB-66, 105–PCB-105, 118–PCB-118, 156–PCB-156, Anth–anthracene, B(a)A–benz(a)anthracene, B(a)P–benzo(a)pyrene, Chrys–chrysene, Fluor–fluoranthene, Phen–phenanthrene, Pyr–pyrene.

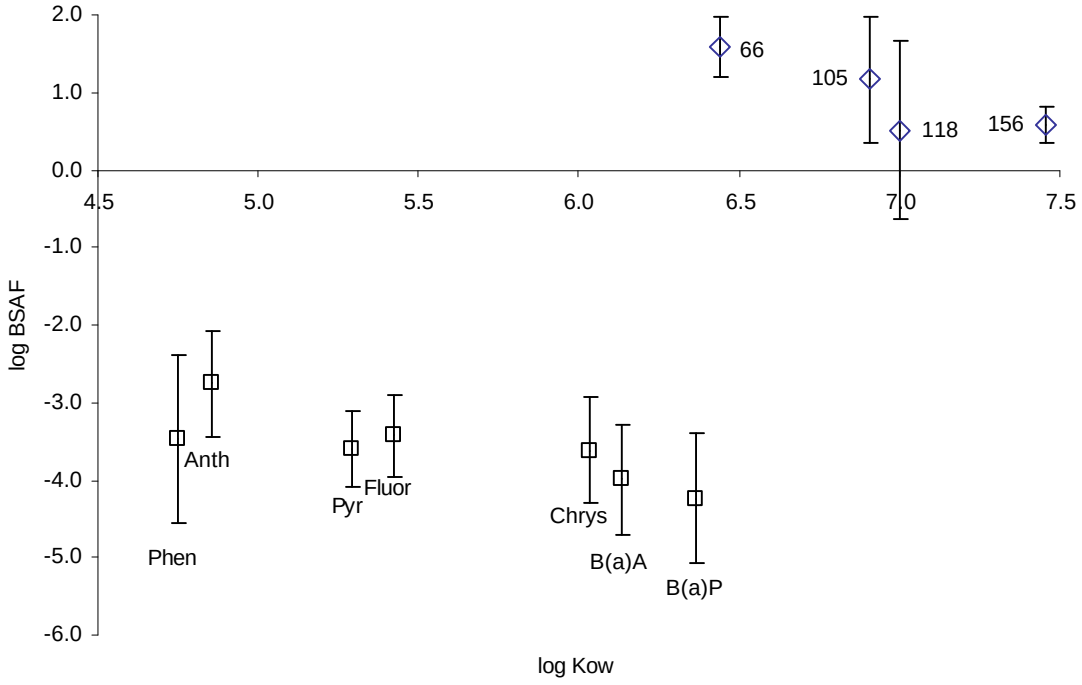

Table 3-2: Log K_{ow}, molar volume and saltwater-adjusted log K_{ow} for PCBs and co-eluting congener groups. log Kow and molar volume based on Mackay et al. (1999) and de Maagd et al. (1998b); log K_{ow} adjusted for saltwater using the method described by Xie et al. (1997). Log Kow of Phase I metabolites estimated using the method described by Bodor and Buchwald (1997).

Chemical Name	Log K_{ow}	Molar Volume (cm^3/mol)[1]	Adjusted Log K_{ow}[3]	Metabolite log K_{ow}[4]
phenanthrene	4.57	199	4.75	3.12
anthracene	4.68	197	4.86	3.23
Pyrene	5.10	214	5.29	3.65
Fluoranthene	5.23	217	5.43	3.78
Chrysene	5.81	251	6.04	4.36
Benz(a)anthracene	5.91	248	6.13	4.46
Benzo(a)pyrene	6.13	263	6.37	4.68

Figure 3-4: Relationship between log K_{sc} and log K_{ow} for PAHs. Ksc values compiled from Jonker and Koelmans (2002, ◇) and Gustafsson et al. (1997; □)

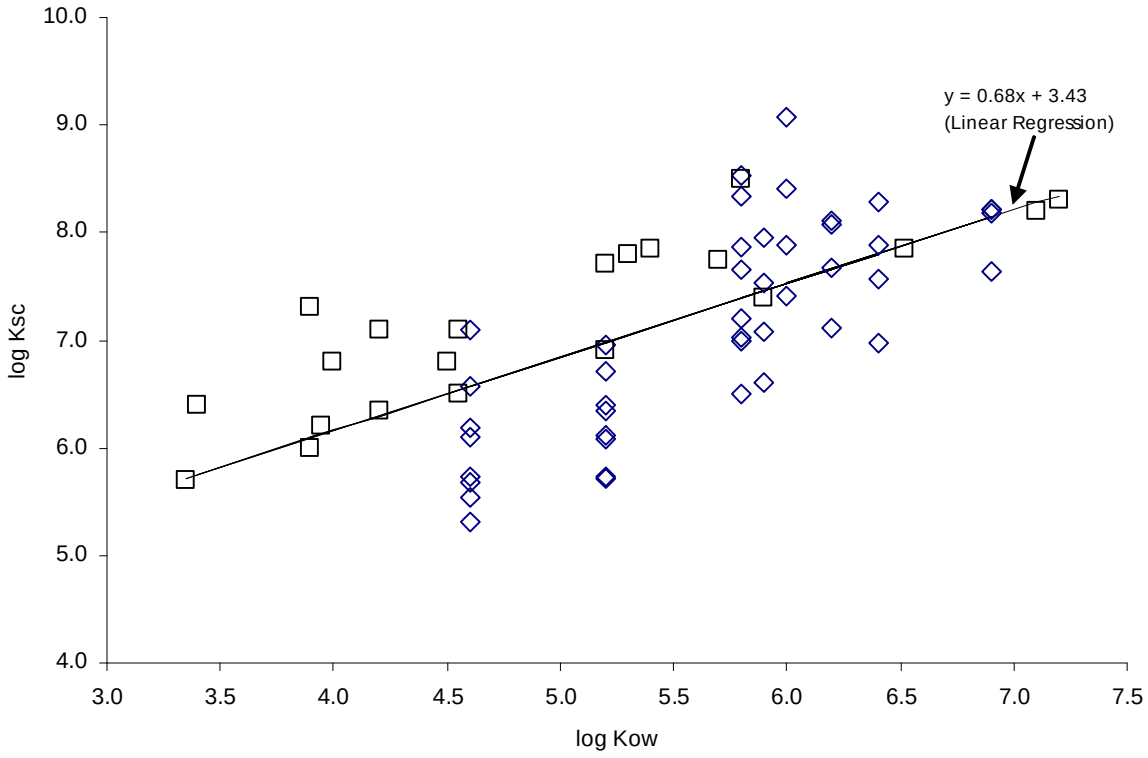

Livingstone (1998) each provide summaries of enzyme activities that have been measured on cellular preparations *in vitro* for marine species (refer to Tables 3-3, and 3-4). Based on these *in vitro* studies, metabolic activity is expected to be relatively low in small infauna and epifauna (e.g., amphipods and annelids), and large infauna (e.g., bivalve mollusks), intermediate in large epifauna (e.g., crabs and shrimp) and highest in fish and larger crustaceans. In addition, Phase II enzyme activities appear to be higher than the activities of Phase I enzymes.

Unfortunately, very few studies allow correlation of *in vitro* enzyme activities with *in vivo* biotransformation rates, because of a lack of quantitative data and the ways in which *in vitro* rates are reported (Sijm and Opperhuizen, 1989). Authors of *in vitro* studies most often report enzyme rates in terms amount of substrate converted per amount of microsomal protein per unit time. Without an estimate of the rate per mass of organism, or the amount of enzyme protein per mass of organism, it is difficult to extrapolate these measured values to live organisms.

Where the data are adequate, laboratory measured enzyme activities may not accurately represent metabolic rates *in vivo* because chemical substrates in organism tissues may not be as available for enzymatic action as chemical substrates in microsomal preparations. This condition is likely to result in overestimates of actual *in vivo* rates of PAH metabolism (James, 1989; Livingstone, 1992). For example, James and Little (1984) measured metabolic rates of 14.16 nmol/min/g hepatopancreas for benzo(a)pyrene in microsomal preparations from the hepatopancreas of male spiny lobsters. The benzo(a)pyrene concentration which yielded this activity was approximately 80 nmol/g, yielding a rate constant for microsomal metabolic transformation of 0.177/min, or 255/day. This *in vitro* rate constant is much higher than *in vivo* rate constants estimated for fish in bioconcentration experiments (De Maagd et al. 1998a; van der Linde et al. , 2001) and those estimated here from radiolabel studies (see below).

There are a limited number of studies that have estimated rate constants for Phase I biotransformation of PAHs in aquatic organisms through the use of experimental data and

Table 3-3: Summary of benzo(a)pyrene hydroxylase (BPH; a Phase I reaction) activities measured *in vitro* for marine organisms. Min-minimum observed rate; Max-maximum observed rate; SE-standard error of the mean.

Organism Class	BPH Activity (nmol/min/mg protein)			Number of Studies	Source
	MIN	MAX	MEAN (±SE)		
Fish	0.027	3.4	0.587 ± 0.305	11	James (1989); Buhler and Williams (1989)
Crustaceans	0.001	1.343	0.437 ± 0.172	9	James (1989); Buhler and Williams (1989)
Mollusks	0.006	0.073	0.038 ± 0.010	6	James (1989); Buhler and Williams (1989)
Annelids	0.015	0.024	0.015 ± 0.009	2	James (1989); Buhler and Williams (1989)
Fish			0.307 ± 0.208	-	Livingstone (1998)
Echinoderms			0.0084 ± 0.0055	-	Livingstone (1998)
Crustaceans			0.04 ± 0.0031	-	Livingstone (1998)
Mollusks			0.0212 ± 0.0034	-	Livingstone (1998)

Table 3-4: Summary of glutathione *S* transferase (GST) and epoxide hydroxylase (EH; both Phase II reactions) activities measured *in vitro* for marine organisms. Min-minimum observed rate; Max-maximum observed rate; n-number of studies. Source: Foureman (1989)

Organism Class	GST Activity (nmol/min/mg protein)				EH Activity (nmol/min/mg protein)			
	min	max	mean	n	min	max	mean	n
Fish	2	131	27	8	<1	4	2	6
Crustaceans	<1	3	1.67	3	2	19	7.75	4
Mollusks			<1	2			2	1

models. De Maagd et al. (1998a) conducted waterborne exposure of benz(a)anthracene to fathead minnow by applying a mechanistic model for elimination rate constants, they were able to deduce a k_M of 1.33/day for benz(a)anthracene in fathead minnow. Van der Linde et al. (2001) compiled experimental data from bioconcentration experiments and deduced k_M for several chemicals and organisms by comparing elimination rates predicted by a mechanistic model (i.e. in the absence eof metabolites) and actual elimination rates observed in the experiments. Their results indicated PAH biotransformation rates of 0.1 to 1 per day in both annelids and fish, although k_M was generally lower in annelids than in fish, an observation consistent with the lower enzyme activity in annelids.

In addition to these studies which explicitly determined rate constants for PAH biotransformation in aquatic species, it is also possible to make broad approximations of k_M from experiments where organisms were exposed to radiolabelled chemicals. These experiments generally involve exposure of animals to radiolabelled PAH compounds in water or sediments. After a given exposure time, the animal tissue is analyzed to determine the proportions of accumulated radioactivity as parent compound or as polar and conjugated metabolites. The average rate of metabolism during the experiment is determined from experimental results as:

$$R = \frac{T \cdot \phi_M}{t} \qquad [44]$$

Where R is the rate of metabolism (pmol/g/day), T is the total radioactivity measured in organism tissue (pmol/g), and ϕ_M is the fraction of radioactivity associated with metabolites, and t is the exposure time (days). Thus, $T \cdot \phi_M$ represents both the amount of parent chemical metabolized and the amount of metabolites produced during the exposure time. k_M (1/day) is estimated by normalizing the rate (pmol/g/day) to the body burden of parent compound (pmol/g) during the exposure period. Landrum and Scavia (1983) applied this method to determine a k_M of 0.6/day for anthracene accumulated from water and sediment in the amphipod, *Hyallela azteca*. The authors cautioned that this value was likely an underestimate because the analysis method did not account for parent compound or metabolite elimination. Livingstone (1991), also applied this method for

estimating metabolic rates (but not rate constants) of several substituted and non-substituted hydrocarbons.

Both Livingstone (1998) and Landrum and Scavia (1983) proposed normalizing the metabolic rate to the body burden of parent chemical at the end of the experiment in order to derive k_M. However, in sediment or water exposures that begin with unexposed organisms, both the overall body burden (i.e., parent chemical and metabolites) and the parent compound body burden are expected to begin at zero and approach a steady state condition. Therefore, with exposure in environmental media, the average parent compound concentration during the experiment is likely to be lower than the concentration at the end of the experiment, and normalizing to the end body burden results in an underestimate of k_M. A potentially more representative method for deriving k_M is to normalize the metabolic rate to the median body burden of parent chemical (e.g., half way between zero and the end body burden), to account for the expected lower average parent compound concentration during the experiment. However, this method may underestimate the parent compound concentration and overestimate k_M if uptake and elimination kinetics neared steady state during the exposure period. Thus, there are two potential equations for estimating k_M, each with some uncertainty:

$$k_M(\text{end}) = \frac{R}{T\cdot(1-\phi_M)} \quad \textit{or} \quad k_M(\text{median}) = \frac{R}{0.5\cdot T\cdot(1-\phi_M)} \qquad [45]$$

Where k_M(end) is based on the concentration of parent PAH congeners at the end of the experiment and is likely to underestimate the *true* k_M, and k_M(median) is based on the median concentration of parent PAH congeners during the experiment and is likely to overestimate *true* k_M. The inclusion of T in both the calculation for R and the normalization to obtain k_M causes a "canceling-out" effect such that the calculated k_M depends only ϕ_M and t. The result is a simple relationship between ϕ_M and t and estimated k_M that can be used to interpret the radiolabel studies. (refer to Figure 3-5).

I applied both methods to estimate k_M values from radiolabel studies with annelids, crustaceans, mollusks and fish. Tables 3-5 to 3-7 present the calculation of k_M for various studies while Table 3-8 provides a summary of the calculated k_M values. Where multiple

Figure 3-5: Relationship between exposure time (t), fraction of metabolites (ϕ_M) and estimated k_M(median) for interpretation of *in vivo* metabolism studies which used radiolabeled PAHs.

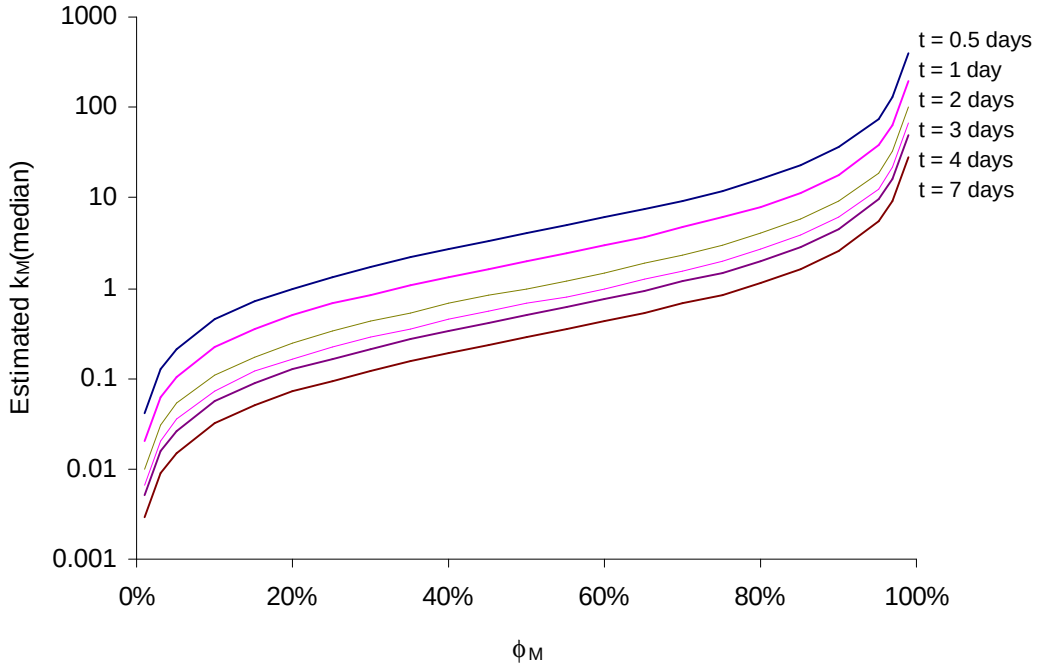

Table 3-5: Estimated rate constants for Phase I PAH metabolism in marine annelid species. k_M(end) and k_M(median) refer to rate constants derived using end or median body burden, respectively, of parent PAHs and metabolites.

Chemical	Organism	Exposure Time (days)	parent chemical	metabolites	Source	k_M (end)	k_M (median)
benzo(a)pyrene	*Nereis diversicolor*	6	6%	94%	Kane-Driscoll and McElroy 1996	2.50	5.00
benzo(a)pyrene	*Scolecolepides viridis*	6	21%	80%	Kane-Driscoll and McElroy 1996	0.65	1.29
benzo(a)pyrene	*S. viridis*	12	17%	83%	Kane-Driscoll and McElroy 1996	0.41	0.81
benzo(a)pyrene	*Leitoscoloplos fragilis*	6	92%	8%	Kane-Driscoll and McElroy 1996	0.01	0.03
benzo(a)pyrene	*N. diversicolor*	9	5%	95%	Kane-Driscoll and McElroy 1996	2.11	4.22
benzo(a)pyrene	*S. viridis*	9	40%	60%	Kane-Driscoll and McElroy 1996	0.17	0.33
benzo(a)pyrene	*L. fragilis*	9	90%	10%	Kane-Driscoll and McElroy 1996	0.01	0.02
benzo(a)pyrene	*L. fragilis*	6	91%	9%	Kane-Driscoll and McElroy 1996	0.02	0.03
benzo(a)pyrene	*Spio setosa*	6	91%	9%	Kane-Driscoll and McElroy 1996	0.02	0.03
benzo(a)pyrene	*Pectinaria gouldii*	6	89%	11%	Kane-Driscoll and McElroy 1996	0.02	0.04
benzo(a)pyrene	*Glyera dibranchiata*	6	86%	14%	Kane-Driscoll and McElroy 1996	0.03	0.05
benzo(a)pyrene	*S. viridis*	6	50%	50%	Kane-Driscoll and McElroy 1996	0.17	0.30
benzo(a)pyrene	*Abarenicola pacifica*	60	71%	29%	Weston 1990	0.01	0.01
benzo(a)pyrene	*A. pacifica*	60	69%	31%	Weston 1990	0.01	0.01
benzo(a)pyrene	*A. pacifica*	60	73%	27%	Weston 1990	0.01	0.01
benzo(a)pyrene	*Nereis succinea*	7	4%	96%	McElroy et al. 2000	3.43	6.23
benzo(a)pyrene	*Capitella sp.*	7	58%	42%	McElroy et al. 2000	0.10	0.19
benzo(a)pyrene	*Haploscolopolous sp.*	7	65%	35%	McElroy et al. 2000	0.08	0.14
benzo(a)pyrene	*Pectinaria gouldii*	7	93%	7%	McElroy et al. 2000	0.01	0.02
benz(a)anthracene	*N. virens*	6	1.2 μg/g	3.8 μg/g	McElroy 1985	0.53	1.06
benz(a)anthracene	*N. virens*	25	6 μg/g	19.6 μg/g	McElroy 1985	0.13	0.26

Table 3-6: Estimated rate constants for Phase I PAH metabolism in marine mollusk species. k_M(end) and k_M(median) refer to rate constants derived using end or median body burden, respectively, of parent PAHs and metabolites.

Chemical	Organism	Exposure Time (days)	parent chemical	metabolites	Source	k_M (end)	k_M (median)
benzo(a)pyrene	*Hydrobia totteni*	7	31%	69%	McElroy et al 2000	**0.32**	0.64
benzo(a)pyrene	*Ilyanasa obsoleta*	7	43%	57%	McElroy et al 2000	**0.19**	0.38
benzo(a)pyrene	*Yodia limatula*	7	75%	25%	McElroy et al 2000	**0.05**	0.10
benzo(a)pyrene	*Gemma gemma*	7	82%	18%	McElroy et al 2000	**0.03**	0.06

Table 3-7: Estimated rate constants for Phase I PAH metabolism in marine crustacean and fish species. k_M(end) and k_M(median) refer to rate constants derived using end or median body burden, respectively, of parent PAHs and metabolites.

Chemical	Organism	Exposure Time (days)	parent chemical	metabolites	Source	k_M (end)	k_M (median)
Amphipods and copepods							
anthracene	*Hyalella azteca*				Landrum and Scavia (1983)	0.54	
benz(a)anthracene	*Ampelisca abdita*	10	87%	13%	Fay et al. (2000)	0.01	0.03
benzo(a)pyrene	*A. abdita*	10	92%	8%	Fay et al. (2000)	0.01	0.02
benzo(a)pyrene	*Edotea triloba*	7	80%	20%	McElroy et al. (2000)	0.04	0.07
benzo(a)pyrene	*Gammarus mucronatus*	7	43%	57%	McElroy et al. (2000)	0.19	0.38
benzo(a)pyrene	*Eohaustorius washingtonianus*	1	2.26 pmol/g	0.72 pmol/g	Reichert et al. (1985)	0.32	0.64
benzo(a)pyrene	*Rhepoxinius abronius*	1	0.94 pmol/g	0.68 pmol/g	Reichert et al. (1985)	0.72	1.44
benzo(a)pyrene	*E. washingtonianus*	7	78%	22%	Varanasi et al. (1985)	0.04	0.08
benzo(a)pyrene	*R. abronius*	7	26%	74%	Varanasi et al. (1985)	0.41	0.81
fluoranthene	*Schizopera knabeni*	4	0.892	0.108	Lotufo (1998)	0.03	0.06

Table 3-7 (continued): Estimated rate constants for Phase I PAH metabolism in marine crustacean and fish species. k_M(end) and k_M(median) refer to rate constants derived using end or median body burden, respectively, of parent PAHs and metabolites.

Chemical	Organism	Exposure Time (days)	parent chemical	metabolites	Source	k_M (end)	k_M (median)
Fluoranthene	*Coullana sp*	4	0.872	0.128	Lotufo (1998)	0.04	0.07
Shrimp, crab and spiny lobster							
benzo(a)pyrene	*Callinectes sapidus* (whole body)	1	326 μg	185 μg	Lee et al. (1976)	0.57	1.13
benzo(a)pyrene	*C. sapidus (*whole body)	1-2	609 μg	495 μg	Lee et al. (1976)	0.51	0.66
benzo(a)pyrene	*Panulirus argus (*hepatopancreas)	0.25	55%	45%	Little et al (1985)	3.27	
benzo(a)pyrene	*P. argus* (hepatopancreas)	1	23%	77%	Little et al (1985)	2.51	1.80
benzo(a)pyrene	*P. argus (*hepatopancreas)	3	7%	93%	Little et al (1985)	3.17	2.05
benzo(a)pyrene	*Pandalus platyceros* (hepatopancreas)	7	6%	94%	Varanasi et al. (1985)	2.24	4.48
Fish							
benzo(a)pyrene	*Parophyrus vetulus* (whole body)	7	6%	94%	Varanasi et al. (1985)	2.24	4.48

Table 3-8: Summary of estimated k_M values for marine annelids, mollusks, amphipods and copepods, larger crustaceans and fish. k_M(end) and k_M(median) refer to rate constants derived using end or median body burden, respectively, of parent PAHs and metabolites. SD-standard deviation, n-number of studies.

Organism	Estimated k_M(end)		Estimated k_M(median)		n
	Range	mean ± SD	Range	mean ± SD	
annelid worms	0.01 - 3.43	0.50 ± 0.96	0.01 - 6.23	0.96 ± 1.80	21
mollusks	0.03 - 0.32	0.15 ± 0.14	0.06 - 0.64	0.29 ± 0.27	4
amphipods and copepods	0.01 - 0.72	0.21 ± 0.25	0.02 - 1.44	0.36 ± 0.47	11
shrimp, crab and lobster	0.51 - 3.27	2.05 ± 1.23	0.66 - 4.48	2.02 ± 1.48	6
English sole		2.24		4.48	

measurements were recorded over time, only the initial exposure period was included in order to minimize uncertainty due to metabolite elimination and other factors such as association of metabolites with non-extractable fractions (e.g., DNA adduct formation). The only exception was for studies where exposure was via injection (i.e., one time exposure) and the time course of elimination was observed.

k_M values derived from the experimental data followed the same general trend as the metabolic capacities for species groups indicated by enzyme activities measured *in vitro,* Marine mollusks appeared to have the lowest ability to metabolize PAHs with mean calculated k_M of either 0.15 or 0.30/day depending on the estimated body burden of parent compound (i.e., end vs. median concentration). This result is consistent with earlier researchers who found PAH metabolism in mollusks to be either low relative to other species or absent (James, 1989; Livingstone, 1991). Based on these data, 0.15 to 0.30/day is expected to be a reasonable range for average k_M in marine mollusks.

Calculated k_M values for small benthic crustaceans (copepods and amphipods) were similarly low, averaging either 0.21 or 0.36 (end vs. median parent PAH concentration). In three studies with larger crustaceans (i.e., shrimp, crab and lobster), calculated k_M values ranged from 0.54 to 4.7/day (k_M(median)), or 0.51 to 3.75/day (k_M(end), and averaged approximately 2/day using both methods. The lower end of these ranges exceeds the maximum observed in smaller crustaceans, suggesting a higher metabolic capacity in larger, more developed crustacean species. It is important to note that two of the studies reported metabolites in hepatopancreas only, and likely overestimated whole body metabolism given the higher metabolic capacity in this organ relative to other tissues. Thus, the upper limit of these calculated ranges are likely higher than the actual *in vivo* metabolism for larger crustaceans. Livingstone (1998) reported a metabolic rate for crustaceans of 2.05 pmol/min/g at 10 nmol/g benzo(a)pyrene which was based on a regression of a subset of the crustacean studies described here. The resulting k_M of 0.3 is closer to the values determined here for smaller crustaceans, likely because of the predominance of studies on small amphipods in Livingstone's data set. Based on these

data, reasonable estimates of average k_M for PAHs are 0.2 to 0.4/day in small crustaceans (e.g., amphipods and copepods) and 1 to 2/day in larger crustaceans (e.g., shrimp, crabs and spiny lobster).

Annelid worms appeared to have an intermediate metabolic capacity with k_M values of 0.50/day and 0.96/day, based on either end parent concentrations or median parent concentrations, respectively. These results are consistent with the range in k_M of 0.1 to 1/day reported by van der Linde et al. (2001) and moderately higher than calculated k_M (0.11/day) for *Nereis virens* metabolizing benz(a)anthracene, derived from data presented in Livingstone (1998). Based on these data, 0.5 to 1/day is a reasonable range for representing the average k_M in annelids.

The one radiolabel study with English sole exposed to benzo(a)pyrene via sediment suggested k_M values of 2.24 and 4.48 (end body burden vs. median body burden) on a whole-body basis. Livingstone (1998) reports metabolic rates for benzo(a)pyrene of 0.49 pmol/min/g at a parent body burden of 0.6-0.7 nmol/g in *Lepomis macrochirus* and 6.2 pmol/min/g at a parent body burden of 3.1 nmol/g. Application of the equation for k_M(end) yielded respective k_M values of 1.08 and 2.88. The values described for the three species above are higher than k_M reported by de Maagd et al. (1998a) in fathead minnow for benz(a)anthracene and van der Linde et al. (2001) for several PAHs and fish species. Thus, based on studies with radiolabeled compounds, and combined experimental/ modelling approaches, average k_M ranging from 1 to 3, is expected to be reasonable for PAHs in fish species.

The metabolic rate constants derived here should be considered estimates only. A large amount of uncertainty is associated with the calculations because they do not account for elimination of metabolites and parent compound via routes other than metabolism. In addition, several factors are expected to influence actual metabolic transformation rates in natural situations, including environmental temperature, intraspecies variability, interspecies variability for aggregated trophic guilds, and the presence of Cytochrome P450 inducers such as PCBs or dioxins. For example, Livingstone (1998) reported that

the presence of inducing agents can increase enzyme activity by one to two orders of magnitude.

Table 3-9 summarizes the expected ranges in average k_M and a reasonable intermediate value for each trophic guild in the BSAF model. As a starting point, the intermediate k_M for each trophic guild was applied for all modelled PAHs. Although enzyme activity is likely to be congener-specific, availability of substrate is expected to be the primary limiting factor in metabolism. Thus, k_M for more hydrophobic PAHs which partition strongly to lipid, may be limited by low substrate availability rather than enzyme affinity. Because of the uncertainty associated with these estimated k_M values, a model fitting analysis was also conducted to determine if other values for k_M would better represent PAH bioaccumulation in Kitimat Arm.

In order to estimate steady state concentrations of Phase I metabolites (i.e., the metabolites responsible for toxic effects), it was also necessary to estimate values for k_{phase2}. Unfortunately, there were no known studies which reported data suitable for estimating Phase II rate constants. Based on the relative activity of BPH (Phase I) and GST and EH (Phase II) *in vitro*, k_{phase2} is expected to be higher than k_M. However, potential rate limiting factors for GST are the availability of Phase I metabolites and glutathione for conjugation. Under high exposure to PAHs or induction of Phase I enzymes, resulting in relatively large fluxes of Phase I metabolites, it is possible for glutathione stores to be depleted, limiting the rate of conjugation by GST. These conditions would result in higher body burdens of Phase I metabolites. This could possibly lead to a higher potential for DNA adduct formation and associated risk of carcinogenesis. There are no known studies that have determined the conditions under which this is likely to occur in marine fish and invertebrates.

Given this lack of information regarding k_{phase2}, it was not specified *a priori*. Instead, sensitivity analysis was conducted to examine the impact of uncertainty in this parameter on predicted metabolite body burdens. In addition, model application for Phase I

Table 3-9: Estimated k_M values for PAH congeners in trophic guilds from the BSAF model. k_M relative to Dungeness crab is based on intermediate values of k_M.

Trophic Guild	Expected Range in k_M	Intermediate Value for k_M	k_M relative to Dungeness crab[1]
zooplankton	0.2 – 0.4	0.3	0.2
small infauna and epifauna	0.2 – 1.0	0.6	0.4
large infauna	0.15 – 0.30	0.2	0.13
large epifauna	0.5 – 2.5	1	0.67
small fish	1 – 3	2	1.33
juvenile flatfish	1 – 3	2	1.33
Dungeness crab	0.5 – 2.5	1.5	1

metabolites was conducted in an evaluative fashion which considered two potential scenarios for Phase II metabolism.

Food Web Structure and Ecosystem Properties

Food web structure and ecosystem properties were generally the same as those used in the PCB BSAF model for Kitimat Arm. The soot carbon content of Kitimat Arm surface sediments is approximately 0.15% near Kitimat Village and range up to 0.7% in the inner and outer harbour (Walt Cretney, personal communication). A value of 0.4 % was chosen to represent the whole of Kitimat Arm.

Sediment and Water Concentrations

Sediment concentrations for individual PAH congeners were obtained from data presented in Harris (1999). These measurements had corresponding data for Dungeness crabs and were used to calculate observed BSAFs. Suspended sediments were assumed to be in equilibrium with bottom sediments. Corresponding data for the concentration of PAHs dissolved in overlying water were not available for Kitimat Arm. Consequently, dissolved water concentrations in overlying water and sediment porewater were estimated using Equations 40 and 41, respectively. The application of soot carbon partitioning for estimating dissolved water concentrations and bioavailable fractions in detritus causes the overall modelled bioavailability (i.e., amount of chemical available for uptake from water and food) to be much lower than would be predicted for non-soot-associated chemicals such as PCBs.

3.3.4 Sensitivity Analysis

Parent PAHs

The goal of sensitivity analysis for parent PAHs was to observe how variability in K_{sc} and k_M affected model-predicted BSAFs.

For K_{sc}, three log K_{sc} vs. log K_{ow} relationships were used (High K_{sc}, Best-fit K_{sc} and Low K_{sc}, refer to Figure 3-6). These three relationships represented the Best-fit to the K_{sc} data and reasonable upper (i.e., High K_{sc}) and lower (i.e., Low K_{sc}) extents for log K_{sc} versus log K_{ow}. The upper and lower bounds were determined by respectively adding or

Figure 3-6: Three potential forms of the relationship for log K_{sc} vs. log K_{ow}.

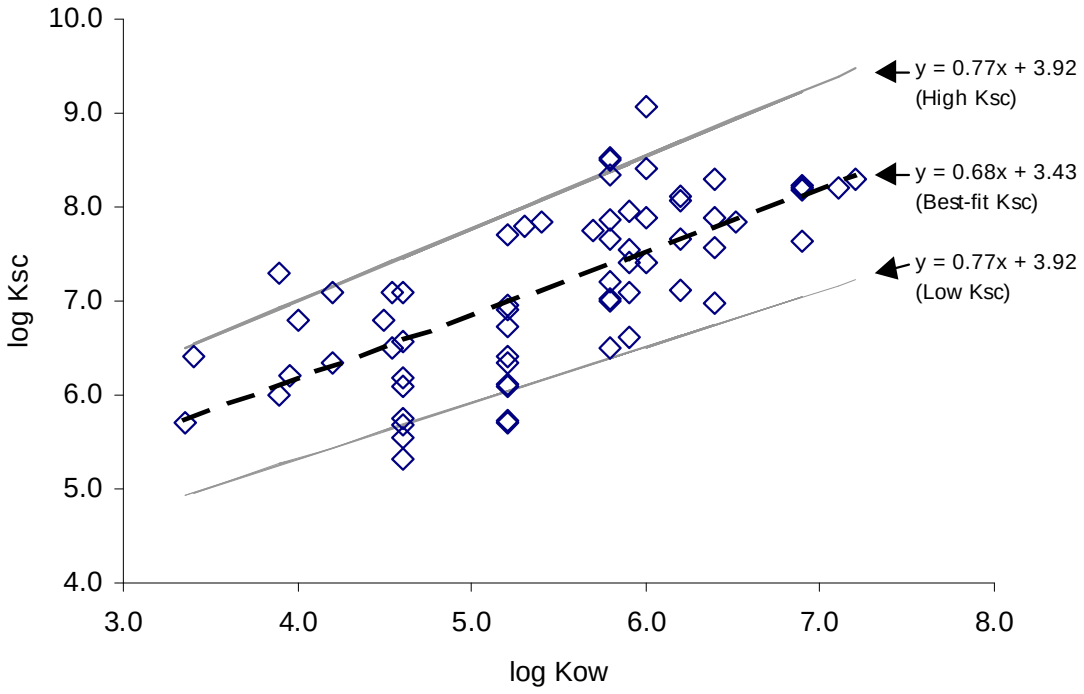

subtracting one standard error from the regression coefficients (both slope and intercept). The sensitivity analysis for K_{sc} was conducted under two conditions: once with k_M=0 for all organisms (to show the effect of K_{sc} in the absence of metabolism) and once with k_M set at the intermediate values from Table 3-9 (to show the effect of K_{sc} when metabolism is also accounted for).

For k_M, three sets of values for trophic guilds were used based on the ranges and intermediate values presented in Table 3-9. These three sets represented the most likely k_M values for trophic guilds in Kitimat Arm (i.e., intermediate k_M, based on the intermediate values from Table 3-9) and reasonable upper (i.e. high k_M) and lower (i.e., low k_M) bounds for k_M. The high k_M in each trophic guild was based on the upper limit of the expected range whereas low k_M in each trophic guild was based on the lower limit of the expected range. The sensitivity analysis for k_M was conducted under two conditions: once without soot carbon partitioning (to show the effect of k_M with normal PAH bioavailability) and once with soot carbon partitioning based on the Best-fit relationship for K_{sc} (to show the effect of k_M under the low bioavailability conditions in Kitimat Arm).

Phase I Metabolites of PAH

The main source of model uncertainty for predicting the mass balance of Phase I metabolites in benthic organisms was the rate of Phase II metabolism (k_{phase2}). There is little information in the literature that allows estimation of rate constants for Phase II metabolism. In order to evaluate the effect of this uncertainty on model predictions, I conducted a sensitivity analysis to determine the relationship between the predicted body burden of Phase I metabolites and the rate of Phase II metabolism (k_{phase2}). k_{phase2} was assumed to be a constant proportion of k_M for all trophic guilds. By varying this proportion, it was possible to determine the relationship between k_{phase2} and the Phase I metabolite concentration. The trend in k_{phase2} among trophic guilds was assumed to parallel the trend in k_M since both of these processes are expected to be a function of the overall metabolic capacity of the organism. For this sensitivity analysis, benzo(a)pyrene was chosen to represent intermediate to higher K_{ow} PAHs which have the potential to cause carcinogenesis following Phase I metabolic activation.

3.3.5 Model Performance Evaluation

Parent PAHs

To evaluate the performance of the model for parent PAHs, BSAF predictions were made for Dungeness crab using intermediate k_M and Best-fit K_{sc} and then compared to observed BSAFs in Kitimat Arm. Initially, I assumed that one k_M value could be applied for all PAH congeners, within a trophic guild. The quantitative criteria used to evaluate model performance was model bias, as discussed in Chapter 2.

To determine if proportionally higher or lower k_M values would better represent bioaccumulation of parent PAHs in Dungeness crab, I conducted a model fitting exercise where k_M for Dungeness crab was varied and k_M in other trophic guilds paralleled that in Dungeness crab according to the relative proportions in Table 3-9. The criterion for the model fitting was minimization of the sum-of-squared deviations (SSQ; refer to Equation 30) between predicted and observed BSAFs for all PAH congeners.

Phase I Metabolites of PAH

Body burdens of Phase I Metabolites of PAH have not been analyzed in benthic organisms from Kitimat Arm. Consequently, it was not possible to evaluate the accuracy of the mass balance model for Phase I metabolites. However, it was still possible to apply the model in an evaluative fashion to see how different assumptions affected model predictions (see below).

3.3.6 Model Application

Once the performance of the model was tested, two model applications were conducted: model-fitting to infer k_M values specific to each PAH congener; and exposure assessment for benzo(a)pyrene (both parent chemical and Phase I metabolites).

Inference of Congener-specific k_M values

While the application of one k_M value for all PAH congeners within a trophic guild provided a general estimate of PAH metabolism, it did not account for differences in metabolic transformation rates between congeners. In addition to organism-specific metabolic capacities, enzyme affinity and resultant *in vivo* metabolic transformation rates

are expected depend on chemical structure. Therefore, a model-fitting exercise was conducted to determine k_M values specific to each PAH congener and the expected variability in these congener-specific k_M values. The criterion used for this analysis was minimization of the deviation (i.e., $BSAF_{p,i}$–$BSAF_{o,i}$) for each congener.

Exposure Assessment for Benzo(a)pyrene

The purpose of the exposure assessment was to examine how metabolism affects the trophic dynamics of parent PAHs and metabolites. Benzo(a)pyrene was chosen as a representative PAH congener since its K_{ow} is near the range where maximal bioaccumulation, but it is known to be rapidly metabolized in many aquatic organisms. In addition, its K_{ow} is similar to that of PCB-66, allowing comparison between non-metabolized PCBs and metabolized PAHs.

The models were used to predict body burdens of parent benzo(a)pyrene and Phase I metabolites of benzo(a)pyrene based on the average sediment benzo(a)pyrene concentration in Kitimat Arm. Because the uncertainty in k_{phase2} and the lack of observed concentration data precluded absolute prediction of Phase I metabolite body burdens, the model was applied in an evaluative fashion to examine the implications of high or low values for k_{phase2}. The evaluative analysis involved two representative scenarios:

1. *Rapid Phase II Metabolism:* This scenario represents the "normal" case in natural systems where Phase II rates are expected to exceed Phase I rates. k_{phase2} was set at $3 \cdot k_M$ for this scenario.
2. *Slow Phase II Metabolism*: This scenario represents the situation where Phase I induction or high PAH exposure levels could cause a high influx of Phase I metabolites which overwhelms the Phase II metabolic pathway (i.e., k_{phase2} lower than k_M). k_{phase2} was set at $0.3 \cdot k_M$ for this scenario.

To evaluate the exposure assessment predictions, flux calculations were made for benzo(a)pyrene and PCB-66. Benzo(a)pyrene and PCB-66 are chemicals of similar K_{ow} that are both present in bottom sediments of Kitimat Arm and, consequently, expected to be bioaccumulated by Dungeness crab. The log K_{ow} for these chemicals (i.e., 6.37 for benzo(a)pyrene, 6.44 for PCB-66) is within the range where maximal biomagnification is

expected; however, parent benzo(a)pyrene undergoes metabolic transformation reducing its body burden. Because of the different environmental concentrations of these chemicals, the total flux of each chemical through a Dungeness crab was expected to be different, even in the absence of metabolic transformation. However, by examining the proportion of the total flux that is attributable to each uptake and depuration process it was possible to observe the driving processes for bioaccumulation of metabolized and non-metabolized chemicals. This comparison was also made for different trophic guilds in order to observe the impact of different life history characteristics and food sources.

It was also possible to compare the fluxes of Phase I metabolites of benzo(a)pyrene under the two scenarios for k_{phase2} to examine the driving processes for the mass balance of PAH metabolites in trophic guilds of Kitimat Arm.

3.4 RESULTS AND DISCUSSION

3.4.1 Sensitivity Analysis

K_{sc} and k_M

The association of smelter-emitted PAHs with soot carbon is expected to lower bioavailable fractions in water and in consumed sediment, reducing exposure and resulting BSAFs for parent PAHs. Figures 3-7 and 3-8 demonstrate how the modelled lower bioavailability reduces the predicted BSAFs, in the absence of metabolism or with metabolism included, respectively. The predictions based on Low K_{sc}, Best-fit K_{sc} and High K_{sc} demonstrate the inverse relationship between K_{sc} and resultant BSAFs. This relationship is expected given that an increase in partitioning to soot carbon results in lower bioavailability. In 3-7, the model predictions for normal bioavailability (i.e., predictions for PCBs) and low bioavailability indicates that, based on the Best-fit relationship for K_{sc}, soot-association of chemicals is expected to lower BSAFs by approximately one order of magnitude. In both Figures 3-7 and 3-8, BSAF predictions with low K_{sc} were approximately half an order of magnitude higher (compared to predictions with Best-fit K_{sc}) and with high K_{sc}, were one order of magnitude lower (compared to predictions with Best-fit K_{sc}). In general, the Best-fit relationship appeared

Figure 3-7: Sensitivity analysis results for K_{sc}, in the absence of metabolism (k_M=0). Symbols represent average observed for BSAFs PCBs (◇) and PAHs (□). Lines represent model predictions for Best-fit Ksc (—), High Ksc (----) Low Ksc (– – –) and PCBs (—). Error bars represent 1 standard deviation.

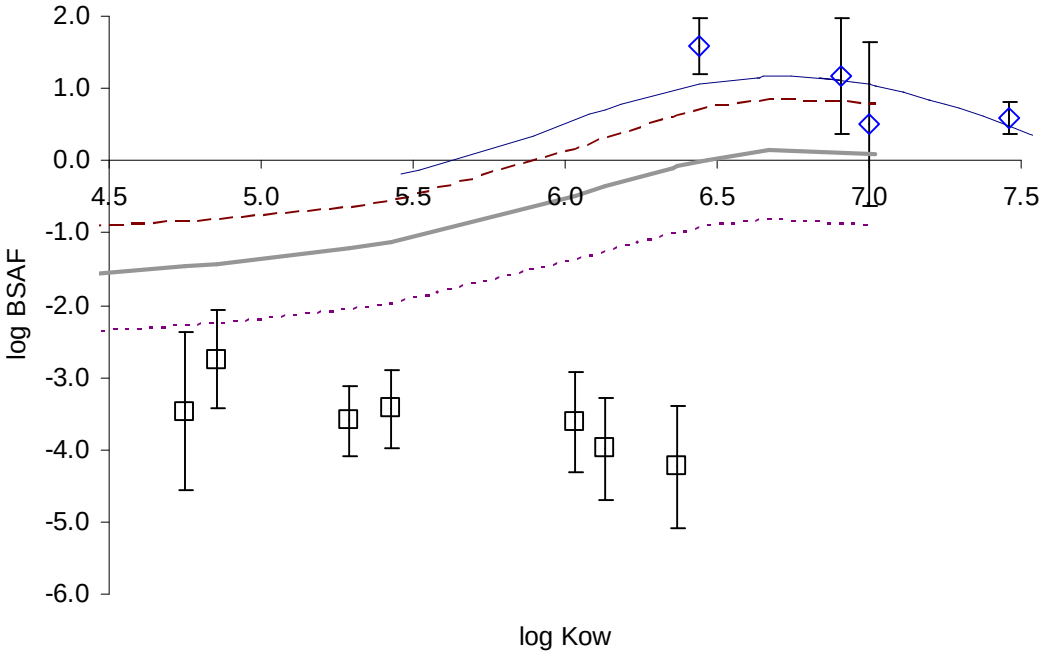

Figure 3-8: Sensitivity analysis results for K_{sc}, with intermediate k_M. Symbols represent observed BSAFs for PCBs (◇) and PAHs (□). Lines represent model predictions for Best-fit Ksc (—), High Ksc (----) Low Ksc (– – –) and PCBs (—). Error bars represent 1 standard deviation.

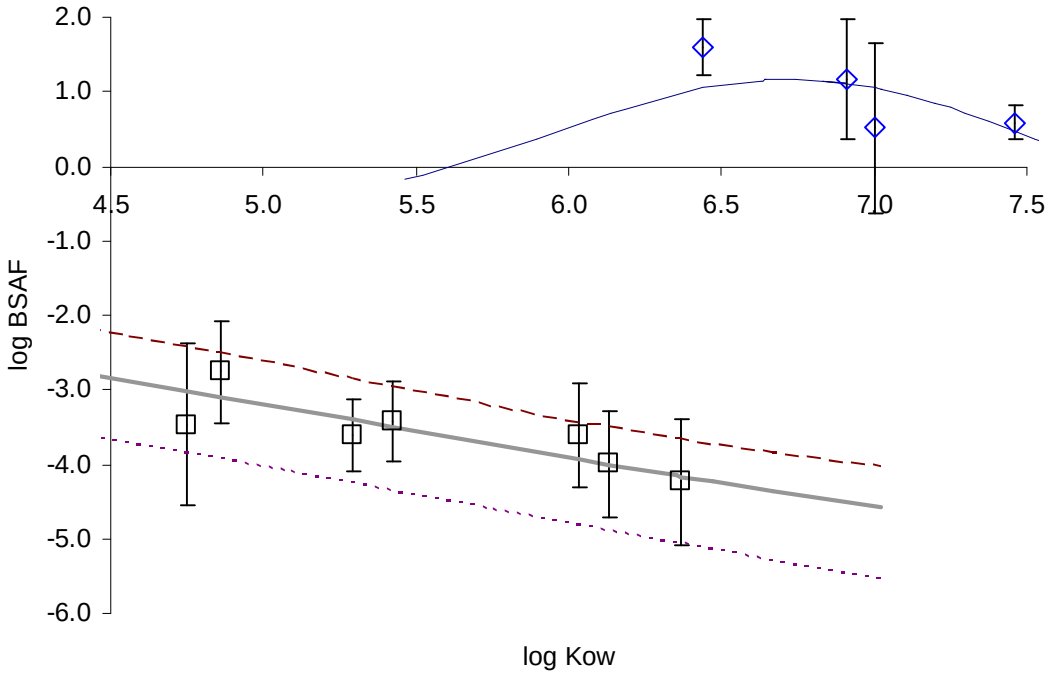

Figure 3-9: Sensitivity analysis results for k_M, in the absence of soot carbon partitioning (i.e., normal bioavailability). Symbols represent observed BSAFs for PCBs (◇) and PAHs (□). Lines represent model predictions for intermediate k_M (—), High k_M (----) Low k_M (– – –) and PCBs (—). Error bars represent 1 standard deviation.

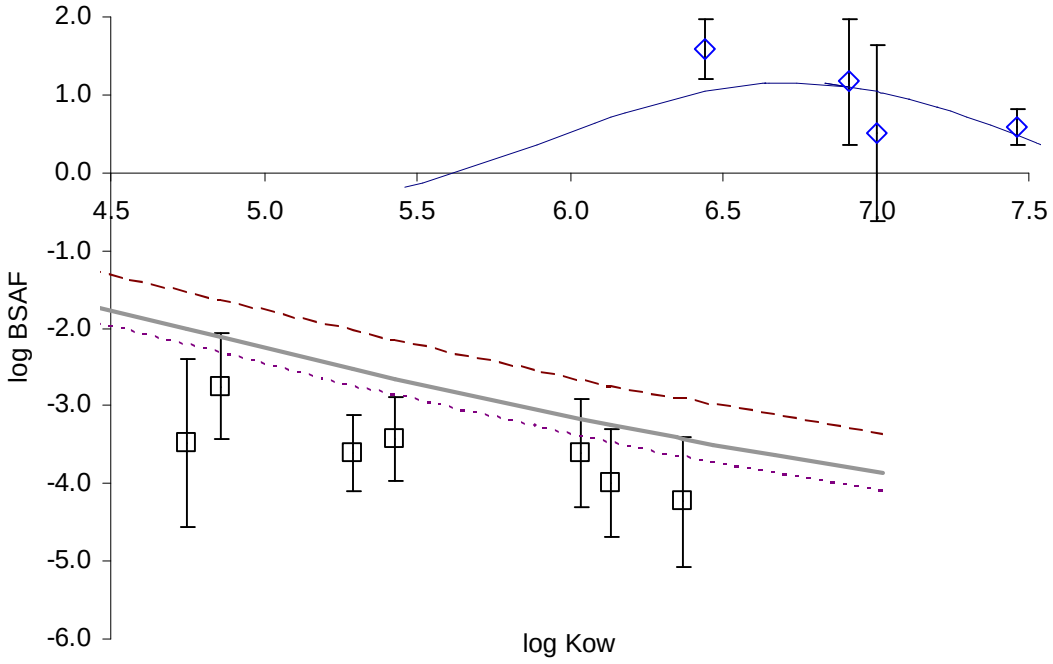

Figure 3-10: Sensitivity analysis results for k_M, with the Best-fit relationship for K_{sc} (i.e., low bioavailability). Symbols represent observed BSAFs for PCBs (◇) and PAHs (□). Lines represent model predictions for intermediate k_M (—), High k_M (----) Low k_M (– – –) and PCBs (—). Error bars represent 1 standard deviation.

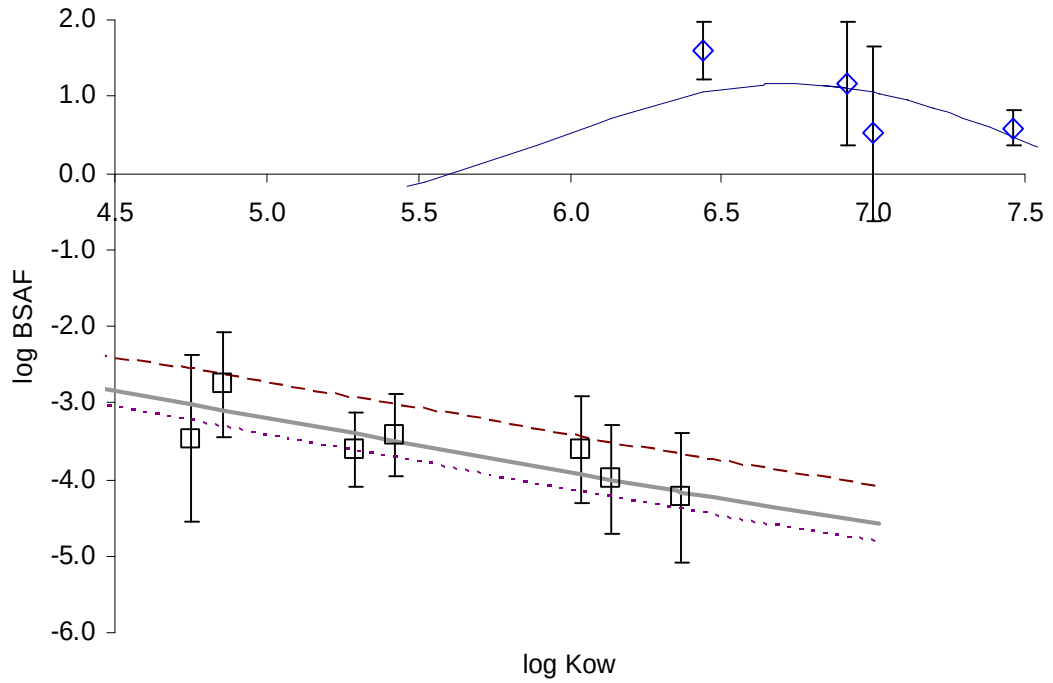

to produce the most accurate representation of BSAFs for PAHs, when k_M is set at intermediate values.

Figures 3-9 and 3-10 depict respective model predictions for three sets of k_M values (low k_M, intermediate k_M and high k_M) with normal bioavailability or low bioavailability due to soot carbon partitioning. k_M values within the ranges reported here result in a 2 to 3 fold reduction in BSAFs for PAHs relative to non-metabolized PCBs. However, with normal bioavailability (i.e., Figure 3-9), the range of model-predicted BSAFs falls above the average observed BSAFs in Kitimat Arm for each PAH congener. Thus, without accounting for soot carbon association, it appears that the model would overpredict BSAFs in Kitimat Arm, even when k_M for each trophic guild is set at the high end of its expected range. When K_{sc} is included in the model using the Best-fit relationship, the range of model predicted BSAFs generally falls about the observed BSAFs for Dungeness crab in Kitimat Arm (refer to Figure 3-10). Intermediate k_M values appear to result in the most accurate representation of BSAFs, when K_{sc} is based on the Best fit relationship.

These results demonstrate that neither soot carbon partitioning alone, nor Phase I metabolism alone, can account for the low magnitude of BSAFs for PAHs in Dungeness crab in Kitimat Arm. Both soot association and Phase I metabolism are instrumental in determining PAH BSAFs for this system.

The dependence of BSAFs for parent PAHs in Kitimat Arm on both Phase I metabolism and soot carbon partitioning is consistent with field observations in Kitimat Arm. Harris (1999) demonstrated that PAH BSAFs for Kitimat Arm Dungeness crabs were three to four orders of magnitude lower than BSAFs for PCBs, compared to the 2-order-of-magnitude difference between PAH and PCBs that is generally reported in the literature. The model results with both these processes combined support this observation. With normal bioavailability, the difference in predicted BSAFs between PAHs and PCBs is more consistent with that reported in the literature (i.e., 2-3 orders of magnitude). The model behaviour also supports the conclusions of Paine et al. (1996) who proposed that

low bioavailability of PAH in Kitimat Arm decreased impacts to the benthic community structure even though PAH concentrations were well above regulatory criteria.k_{phase2}

Figure 3-11 summarizes the results of the sensitivity analysis for k_{phase2}. The model predicts that the body burden of Phase I metabolites is approximately inversely proportional to the rate of Phase II metabolism, especially if k_{phase2} is high relative to k_M. For example, in Dungeness crab, an increase in k_{phase2} from $1 \cdot k_M$ to $10 \cdot k_M$ results in a predicted decrease in the Phase I metabolite concentration from 1.87 ng/g to 0.183 ng/g. For two lower trophic guilds (small infauna and epifauna; large infauna), the Phase I metabolite concentration is less dependent on k_{phase2} when k_{phase2} is low relative to k_M, because elimination via other routes (i.e., gill elimination) have a larger relative effect. For zooplankton, the Phase I metabolite concentrations were not as sensitive to k_{phase2}, likely because gill elimination is the primary elimination route for parent compound and metabolites for this trophic guild (see flux calculations below).

These results highlight the need for further information regarding *in vivo* rates of Phase II metabolism to accurately characterize the body burdens of Phase I metabolites that result from PAH exposure, especially for higher trophic levels.

3.4.2 Model Performance Evaluation

Preliminary predictions of BSAFs for PAHs in Dungeness crab from Kitimat Arm were made by applying the Best-fit K_{sc} relationship and intermediate values for k_M. Figure 3-12 compares model predictions to the observed BSAFs. With this parameter set, model predictions were within one standard deviation of the observed average BSAF for each congener. Model bias ranged from 0.46 to 2.84 with an average value of 0.99 (refer to Figure 3-13). This result indicates that accounting for soot carbon partitioning in Kitimat Arm, and applying non-congener-specific k_M values derived from data available in the literature, resulted in model predictions within a factor of three of observed BSAFs for the PAH congeners examined here.

Figure 3-11: Sensitivity analysis for k_{phase2}. Lines and symbols represent results for Phase I metabolites of benzo(a)pyrene in individual trophic guilds (see Legend).

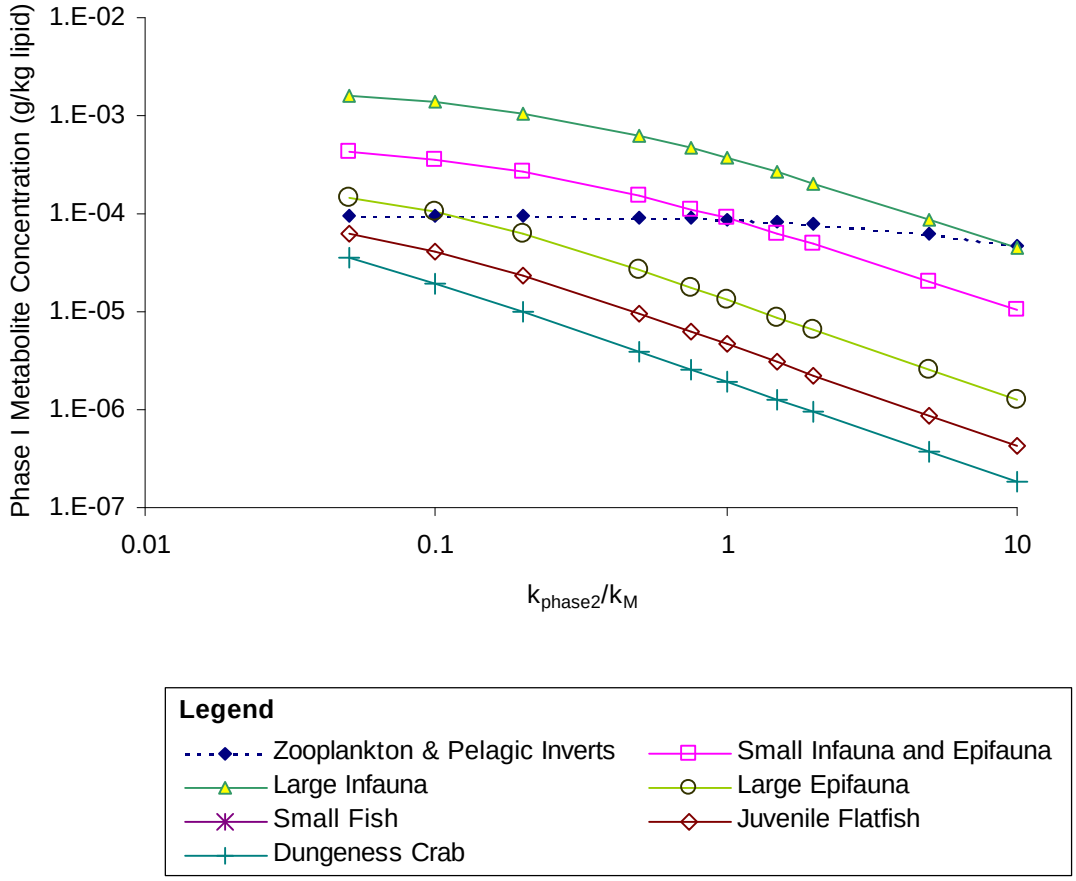

Figure 3-12: Comparison of model-predicted BSAFs, based on intermediate k_M and Best-fit K_{sc}, to observed BSAFs in Kitimat Arm. Symbols represent observed BSAFs for PCBs (◇) and PAHs (□). Lines represent model predictions for PAHs (—) and PCBs (—)

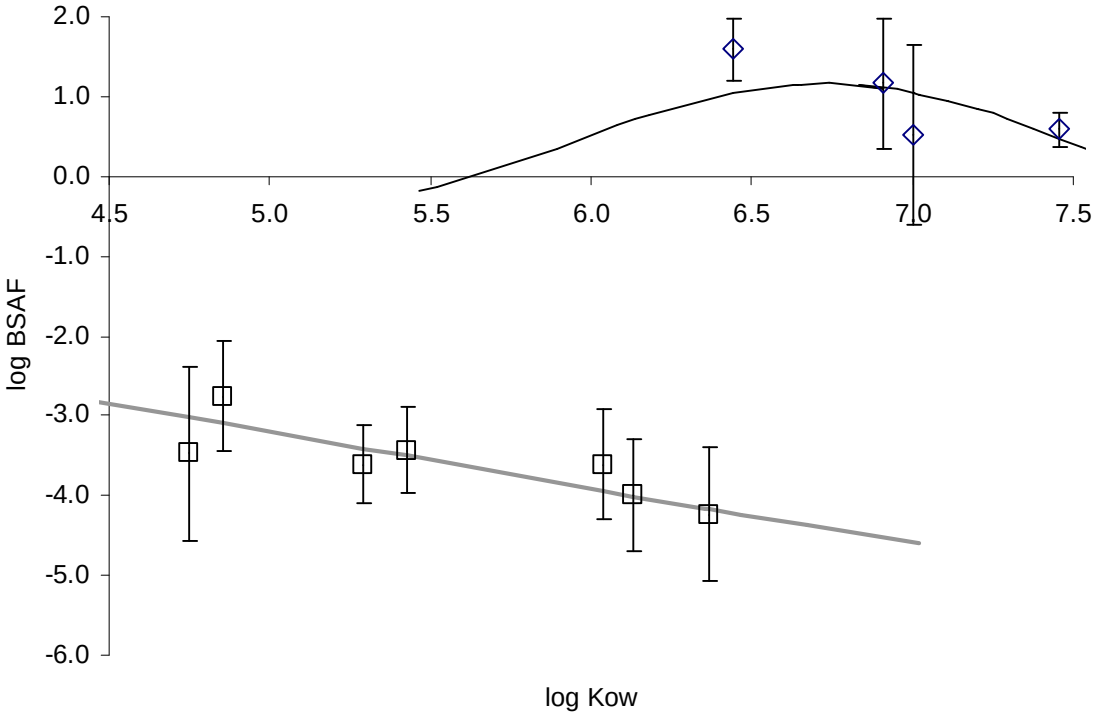

Figure 3-13: Model bias (MB) vs. log K_{ow} for predicted BSAFs of PAHs in Dungeness crab from Kitimat Arm.

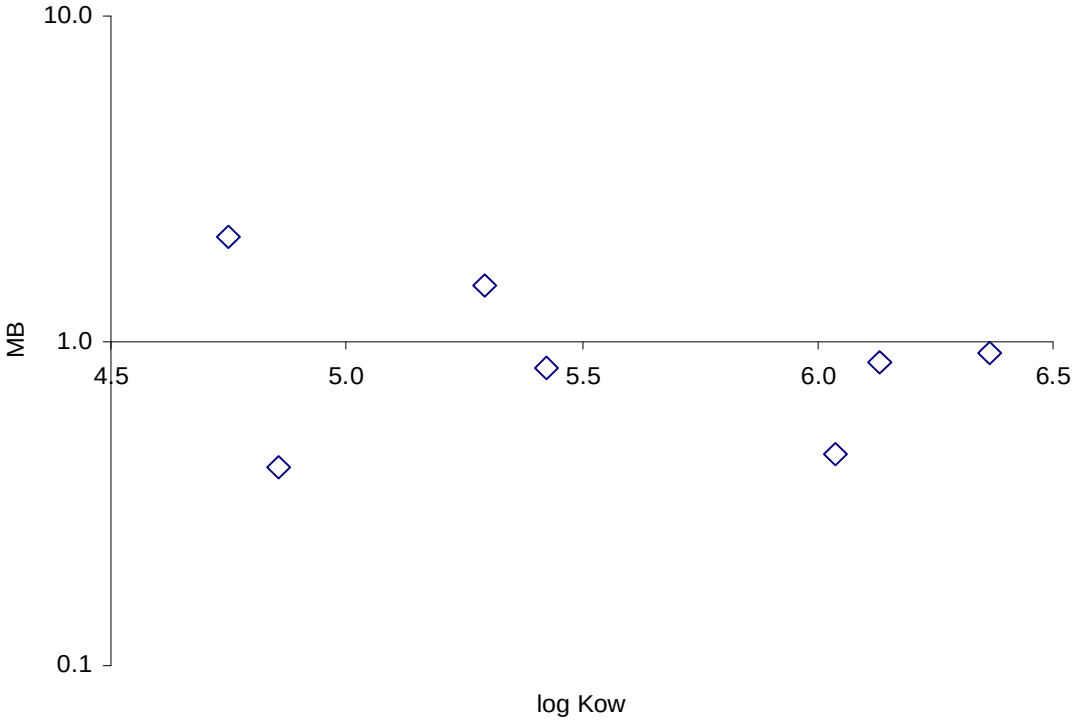

Following this initial model evaluation, the model-fitting exercise for k_M values across all PAH congeners was conducted, where the proportionality of k_M values in trophic guilds, relative to Dungeness crab, was kept constant. The fitted k_M values were virtually the same as the intermediate k_M values derived from literature studies, supporting the validity of the literature-derived values (refer to Table 3-10). The literature values were based primarily on studies with benzo(a)pyrene plus a few additional congeners and are potentially representative of k_M for this congener and other congeners with similar size and structure, assuming similar enzyme affinity.

Tissue burdens of Phase I metabolites have not been determined in Dungeness crab from Kitimat Arm. Consequently, it was not possible to evaluate model performance for Phase I metabolites.

3.4.3 Model Application

Inference of Congener-Specific k_M values

Because there was uncertainty as to the applicability of the non-congener-specific k_M values to PAH congeners with different size and structure, a separate, congener-specific model-fitting analysis was also conducted. Table 3-10 presents the results of this analysis.

Fitted congener-specific k_M values for Dungeness crab ranged from 0.68/day for anthracene to 4.31/day for phenanthrene compared to the non-specific value of approximately 1.5/day that was determined from literature data and combined calibration. As noted above, k_M in other trophic guilds varied in proportion to the values for Dungeness crab. The congener- specific analysis demonstrates the range of variability expected for *in vivo* metabolic rates between the PAHs studied here. For example, in Dungeness crab, this model application suggests that metabolic transformation rates for the PAH congeners examined here would range from 0.68/day to 4.31/day. For other congeners of similar size and structure (i.e., with 3 or more rings), k_M values are also likely to fall within this range.

Table 3-10: Comparison of non-congener-specific k_M values for PAHs to congener-specific k_M values for phenanthrene, anthracene, fluoranthene, pyrene, benz(a)anthracene, chrysene and benzo(a)pyrene. Non-congener-specific values were determined from literature data and model fitting for all congeners. Congener specific values were determined by model fitting for individual congeners.

	Non-congener-specific k_M values		**Congener-specific k_M values**						
Trophic Guild	**Non-congner-specific k_M values**	**Literature-derived Range**	**Phenanthrene**	**Anthracene**	**Fluoranthene**	**Pyrene**	**Benz(a)anthracene**	**Chrysene**	**Benzo(a)pyrene**
zooplankton	0.30	0.2 – 0.4	0.86	0.14	0.26	0.47	0.29	0.15	0.35
small infauna and epifauna	0.59	0.2 – 1.0	1.72	0.27	0.51	0.95	0.58	0.29	0.69
large infauna	0.19	0.15 – 0.30	0.56	0.09	0.17	0.31	0.19	0.09	0.22
large epifauna	0.98	0.5 – 2.5	2.87	0.45	0.85	1.57	0.96	0.48	1.15
small fish	1.96	1 – 3	5.73	0.90	1.70	3.14	1.92	0.97	2.30
juvenile flatfish	1.96	1 – 3	5.73	0.90	1.70	3.14	1.92	0.97	2.30
Dungeness crab	1.48	0.5 – 2.5	4.31	0.68	1.28	2.36	1.44	0.73	1.73

Based primarily on *in vitro* studies, several authors have suggested that higher rates of metabolism are expected for higher molecular weight congeners (for reviews see James, 1989; and Varanasi et al., 1989b). However, the congener-specific calibration results do not support this conclusion. For the seven PAH congeners examined here, there was no apparent increasing trend in k_M with increasing K_{ow} or number of aromatic rings.

Exposure Assessment for Benzo(a)pyrene

Figure 3-14 presents the predicted body burdens of parent benzo(a)pyrene and Phase I metabolites of benzo(a)pyrene in trophic guilds from Kitimat Arm under the two scenarios for k_{phase2} (i.e., $k_{phase2} = 3 \cdot k_M$ and $k_{phase2} = 0.3 \cdot k_M$). Note that only the predicted Phase I metabolite body burdens varied between scenarios because parent PAH concentrations are not dependent on the rate of Phase II metabolism.

Under the first scenario (i.e., $k_{phase2} = 3 \cdot k_M$), the model predicted generally low Phase I metabolite concentrations relative to parent compound. The second scenario (i.e., $k_{phase2} = 0.3 \cdot k_M$) resulted in much higher concentrations of Phase I metabolites with the metabolite concentration exceeding the parent concentration by up to three-fold. These trends were observed for all trophic guilds except zooplankton. For both scenarios, large infauna exhibited the highest body burdens of both benzo(a)pyrene and Phase I metabolites.

The most important generalization that can be made for both scenarios is that, in predatory trophic guilds (i.e., those feeding primarily on other animals rather than phytoplankton and detritus), both parent benzo(a)pyrene concentrations and Phase I metabolite concentrations decrease with increasing trophic status. Based on this observation, neither parent benzo(a)pyrene nor benzo(a)pyrene Phase I metabolites appear likely to undergo food web biomagnification. For lower trophic guilds which feed primarily on phytoplankton and detritus, parent PAH and metabolite body burdens were much higher than for higher trophic guilds.

Figure 3-15 compares the model-predicted fluxes for parent benzo(a)pyrene and PCB-66 in Dungeness crab. For a non-metabolized hydrophobic chemical such as PCB-66, influx of chemical into the organism is dominated by dietary absorption. The low chemical

Figure 3-14: Predicted body burdens of parent B(a)P (light shading) and Phase I B(a)P metabolites (dark shading) in trophic guilds under two representative scenarios. Note differing scales on y-axis.

Scenario 1: Rapid Phase II Metabolism ($k_{phase2} = 3 \cdot k_M$)

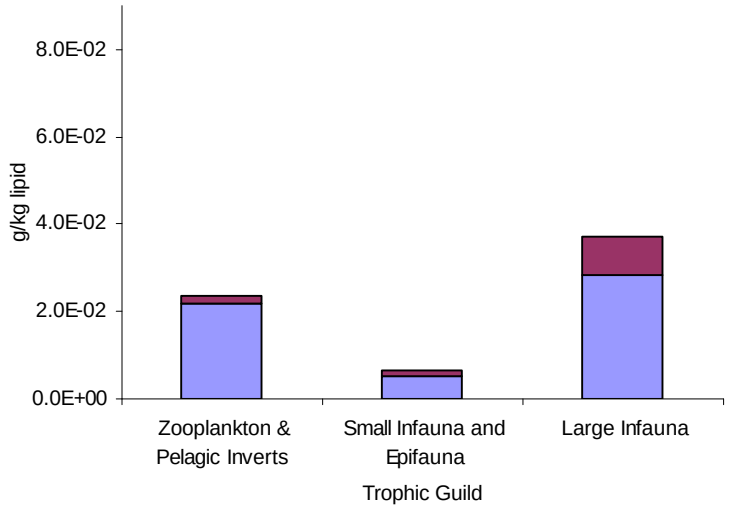

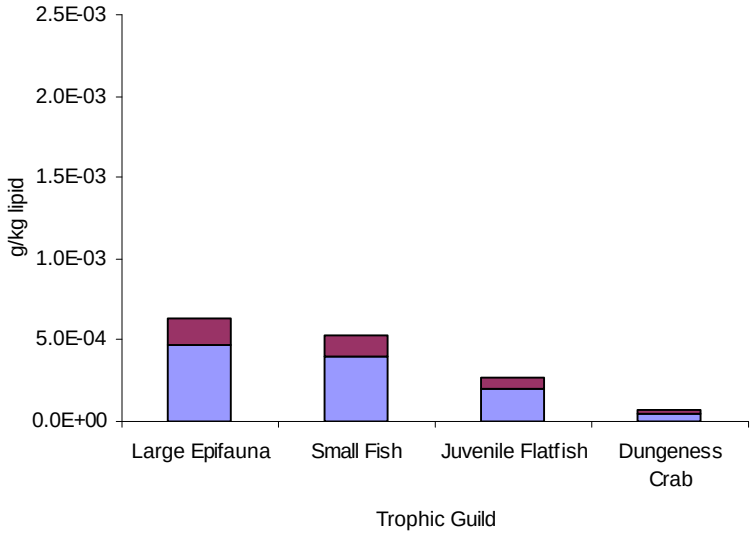

Scenario 2: Slow Phase II Metabolism ($k_{phase2} = 0.3 \cdot k_M$)

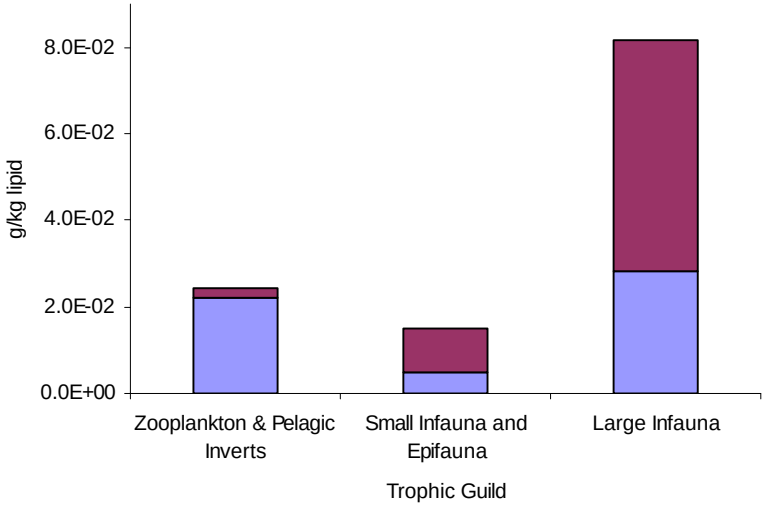

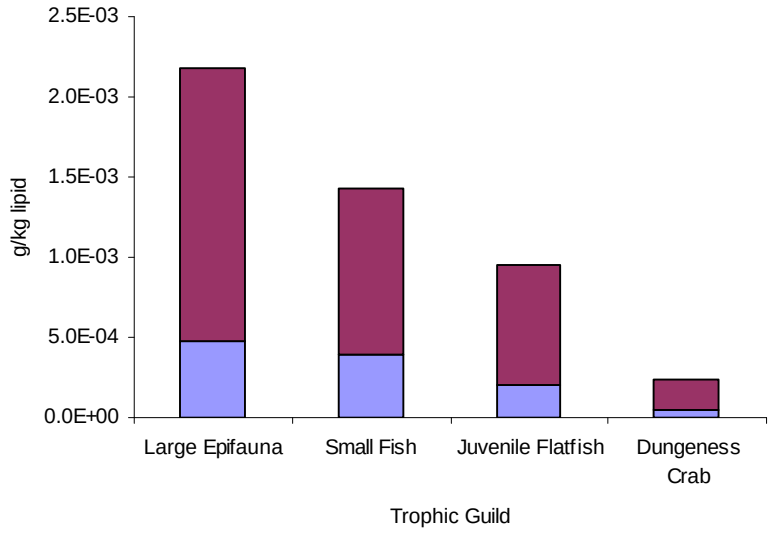

concentration in water (i.e., due to high K_{ow} and sediment-water disequilibrium), means that uptake at respiratory surfaces is low relative to the total chemical flux. The outward flux of chemical results from a combination of growth dilution, faecal egestion and gill elimination, with gill elimination being the most important route. In contrast, gill uptake is the primary route of benzo(a)pyrene accumulation in Dungeness crab, with dietary uptake only 10% of the total influx. Adult Dungeness crab are expected to be primarily predatory, with only incidental sediment ingestion. Thus, the relatively low dietary flux of parent benzo(a)pyrene can be attributed to PAH biotransformation in lower trophic guilds. Phase I metabolism is the predominant route of parent chemical elimination for benzo(a)pyrene, demonstrating the importance of metabolism for reducing body burdens of this chemical. The relatively large k_M in Dungeness crab results in a predicted BSAF for benzo(a)pyrene of 0.00007, compared to a BSAF of 11.5 for PCB-66.

Figure 3-16 summarizes parent compound fluxes for benzo(a)pyrene and PCB-66 in large epifauna. The uptake and elimination fluxes of PCB-66 for this trophic guild have similar proportions to Dungeness crab with the dietary route dominating uptake, and gill surfaces dominating elimination. Dietary uptake of parent benzo(a)pyrene plays a larger role in chemical influx relative to that predicted in Dungeness crab. Large epifauna are expected to feed lower in the food web than Dungeness crab, consuming a combination of detritus and smaller benthic invertebrates. Thus, the higher dietary influx of benzo(a)pyrene is due to its high concentration in detritus (i.e., where metabolism is not occurring), and lower rates biotransformation in lower trophic guilds. Again, Phase I metabolism is predicted to be the primary route of elimination for benzo(a)pyrene.

Table 3-11 summarizes the estimated fluxes of benzo(a)pyrene for all trophic guilds in Kitimat Arm. In general, model predictions for these organisms exhibited similar trends in influx and outflux with the dietary route becoming progressively more significant in lower trophic guilds feeding on detritus. The highest total flux was observed for zooplankton, followed by large infauna. Both of these trophic guilds ventilate large volumes of water relative to their size and feed primarily on detritus (where biotransformation does not occur) resulting in significant benzo(a)pyrene uptake via

Figure 3-15: Comparison of model-predicted parent compound fluxes for benzo(a)pyrene and PCB-66 in Dungeness crab from Kitimat Arm.

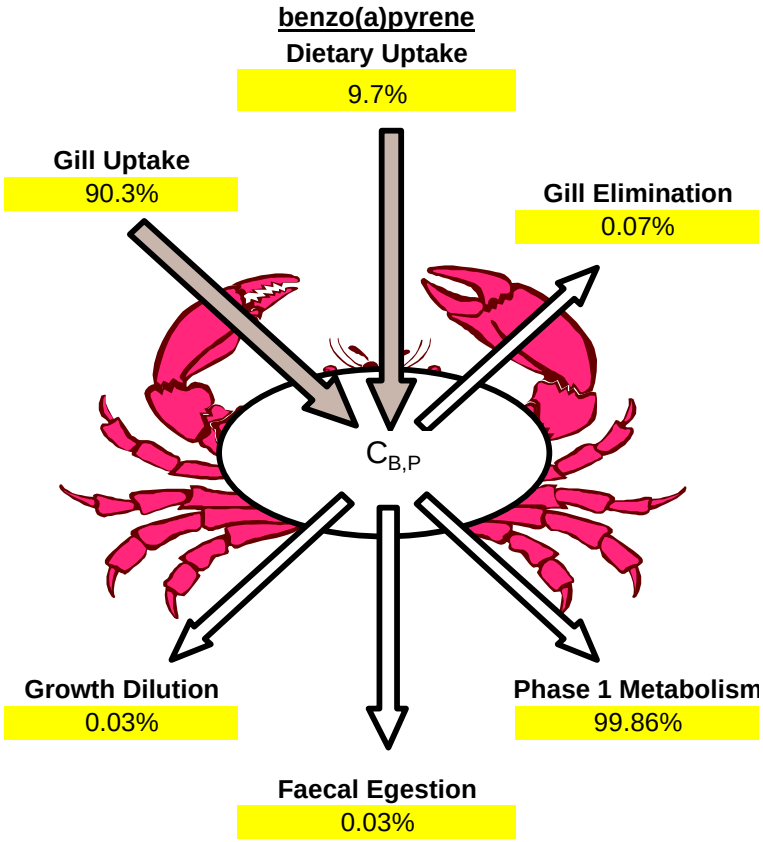

Sediment Concentration: 9610 ng/g

Tissue Concentration: 1.82 ng/g

BSAF: 6.75x10-5

Total Chemical Flux: 2.74 ng/g/day

Sediment Concentration: 1.8x10-2 ng/g

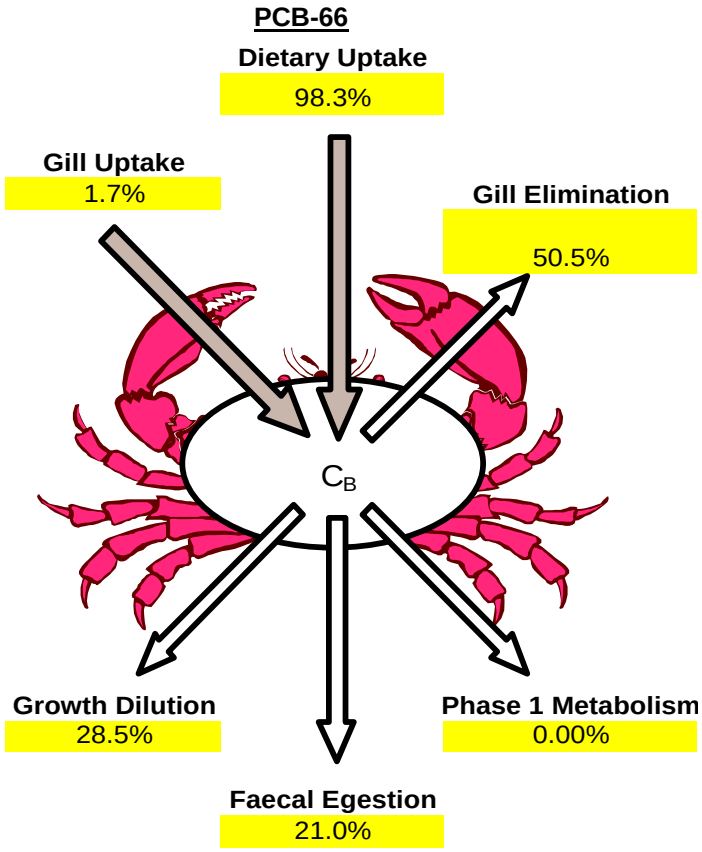

Tissue Concentration: 0.57 ng/g

BSAF: 11.4

Total Chemical Flux: 1.06x10-3 ng/g/day

Figure 3-16: Comparison of model-predicted parent compound fluxes for benzo(a)pyrene and PCB-66 in large epifauna from Kitimat Arm.

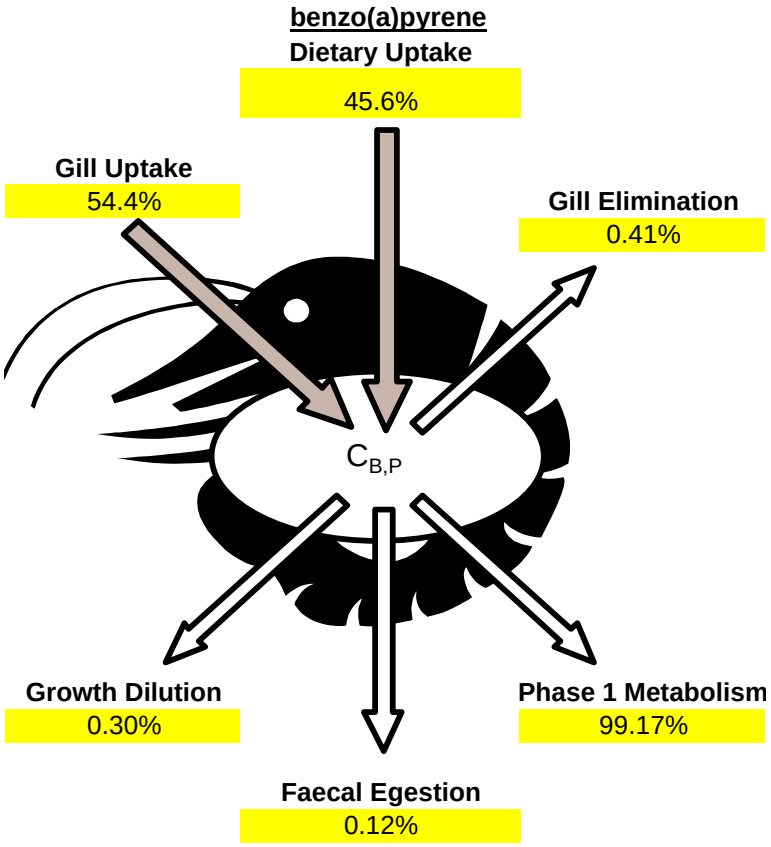

Sediment Concentration: 9610 ng/g

Tissue Concentration: 12.23 ng/g

BSAF: 0.006

Total Chemical Flux: 12.3 ng/g/day

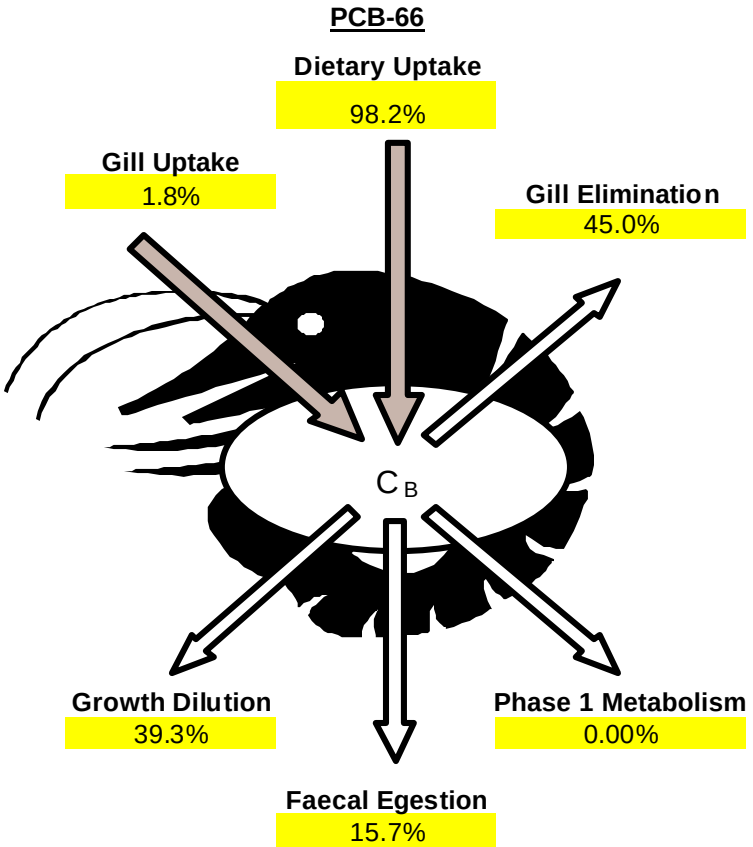

Sediment Concentration: : 1.8x10-2 ng/g

Tissue Concentration: 0.34 ng/g

BSAF: 9.30

Total Chemical Flux: 2.62×10^{-3} ng/g/day

Table 3-11: Summary of model-predicted BSAFs, total chemical fluxes, and proportion of flux associated with gill uptake, dietary uptake, gill elimination, faecal egestion, growth dilution and Phase I metabolism, for benzo(a)pyrene in trophic guilds of Kitimat Arm.

	Dungeness crab	juvenile flatfish	large epifauna	small fish	large infauna	small infauna and epifauna	zooplankton
Predicted BSAF	$6.75 \cdot 10^{-5}$	0.0003	0.0006	0.0005	0.037	0.007	0.03
Total Chemical Flux (ng/g/d)	2.74	8.51	12.3	28.5	123	65.6	375
Gill Uptake	90.3%	79.5%	54.4%	61.3%	51.8%	8.8%	65.5%
Dietary Uptake	9.7%	20.5%	45.6%	38.7%	48.2%	91.2%	34.5%
Gill Elimination	0.07%	0.25%	0.41%	0.39%	23.3%	0.71%	22.8%
Faecal Egestion	0.03%	0.04%	0.12%	0.07%	0.65%	0.59%	1.79%
Growth Dilution	0.03%	0.04%	0.30%	0.07%	3.0%	1.14%	4.7%
Phase 1 Metabolism	99.9%	99.7%	99.2%	99.5%	73.1%	97.6%	70.7%

Table 3-12: Summary of model-predicted BSAFs, total chemical fluxes, and proportion of flux associated with gill uptake, dietary uptake, gill elimination, faecal egestion, growth dilution and Phase I metabolism, for PCB-66 in trophic guilds of Kitimat Arm.

	Dungeness crab	juvenile flatfish	large epifauna	small fish	large infauna	small infauna and epifauna	zooplankton
Predicted BSAF	11.36	8.19	9.29	1.30	1.72	7.21	0.51
Total Chemical Flux (ng/g/d)	$1.06 \cdot 10^{-03}$	$1.46 \cdot 10^{-03}$	$2.62 \cdot 10^{-03}$	$6.11 \cdot 10^{-04}$	$2.46 \cdot 10^{-03}$	$3.07 \cdot 10^{-03}$	$3.15 \cdot 10^{-03}$
Gill Uptake	1.7%	3.3%	1.8%	20.5%	18.6%	1.4%	55.9%
Dietary Uptake	98.3%	96.7%	98.2%	79.5%	81.4%	98.6%	44.1%
Gill Elimination	50.5%	72.0%	45.0%	70.4%	84.4%	25.9%	74.9%
Faecal Egestion	21.0%	13.8%	15.7%	14.0%	2.7%	24.7%	6.7%
Growth Dilution	28.5%	14.2%	39.3%	15.6%	12.9%	49.4%	18.4%
Phase 1 Metabolism	0.0%	0.0%	0.0%	0.0%	0.0%	0.0%	0.0%

respiratory surfaces and the diet. In addition, for these two trophic guilds, benzo(a)pyrene elimination via biotransformation was less significant relative to other trophic guilds. The low k_M values for these trophic guilds likely cause other elimination routes to be more significant. This combination of high exposure and lower metabolic transformation rates explains why zooplankton and large infauna have the highest predicted body burdens of parent benzo(a)pyrene.

In contrast, for PCB-66, dietary uptake is the most important uptake route for all trophic guilds because PCB-66 is eliminated slowly by most organisms (refer to Table 3-12). Elimination of PCB-66 occurs via a combination of gill elimination, faecal egestion and growth dilution rather than metabolic transformation (k_M is zero for this chemical).

The fluxes of Phase I benzo(a)pyrene metabolites in Dungeness crab under the two scenarios are summarized in Figure 3-17. Under Scenario 1 where k_{phase2} is relatively high, the flux of Phase I metabolites into the organism is primarily via Phase I metabolism of parent chemical, with dietary uptake of Phase I metabolites comprising only a small percentage of the total influx. Phase I metabolites are eliminated primarily via Phase II metabolism due to the high rate constant for this pathway, compared to other elimination routes. As demonstrated above, under this scenario the body burden of Phase I metabolites is low relative to the parent chemical concentration.

With Scenario 2 where k_{phase2} is low relative to k_M, Phase I metabolite influx in Dungeness crab is still dominated by parent compound biotransformation but dietary uptake of metabolites is somewhat more significant. In addition, the rate of Phase II metabolism is lower relative to other metabolism processes, meaning that gill elimination constitutes a higher proportion of the total outflux.

Table 3-13 summarizes the Phase I metabolite fluxes for benzo(a)pyrene in each trophic guild, under the two scenarios. For Scenario 1, all trophic guilds except zooplankton displayed the same pattern as Dungeness crab with the influx of Phase I metabolites dominated by parent compound biotransformation within the organism and outflux

Figure 3-17: Comparison of fluxes for Phase I metabolites of benzo(a)pyrene in Dungeness crab under two representative scenarios.

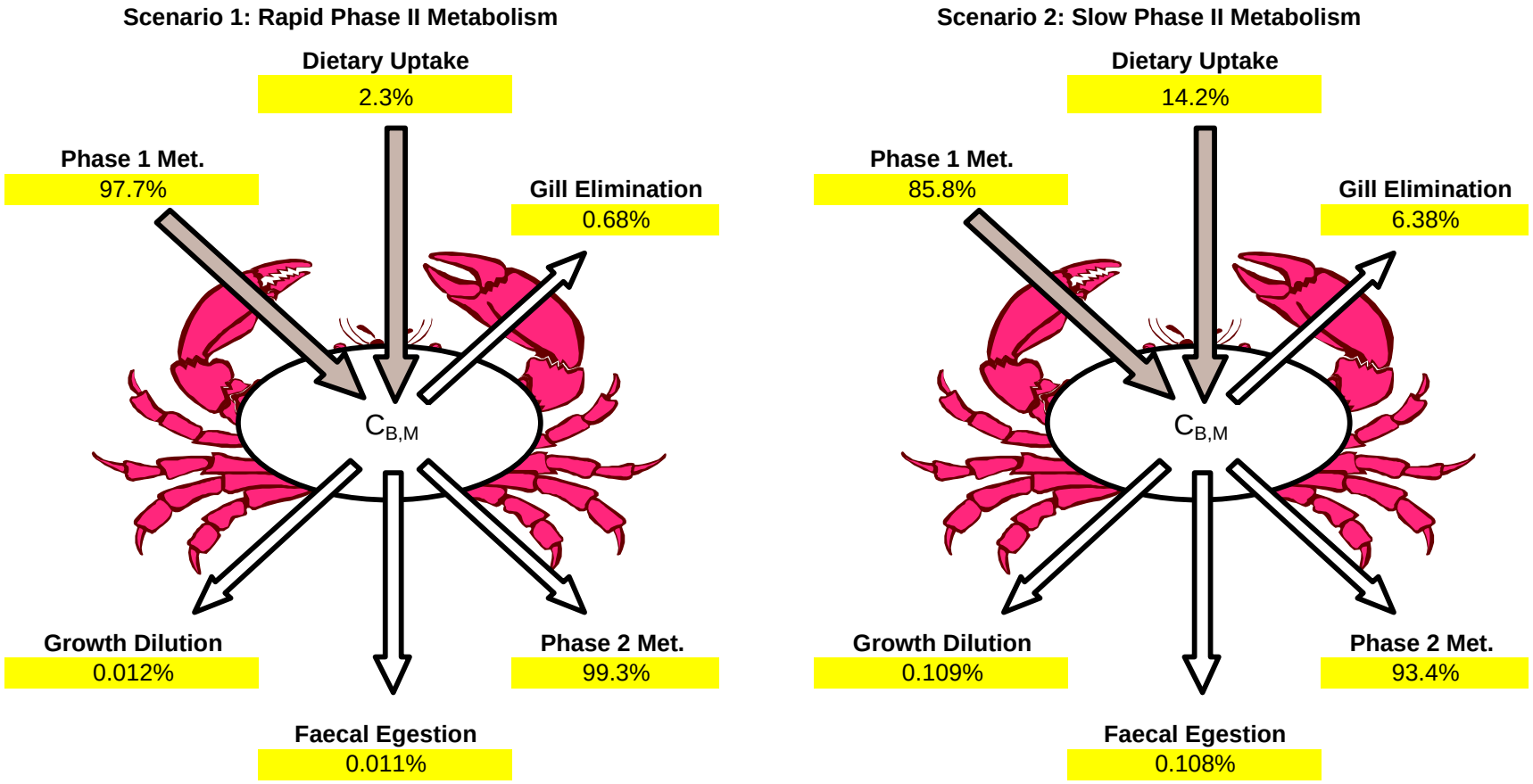

Table 3-13: Summary of model-predicted fluxes and proportion of fluxes associated with gill uptake, dietary uptake, gill elimination, faecal egestion, growth dilution and Phase I metabolism, for Phase I metabolites of benzo(a)pyrene in trophic guilds of Kitimat Arm, under two scenarios.

(a) Rapid Phase II Metabolism

	Dungeness crab	juvenile flatfish	large epifauna	small fish	large infauna	small infauna and epifauna	zooplankton
Phase I Metabolite Flux (ng/g/d)	2.8	9.03	29.5	13.2	90	64.4	267
Phase 1 Metabolism	97.7%	94.0%	92.4%	96.0%	100.0%	99.3%	99.6%
Dietary Uptake	2.3%	6.0%	7.6%	4.0%	0.0%	0.7%	0.4%
Phase 2 Met	99.3%	97.7%	96.2%	96.5%	92.8%	93.3%	24.8%
Gill Elimination	0.68%	2.32%	3.67%	3.50%	5.6%	6.3%	74.3%
Faecal Egestion	0.01%	0.02%	0.05%	0.03%	0.4%	0.0%	0.3%
Growth Dilution	0.01%	0.01%	0.10%	0.02%	1.3%	0.4%	0.6%

(b) Slow Phase II Metabolism

	Dungeness crab	juvenile flatfish	large epifauna	small fish	large infauna	small infauna and epifauna	zooplankton
Phase I Metabolite Flux (ng/g/d)	3.19	11.8	30	18.5	90	65.7	267
Phase 1 Metabolism	85.8%	71.7%	66.1%	94.5%	100.0%	97.4%	99.5%
Dietary Uptake	14.2%	28.3%	33.9%	5.5%	0.0%	2.6%	0.5%
Phase 2 Met	93.4%	80.6%	71.6%	73.1%	56.2%	58.4%	3.2%
Gill Elimination	6.38%	19.1%	27.3%	26.5%	33.9%	39.4%	95.7%
Faecal Egestion	0.11%	0.15%	0.39%	0.21%	2.2%	0.0%	0.3%
Growth Dilution	0.11%	0.11%	0.72%	0.18%	7.7%	2.3%	0.7%

dominated by Phase II metabolism. This first scenario is most likely to represent the situation in many natural systems where relatively fast Phase II metabolism results in rapid elimination and very low dietary fluxes of Phase I metabolites.

Under Scenario 2, dietary uptake of Phase I metabolites constitutes a larger proportion of the total metabolite influx in the higher trophic guilds which feed primarily on other organisms. As with Dungeness crab, gill elimination is a more significant flux out of the organisms. Scenario 2 represents a *special-case* in natural systems where the Phase II pathway is potentially overwhelmed due to Phase I induction and/or very high exposure to PAHs.

For zooplankton, the outflux of Phase I metabolites is dominated by gill elimination under both scenarios. This explains why the predicted metabolite body burden for this trophic guild is not as dependent on k_{phase2}, relative to other trophic guilds (refer to Figures 3-11 and 3-14). Although large infauna have a small total flux of Phase I metabolites under both scenarios, gill elimination is less significant than for zooplankton. Combined with the high exposure to and body burdens of parent benzo(a)pyrene, this causes the higher metabolite body burdens that are predicted by the model (refer to Figure 3-14).

It is noteworthy that for both scenarios the influx of Phase I metabolites (i.e., the potential cause of PAH carcinogenesis) is dominated by biotransformation of parent compound within an organism, rather than food web exposure and dietary uptake. This model behaviour suggests that in natural situations, metabolic transformation of parent PAHs will cause trophic dilution of parent PAHs and Phase I metabolites even under conditions of Phase I induction or Phase II limitation.

3.5 CONCLUSION

This analysis describes the application of mechanistic food web modelling to predict the bioaccumulation of PAHs in a representative benthic food web of the BC Coast. Incorporating soot-partitioning and PAH metabolism into the BSAF model results in a reasonably accurate representation of PAH BSAFs for Kitimat Arm. In addition, the

evaluative application of the mass balance model for Phase I metabolites integrates knowledge of metabolic processes and highlights areas where further study is needed. By conducting sensitivity analysis it has been possible to determine important factors affecting exposure of benthic fish and invertebrates to PAH and PAH metabolites.

While several studies describe models of bioaccumulation of non-metabolized substances such as PCBs, few authors have extended this approach to predict BSAFs for PAHs in organisms where significant PAH metabolism is expected. One notable exception is Thomann and Komlos (1999), who developed a model for PAH BSAFs in a simple freshwater food chain and applied it in an evaluative fashion to explore how factors such as PAH bioavailability, uptake efficiency and metabolism affected resultant BSAFs. I know of no previous attempts at modelling the steady state mass balance of PAH metabolites in aquatic organisms. Therefore, this is an important first step for exposure assessment of both PAH and PAH metabolites.

In general, the k_M values based on literature studies and combined calibration (i.e., ignoring congener-specific factors) appear to provide a reasonable approximation of the metabolic transformation rates for PAHs in marine organisms. The ability of a non-specific k_M value to reasonably predict BSAFs in Dungeness crab lends support to the hypothesis that PAH metabolism *in vivo* is dependent not only on enzyme affinity for particular substrates, but also other factors such as the availability of chemical substrates which partition strongly to lipid phases.

As expected from previous studies (Parkerton, 1993; Tracey and Hansen, 1996), the model predicts a decline in BSAFs for parent PAHs with increasing trophic status of predatory benthic organisms which feed primarily on other organisms rather than detritus (refer to Figure 3-16). Comparison of parent chemical flux for benzo(a)pyrene and PCB-66 demonstrates that parent PAHs is rapidly biotransformed by Phase I metabolism in all modelled organisms, reducing parent PAH concentrations and resulting food web transfer of parent chemical. The predicted parent PAH BSAF was highest in large infauna which are representative of detritus-feeding bivalve mollusks. Bivalve mollusks generally have

low metabolic rates relative to other organisms resulting in slower PAH elimination via biotransformation and higher overall accumulation. This model result supports the continued use of bivalve mollusks such as mussels as sentinel species for biomonitoring of PAH contamination, since they are likely to accumulate the highest body burdens of these chemicals.

The evaluative analysis for Phase I metabolites of benzo(a)pyrene was useful to evaluate the expected ecosystem behaviour under various conditions (i.e., rapid Phase II metabolism and low Phase II metabolism). For both cases, the predicted lipid-normalized body burden of Phase I metabolites declined with increasing trophic level in the model food web, although predicted body burdens were much higher in all trophic guilds under the second scenario (refer to Figure 3-16). The explanation for the lack of food web transfer of Phase I metabolites is that the influx of these constituents is generally dominated by Phase I metabolism of parent compound rather than dietary uptake of metabolites. For trophic guilds in the model, the Phase I pathway constituted over 90% of the metabolite influx under the rapid Phase II scenario and at least 66% of the metabolite influx under the Phase II limitation scenario. Thus, the body burden of Phase I metabolites is expected to depend primarily on uptake and subsequent biotransformation of parent chemical. The decline in parent chemical body burdens with increasing trophic status results in a parallel decline in Phase I metabolites.

Although the flux calculations for both parent chemical and Phase I metabolites focussed on the food web dynamics of benzo(a)pyrene, the conclusions drawn from the analysis are expected to have general applicability to other PAHs, especially those with similar K_{ow} to benzo(a)pyrene. For lower K_{ow} PAHs, dietary uptake of parent chemical would be lower than for benzo(a)pyrene and gill absorption would therefore become more significant in lower trophic guilds. Likewise gill elimination may be a more significant route of depuration of parent chemical and Phase I metabolites, although the high rate of Phase II metabolism expected under normal conditions is still likely to dominate elimination kinetics.

In addition to making predictions of BSAFs for PAHs and examining metabolite dynamics, this study integrates existing knowledge relating to bioaccumulation modelling of PAHs and highlights important uncertainties. While the addition of soot carbon partitioning and PAH metabolism resulted in accurate prediction of PAH BSAFs in Dungeness crab, there are significant uncertainties associated with the submodels for each of these processes. Due to a lack of data for PAHs dissolved in surface waters and porewaters of Kitimat Arm, it was not possible to directly validate the model-predicted bioavailability in these media. Thus, further field measurement would be necessary to test the accuracy of this submodel and potentially calibrate it to better represent the environmental condition in Kitimat Arm.

The literature-derived k_M values used in the BSAF model varied among trophic guilds. However, because, BSAF data for PAHs and PCBs were only available for Dungeness crab, model predictions and k_M values could only be validated for this trophic guild. There were no data to test model predictions for lower trophic guilds and consequently there is high uncertainty in the validity of the k_M values selected for these organisms. It is possible that alternate combinations of values for k_M in the lower trophic guilds would still result in similar dietary PAH exposure in Dungeness crab, resulting in similar BSAFs. Collection of additional BSAF data for these trophic guilds would allow for complete validation of model predictions.

It is also important to note that aside from enzyme activity and induction studies conducted primarily with benzo(a)pyrene, there is a paucity of studies that have examined the factors affecting realized rates of PAH Phase I metabolism, especially for other congeners. While the published radiolabel studies provide some information, these studies need to be augmented to include measurements of the time course of PAH uptake and metabolism, estimates of metabolite and parent compound elimination during the exposure period, and PAH congeners with a variety of structures. The combination of exposure studies and mechanistic modeling applied by van der Linde et al. (2001) and others is also a potentially effective approach.

The evaluative analysis of metabolism highlights important uncertainties which preclude prediction of Phase I metabolite body burdens. Metabolite concentrations in tissues have generally not been measured in field collected marine organisms due to analytical constraints. While several researchers (e.g., Krahn et al., 1986; Collier and Varanasi, 1991) have used bile fluorescence as a surrogate for PAH metabolite body burdens, the concentration of metabolites in bile is a function of the feeding status of the organism. Furthermore, the presence of metabolites in fish bile is an indicator of what is being eliminated from the fish rather than the internal concentration of potentially toxic Phase I metabolites.

The laboratory studies with radiolabelled chemicals have provided useful "ballpark" estimates of k_M for representative marine organisms. However, there are few *in vivo* studies that allow estimation of Phase II rate constants for PAHs. Because of the lack of body burden data for Phase I metabolites and lack of information for *in vivo* Phase II metabolic rates, it is not currently possible to validate the mass balance model for Phase I metabolites. Further research is needed to improve understanding of the Phase II metabolic pathway.

4 CONCLUSION AND IMPLICATIONS FOR RISK ASSESSMENT

This research has demonstrated the application of mechanistic environmental modelling to assess the exposure of benthic marine organisms to non-metabolized and metabolized persistent organic pollutants. Human health and ecological risk assessment methods involve the integration of an exposure profile and toxicological response relationship in order to characterize risks to receptors of concern (USEPA, 1998). For bioaccumulative chemicals, assessment of toxicological responses in ecological receptors is generally based on internal body residues, whereas for human receptors they are generally based on dietary consumption levels. The modelling approach applied here represents the exposure assessment phase of risk assessment and is a critical step to characterizing the human health and ecological risks of persistent organic pollutants such as PCBs and PAHs that are present in marine systems.

4.1 KEY CONCLUSIONS

The model developed for PCBs in Chapter 2 augments the current methods for predicting bioaccumulation of non-metabolized substances in aquatic systems (e.g., Gobas, 1993; Morrison et al., 1996; Connolly, 1991) by integrating a bioenergetic feeding model, quantitatively evaluating gastrointestinal magnification, and applying a strategy for estimating sediment-water disequilibrium (devised by Gobas and Maclean, 2003) in the absence of measured water concentrations. The calibrated model provides a reasonably accurate representation of PCB bioaccumulation in benthic organisms with model-predicted BSAFs within a factor of four of observed values for Dungeness crab, the upper trophic-level receptor of interest. Model calibration results indicate that the dietary transfer efficiency of neutral hydrophobic chemicals begins to decline at a lower K_{ow} than that indicated by laboratory studies, an observation also made by Connolly (1991).

The model development and application for PAHs in Chapter 3 integrates strategies for quantifying reduced bioavailability due to soot carbon partitioning, metabolic transformation of parent chemicals and the mass balance of potentially toxic metabolites. By incorporating the soot carbon model of Gustaffson et al (1997) and k_M values for PAHs that can be derived from laboratory studies reported in the literature, the model

produces a reasonably accurate representation of PAH BSAFs for Kitimat Arm. A non-congener-specific k_M value for PAHs in Dungeness crab of 1.48/day resulted in the *best-fit* to observed BSAF data in Kitimat Arm, and was also consistent with k_M values derived from literature data. k_M values for other benthic organisms were expected to be higher for fish species and lower for lower level invertebrates. With these k_M values, the model predicts a decline in BSAFs for parent PAHs with increasing trophic status of predatory benthic organisms which feed primarily on other organisms rather than detritus.

The mass balance model for Phase I metabolites of PAHs is a novel approach to assessing the potential metabolic burden of PAH Phase I metabolites which cause toxic carcinogenesis and other toxic effects. Despite uncertainty in metabolite behaviour and rates of Phase II conjugation reactions, it was possible to draw general conclusions by applying the model in an evaluative fashion. Under two scenarios representing either rapid Phase II reactions or Phase II limitation, the predicted lipid-normalized body burden of Phase I metabolites declined with increasing trophic level in the model food web, although predicted body burdens were much higher in all trophic guilds under the second scenario. Thus, based on the model application for PAHs, it can be hypothesized that both parent PAHs *and* Phase I metabolites of PAH are expected to undergo trophic dilution, exhibiting a decrease in lipid-normalized concentrations with increasing trophic status.

Despite some significant uncertainties in metabolic processes, the model development and application in Chapter 3 represents a viable assessment strategy for predicting food web bioaccumulation of parent PAHs, resultant exposure, and metabolite formation for marine benthic organisms. Accordingly, it has potential application in exposure assessment for human health risk assessment and ecological risk assessment. An important gap in knowledge that must be addressed to facilitate this application is the estimation of rate constants for the Phase II metabolic pathway.

4.2 IMPLICATIONS FOR RISK ASSESSMENT

The models developed here focus on exposure assessment of PAHs and Phase I metabolites. The next phase for risk assessment is to evaluate the toxicological

significance of predicted body burdens of parent PAHs and metabolites. This is an area of uncertainty and ongoing research, especially for toxic effects in ecological receptors. The significance of PAH bioaccumulation and metabolism to ecological and human health risks is discussed briefly in the following sections.

4.2.1 Ecological Significance

Because they are rapidly metabolized, the more hydrophobic PAH congeners (i.e., those with three or more rings) are unlikely to cause acute toxicity at typical environmental concentrations (Eisler, 1987; CEPA, 1994). However, as discussed herein, metabolic pathways may lead to reactive intermediates which can cause toxic effects through binding to DNA or other cellular macromolecules. Studies with rodents suggest that benzo(a)pyrene and benz(a)anthracene exert carcinogenic effects only after metabolic activation (Varanasi et al., 1989b)

For marine organisms, most studies of toxic effects due to PAH exposure have been with flatfish such as English sole displaying hepatic tumours and liver disease. The first reports of liver neoplasia in Puget Sound flatfish occurred in the 1970s (Baumann, 1989). Since then, a wealth of research has been conducted to (i) link liver disease to chemical contaminants in sediments (e.g., Malins et al, 1985; Reichert et al., 1998), (ii) determine that PAHs are one of the major causes of liver carcinogenesis in flatfish (e.g., Malins et al., 1985; Reichert et al., 1998); and (iii) develop biomarkers which indicate exposure to PAHs and probable metabolic stress (e.g., Krahn et al., 1986; Myers et al., 1998a). Krahn et al. (1986) developed methods to identify PAH metabolites in fish bile as an indicator of PAH exposure and found a significant correlation with liver lesions suggesting PAHs as a causative agent. Collier and Varanasi (1991) conducted laboratory exposures of English sole to PAHs and found that both bile metabolite concentrations and liver metabolic activity were related to PAH exposure suggesting a link between sediment PAHs and metabolic activation of accumulated PAH chemicals. In addition, French et al. (1996), Myers et al. (1998b) and Reichert et al. (1998) each described statistical associations between sediment PAH concentrations, metabolites in bile, liver metabolic activity, DNA adduct formation, and resulting liver lesion prevalence.

In general these studies provide a weight of evidence supporting the mode of action for PAH carcinogenesis described by Varanasi et al. (1989a) whereby PAHs are taken up into fish and then transformed by Phase I metabolic processes. Reactive metabolites formed by Phase I processes which are not rapidly conjugated may form DNA adducts through covalent binding. The formation of DNA adducts leads to the formation of degenerative/necrotic liver lesions which lead to lesion prevalence and advanced liver disease. Myers et al. (1998a) used stepwise logistic regression to formulate risk factors for lesion prevalence and found that the presence of DNA adducts was the strongest predictor of lesion occurrence. This conclusion is supported by Shaw and Connel (2001) who reported that for aquatic species, DNA adducts produce better correlation with PAH exposure than internal parent PAH residues. In addition, Myers et al, (1998b) demonstrated that the occurrence of liver lesions in juvenile fish was lower than that reported in adult fish. Liver lesions may result from long-term chronic exposure to PAH and the resulting presence of reactive metabolites. Over the longer time period, there is a higher probability that DNA repair mechanisms will be unable to repair all accumulated DNA adducts.

While PAH-induced carcinogenesis in marine flatfish has been studied extensively there has been only limited study of PAH metabolite-related effects in marine invertebrates. Fossi et al. (1997) evaluated a multi-biomarker approach to assessing contaminant exposure and effects in the Mediterranean crab (*Carcinus aestuarii*) and found that benzo(a)pyrene exposure resulted in elevated mixed-function oxidase activity and DNA damage. Given that similar biomarker responses are known to be associated with liver lesions in flatfish, it is reasonable to presume a potential for hepatic disease in crabs resulting from PAH uptake and metabolism. This presumption is supported by the results of Shaw and Connell (2001) who found similar levels of DNA adducts in crabs and fish collected from a PAH-contaminated creek in Australia.

Although there is strong statistical evidence linking carcinogenesis to PAH metabolism and DNA adduct formation in aquatic organisms, no authors have explicitly formulated a

causative dose response relationship for either DNA adduct formation or lesion prevalence based on tissue burdens of parent PAHs and metabolites. Bile metabolites indicate PAH exposure and subsequent transformation, but bile metabolite concentrations depend on both exposure levels and the feeding status of the organism, and generally do not correlate with sediment PAH concentrations (Baumann, 1989). Furthermore, metabolites in bile are an indicator of effective Phase II metabolism and excretion of reactive Phase I metabolites and may not accurately reflect the body burden of Phase I metabolites.

Finally, Bailey et al (1989) state that: “demonstration of cause and effect (for PAH exposure and hepatic disease) would require that the suspect etiological agents be show to induce tumors in the appropriate host organ under exposure protocols and doses which mimic environmental conditions...” To date this research has not been conducted. Development of a dose-response for PAH metabolite carcinogenesis is further complicated by factors affecting tumor formation such as age at exposure, route of exposure, genetic variation nutrition, growth rate, nutrient and non-nutrient carcinogen modulators and water temperature (Bailey et al., 1989).

Despite the lack of a dose-response relationship for PAH metabolites, it *is* possible to use the model results to make comparative predictions of risks between trophic levels. One of the central beliefs in toxicology is the idea that “the dose makes the poison” (Paracelsus, *circa* 1500). While there is some evidence to suggest that hormesis occurs for low level doses of a wide range of toxicants (Calabrese and Baldwin, 2003), above these levels, the degree of ecological impairment is generally related to toxicant concentration and availability at an active site (McCarty and Mackay, 1993). Accordingly, as PAH exposure increases, increased levels of DNA adducts and incidence of hepatic disease are expected. Given that these biomarker responses and biological effects are related to an increase in certain Phase I metabolites, such as the 7,8 diol of benzo(a)pyrene, the production and resultant tissue residue of Phase I metabolites can be used as an indicator of carcinogenic stress and resultant ecological risk.

The predicted tissue residue of Phase I metabolites of benzo(a)pyrene in trophic guilds from Kitimat Arm are presented for two scenarios (i.e., rapid Phase II metabolism and slow Phase II metabolism) in Figure 4-1. Metabolite residues are highest in the lower trophic guilds which feed exclusively on phytoplankton and detritus, food resources in which parent PAHs are not biotransformed. Of the three lower trophic guilds, large infauna exhibit the highest tissue residues of Phase I metabolites of benzo(a)pyrene. For higher trophic guilds (i.e., those feeding primarily on other organisms rather than detritus), Phase I metabolite concentrations are lowest in the highest trophic levels (juvenile flatfish and Dungeness crab).

Based on these predictions, the risk of carcinogenesis and other PAH-metabolite-mediated effects can generally be expected to be highest in large infauna (i.e., bivalve mollusks) but then decrease with increasing trophic status in higher trophic guilds. The model results therefore suggest that PAH metabolism not only prevents parent compound biomagnification but may also reduce the dose of PAH metabolites and resultant ecological risks to higher trophic levels such as Dungeness crab. It is important to note that this conclusion is a broad generalization and individual species sensitivity may have a large impact on actual risks to marine organisms. For example, English sole occupy the trophic guild just below adult Dungeness crab but have very high sensitivity to PAH carcinogenesis.

4.2.2 Human Health Significance

To protect human consumers of fish and shellfish in British Columbia from unacceptable cancer risks, interim tissue quality criteria have been developed for benzo(a)pyrene (Nagpal, 1993). The model developed for PAHs in Chapter 3 has utility in evaluating the potential effectiveness of the tissue criteria for benzo(a)pyrene.

The tissue criteria are based on the model for cancer risk assessment used by US EPA. Its general form is:

$$R(d) = q \cdot d \qquad [46]$$

Figure 4-1: Model-Predicted body burdens of Phase I B(a)P metabolites in trophic guilds under two representative scenarios, based on a sediment B(a)P concentration of 0.00961 g/kg. Note log scale on y-axis.

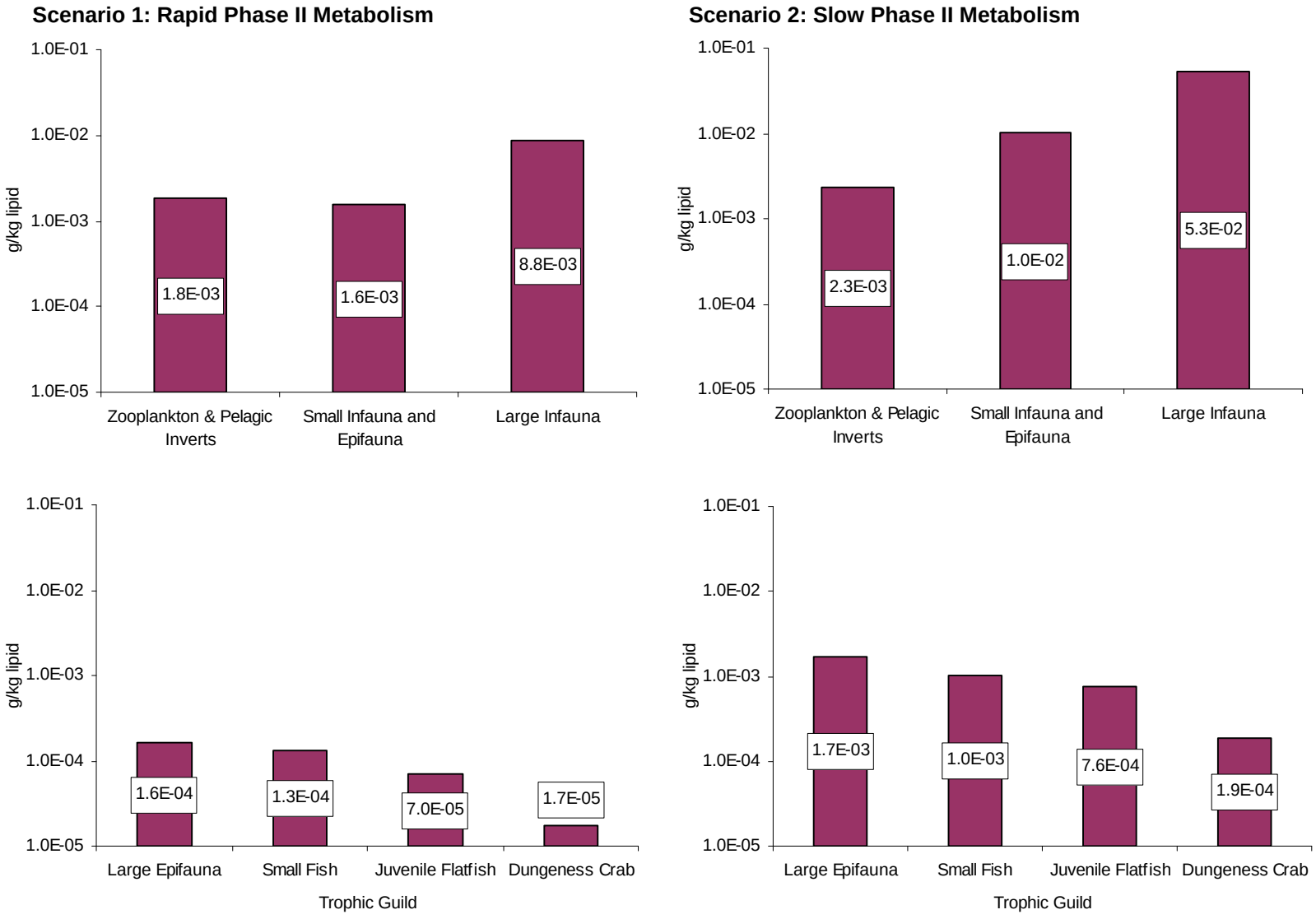

where R(d) is the excess (over background) lifetime risk of cancer at a given dose, d is the dose of chemical (mg/kg/day) and q is the cancer potency factor determined from a dose/tumour frequency relationship. By assuming an acceptable excess risk level (R(d)) of 7 in 1000000, and a cancer potency factor of 11.5 for benzo(a)pyrene (based on the range reported in IRIS (1994)), Nagpal (1993) calculated acceptable tissue concentrations for a 70 kg person under three seafood consumption levels (refer to Table 4-1). In general, these tissue criteria are intended to prevent excess cancer risks in the population of seafood consumers from exceeding 7 in 1000000.

However, the presence of Phase I metabolites, in addition to parent benzo(a)pyrene, could potentially increase excess cancer risks in seafood consumers over the acceptable limit. Given that the mechanism of carcinogenesis for PAHs is the production of Phase I metabolites and subsequent DNA adduct formation by the metabolites, certain Phase I metabolites can be expected to be at least as potent at causing tumours as parent benzo(a)pyrene. Figure 4-2 presents expected tissue burdens of Phase I metabolites in Dungeness crab when parent benzo(a)pyrene tissue burdens meet the intermediate criterion (i.e., 2 μg/kg, based on consumption of 100g of crab tissue per week). Note that the two scenarios again refer to situations when Phase II metabolism is rapid relative to Phase I or when Phase II metabolism is overwhelmed by either Phase I induction or high PAH exposure. In general, these two scenarios represent the best- and worst-case scenarios for exposure to benzo(a)pyrene metabolites by consumers of Dungeness crab. With high Phase II metabolism, the tissue burden of Phase I metabolites is low relative to parent chemical, but their presence could still result in an elevation of the excess cancer risk over the acceptable limit of 7 in 1000000. With low Phase II metabolism, the tissue burden of Phase I metabolites is much higher relative to parent chemical and could potentially cause a significant increase in cancer risk.

As a hypothetical example, if Phase I metabolites are assumed to have equal potency to parent benzo(a)pyrene, the predicted excess cancer risk under the high Phase II scenario from both parent compound and metabolites is 9 in 1,000,000. Under the low Phase II

Table 4-1: Interim tissue criteria for benzo(a)pyrene to protect human consumers of fish and shellfish. Source: Nagpal (1993)

Tissue Criterion (mg/kg wet weight)	Weekly Consumption Rate (g wet weight/week)
4	50
2	100
1	200

Figure 4-2: Predicted tissue burdens of Phase I metabolites of benzo(a)pyrene (dark shading) in Dungeness crab when parent benzo(a)pyrene (light shading) concentrations meet the tissue criterion of 2 μg/kg.

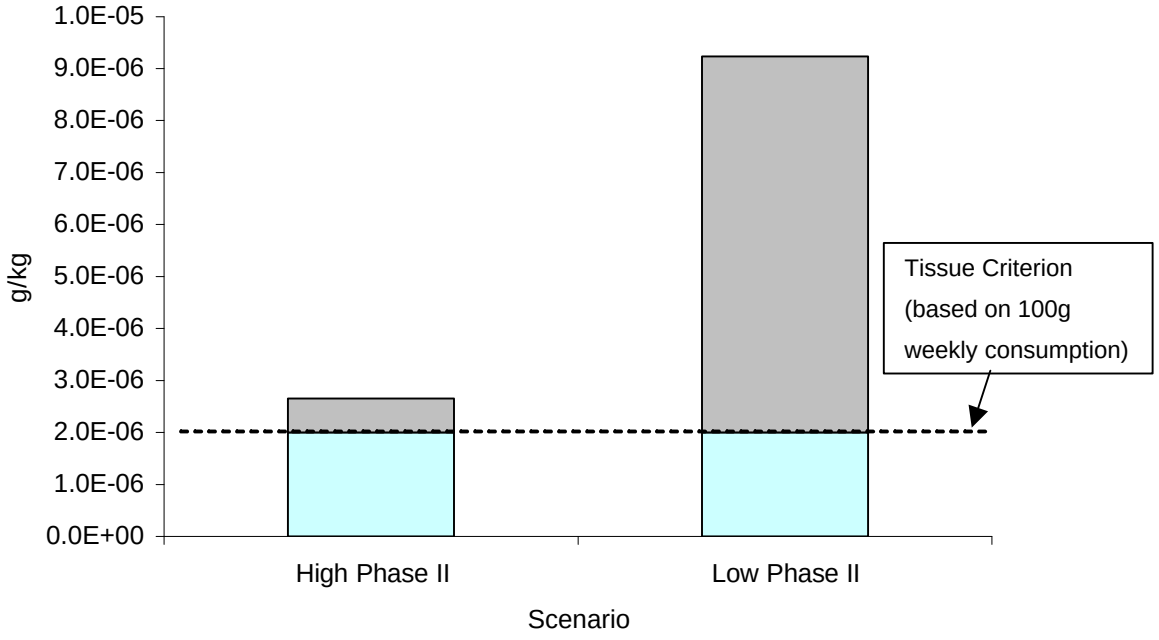

High Phase II – Scenario where the rate of Phase II metabolism of Phase I metabolites exceeds the rate of Phase I metabolism by 3-fold. This is the "normal" case in natural systems.

Low Phase II – Scenario where the rate of Phase II metabolism of Phase I metabolites is significantly lower than the rate of Phase I metabolism (i.e., 3-fold lower). This condition could be caused by Phase II limitation relative to Phase I due to Phase I induction or high PAH exposure levels.

scenario, the predicted excess cancer risk is 24 in 1,00,0000. The calculated tissue residues of parent compound which result in the *acceptable* excess cancer risk of 7 in 1,000,000 would be 1.46 μg/kg for the first scenario and 0.4 μg/kg for the second scenario.

It is important to note that this example is intended to illustrate the potential human health significance of PAH metabolism but shouldn't be interpreted to represent the actual case in Kitimat Arm. Phase II metabolism is generally expected to be rapid relative to Phase I metabolism, reducing tissue residues of metabolites for most situation. Under certain situations, Phase II metabolism may be limited but this condition would likely only persist in areas with relatively high PAH contamination and Phase I inducers present. In addition, the potencies of specific Phase I metabolites are likely to vary with some being non-carcinogenic (i.e., q = 0) and some potentially with higher potency, having already passed through the first stage of metabolic activation. Finally, fish and shellfish contaminated with parent benzo(a)pyrene and benzo(a)pyrene metabolites are likely to also contain other PAH and metabolites, and this mix of chemicals would potentially result in higher risk than benzo(a)pyrene alone. These factors require further study to accurately assess health risks from parent PAHs and PAH metabolites in human consumers of fish and shellfish.

4.3 RECOMMENDATIONS

By first developing and calibrating a model for non-metabolized PCBs and then applying it to PAHs, which undergo metabolic transformation in marine organisms, it has been possible to initiate the development of an assessment strategy for metabolized chemicals with potentially toxic metabolites. By integrating the current knowledge of the processes of bioaccumulation, metabolism and toxicity of parent PAHs and PAH metabolites, it has been possible to identify the following research needs and recommendations for management:

1. **The BSAF model and associated k_M values should be tested in other systems.** Application of the model in other systems would verify its ability to represent PAH dynamics, improving the confidence in model predictions and allowing for

refinement of model parameters. In addition, application and testing of the k_M values for all trophic guilds (i.e., by comparing model predictions to observed data) would validate the k_M values for representative organism groups, lending support to their general applicability to marine organisms. Two systems where data (i.e., sediment and biota) may be adequate for further model application and testing include False Creek, BC and smelter-impacted fjords in Norway.

2. **Research and assessment of PAH-related impacts to marine organisms should be focussed on species with high exposure to parent PAHs and metabolites, and high sensitivity to metabolite-mediated effects.** The results of model sensitivity analysis suggest that bivalve mollusks have the highest metabolite body burdens due to their high parent PAH exposure in food (i.e., sediment and detritus), and low metabolic rates. This prediction supports the continued use of bivalve mollusks as biomonitors of PAH pollution. Based on extensive research in Puget Sound, English sole are known to be highly sensitive to carcinogenesis caused by Phase I PAH metabolites. Thus, while the predicted exposure to Phase I metabolites is low relative to invertebrate detritivores, the risk to this species is may be relatively high because of its toxicological sensitivity. Further research is needed to determine other species high with sensitivity to PAH carcinogenesis.

3. **Environmental assessment and management of PAHs and other metabolized chemicals should consider the risks associated with exposure to both parent chemical and potentially toxic metabolites.** The preceding discussion demonstrates both the links between metabolism and ecological effects, and the potential human exposure to parent PAHs and metabolites. It is important that environmental managers explicitly consider metabolite exposure and potential toxicity in setting environmental criteria and assessing ecological and human health risks. Although the current uncertainty in metabolic rates and the dose-response relationship for PAH metabolites precludes quantitative analysis, precautionary assumptions may be required to prevent metabolite-mediated effects even when parent PAH concentrations are observed to be low. In the future, improved methods for metabolite

analysis, exposure studies to infer metabolic rate constants in live organisms, and toxicity studies to formulate dose-responses for multiple PAHs may all facilitate the finalization of a quantitative assessment strategy for parent PAHs and metabolites.

4. **Further research is necessary to support the development of a quantitative assessment strategy for PAHs and PAH metabolites.** Methods for direct analysis of PAH metabolites in organism tissue are generally lacking, as is knowledge of the dose response-relationship for Phase I metabolites of individual PAH congeners. The inability to directly measure Phase I metabolites in representative organism tissues (i.e., the liver or hepatopancreas) prevents field validation of the model developed here for the mass balance of Phase I metabolites. New chemical analysis techniques would allow for this validation using field-collected organism from contaminated areas. However, while the validated model would allow for exposure assessment, knowledge of the dose-response relationship for PAH metabolites is currently inadequate for risk assessment. To formulate this dose response, long-term life cycle experiments are required to determine the likelihood of carcinogenesis in fish and invertebrates which experience significant PAH exposure during critical life stages or throughout their life cycle. Unfortunately, the cost and time requirements of this type of experimentation may be prohibitive; this is an emerging issue for the assessment of the long-term chronic effects of POPs in aquatic organisms. The k_M values determined from radiolabel studies are first approximations of metabolic rates for PAHs. Additional laboratory experimentation with radiolabelled chemicals could yield valuable information. For example, estimates of k_M and k_{phase2} could be made by fitting a mechanistic model to experimental data for a time course of uptake and elimination of parent PAHs, Phase I metabolites, and conjugated metabolites. By conducting these experiments with different species groups and multiple PAHs, more accurate, congener-specific estimates of k_M and k_{phase2} could be made for broad organism classes.
5. **Further research is necessary regarding the bioavailability of soot-associated PAHs.** Soot association appears to cause a significant reduction in exposure and resultant BSAFs for parent PAHs. While current research and theories allow for

estimation of bioavailable fractions in water, there is little information regarding the dietary uptake of PAH from soot.

The enactment of some or all of these recommendations would serve to improve the current assessment approaches for the impacts of PAHs in marine ecosystems.

REFERENCES

Aller, RC. 1983. The importance of the diffusive permeability of animal burrow linings in determining marine sediment chemistry. J. Mar. Res. 41: 299-322.

Arnot, J. 2003. Bioaccumulation modelling of organic chemicals in aquatic ecosystems. Master's Thesis. Department of Biology. Simon Fraser University. April 2003.

Bailey, GS, DE Goeger and J Hendricks. 1989. Factors influencing experimental carcinogenesis in laboratory fish models. In: Varanasi, U (ed.). 1989. Metabolism of polycyclic aromatic hydrocarbons in the aquatic environment. CRC Press. Boca Raton.

Baumann, PC. 1989. PAH, metabolism, and neoplasia in feral fish populations. In: Varanasi, U (ed.). 1989. Metabolism of polycyclic aromatic hydrocarbons in the aquatic environment. CRC Press. Boca Raton.

BCMELP (BC Ministry of Environment Lands and Parks). 1997. Ambient Water Quality Criteria for Dissolved Oxygen. Prepared pursuant to Section 2(e) of the Environment Management Act, 1981 February 1997

Bodor, N and P Buchwald. 1997. Molecular size based approach to estimate partition properties for organic solutes. J. Phys. Chem. B 101: 3403-3412.

Boehm, PD and JG Quinn. 1977. The persistence of chronically accumulated hydrocarbons in the hard shell clam *Mercenaria mercenaria*. Mar. Biol. 44: 227-233.

Boese, BL, M Winsor, HL Lee, S Echols, J Pelletier, and R Randall. 1995. PCB congeners and hexachlorobenzene biota sediment accumulation factors for *Macoma nasuta* exposed to sediments with different total organic carbon contents. Environ. Toxicol. Chem. 14(2): 303-310

Brett, JR. 1995. Chapter 1 - Energetics. *in:* Groot, C, L Margolis, and WC Clarke (eds.). 1995. Physiological ecology of Pacific salmon. UBC Press, Vancouver.

Brown, CA and NB Terwilliger. 1999. Developmental changes in oxygen uptake in *Cancer magister* (Dana) in response to changes in salinity and temperature. J. Exp. Mar. Biol. Ecol. 241: 179-192.

Buhler, DR and DE Williams. 1989. Enzymes involved in metabolism of PAH by fishes and other aquatic animals: oxidative enzymes (or Phase I enzymes). In: Varanasi, U (ed.). 1989. Metabolism of polycyclic aromatic hydrocarbons in the aquatic environment. CRC Press. Boca Raton.

Cahill, TM, I Cousins and D Mackay. 2003. Development and application of a generalized physiologically based pharmacokinetic model for multiple environmental contaminants. Environ. Toxicol. Chem. 22(1): 26-34.

Calabrese, EJ and LA Baldwin. 2003. Commentary: Toxicology rethinks its central belief – hormesis demands a reappraisal of the way risks are assessed. Nature 42: 691-692.

Campfens, J and D Mackay. 1997. Fugacity-based model of PCB bioaccumulation in complex aquatic food webs. Environ. Sci. Technol. 31: 577-583.

CEPA (Canadian Environmental Protection Act). 1999. Canada Gazette Part III: Vol. 22 No.3 November 4, 1999. Statutes of Canada, 1999, Chapters 33 and 34, Acts assented to from 18 June to 14 September, 1999. Ottawa, Canada: the Minister of Public Works and Government Services, the Queen's Printer for Canada.

CEPA. 1994. Priority substances list assessment report – polycyclic aromatic hydrocarbons. Environment Canada/Health Canada.

Collier, TK and U Varanasi. 1991. Hepatic activities of xenobiotic metabolizing enzymes and biliary levels of xenobiotics in English sole (Parophrys vetulus) exposed to environmental contaminants. Arch. Environ. Contam. Toxicol.. 20: 462-473.

Connolly, JP. 1991. Application of a food chain model to polychlorinated biphenyl contamination of the lobster and winter flounder food chains in New Bedford Harbor. Environ. Sci. Technol. 25: 760-770.

Cretney, WJ, CS Wong, MacDonald, RW, Erickson, PE, and BR Fowler. 1983. Polycyclic aromatic hydrocarbons in surface sediments and age-dated cores from Kitimat Arm, Douglas Channel and adjoining waterways. pp. 162-195 *in*: MacDonald, RW (ed). 1983. Proceedings of a workshop on the Kitimat marine environment. Can. Tech. Rep. Hydro. Ocean Sci. No. 18.

de Maagd, PG, DTEM ten Hulscher, H van den Heuvel, A Opperhuizen and DTHM Sijm. 1998b. Physicochemical properties of polycyclic aromatic hydrocarbons: aqueous solubilities, *n*-ocatanol/water partition coefficients, and Henry's law constants. Environ. Toxicol. Chem. 17(2): 251-257.

de Maagd, PG, J de Poorte, A Opperhuizen and DTHM Sijm. 1998a. No influence after various exposure times on the biotransformation rate constants of benzo(a)anthracene in fathead minnow (*Pimephales promelas*). Aquatic Toxicology 40: 157-169.

Di Toro, DM, CS Zarba, D Hansen, WJ Berry, RC Swartz. CD Cowan, SP Pavlou, HE Allen, NA Thomas, and PR Paquin. 1991. Technical basis for establishing sediment quality criteria for nonionic organic chemicals using equilibrium partitioning. Environ. Toxicol. Chem. 10: 1541-1583.

Eickhoff, CV, S He, FAPC Gobas and FCP Law. 2003. Determination of polycyclic aromatic hydrocarbons in Dungeness crabs (Cancer magister) near an aluminum smelter in Kitimat Arm, British Columbia, Canada. Environ. Toxicol. Chem. 22(1): 50-58. l

Eisler, R. 1987. Polycyclic aromatic hydrocarbon hazards to fish, wildlife, and invertebrates: a synoptic review. Contaminant Hazard Review. Fish and Wildlife Service Biological Report 85(1.11). Washington, D.C.

Environment Canada. 2000. A guide to the Canadian Environmental Protection Act, 1999. March 2000.

EVS and PLA (EVS Environment Consultants and Paine, Ledge and Associates). 1997. Alcan marine monitoring program: 1997 intensive study. Report prepared for Alcan Ltd.

EVS Environment Consultants, Sea Science and Frank Gobas Environmental Consulting. 1996. Modelling the fate of contaminant discharges in Burrard Inlet. A report to the Burrard Inlet Environmental Action Program, Vancouver, BC.

Fay, AA, BJ Brownawell, AA Elskus, and AE McElroy. 2000. Critical body residues in the marine amphipod Ampelisca abdita: sediment exposures with nonionic organic contaminants. Environ. Toxicol. Chem. 19(4): 1028-1035.

Fisk AT, RJ Norstrom, CD Cymbalisty, DCG Muir. 1998. Dietary accumulation and depuration of hydrophobic organochlorines: bioaccumulation parameters and their relationship with the octanol/water partition coefficient. Environ. Toxicol. Chem. 17(5): 951-961.

Fossi, MC, C. Savelli, S. Casini, E. Franchi, N. Mattei and I. Corsi. 1997. Multi-response biomarker approach in the crab Carcinus aestuarii experimentally exposed to benzo(a)pyrene, polychlorobiphenyls and methyl-mercury. Biomarkers 2: 311-319

Foureman, GL. 1989. Enzymes involved in metabolism of PAH by fishes and other aquatic animals: hydrolysis and conjugation enzymes (or Phase II enzymes). In: Varanasi, U (ed.). 1989. Metabolism of polycyclic aromatic hydrocarbons in the aquatic environment. CRC Press. Boca Raton.

French, BL, WL Reichert, T Hom, M Nishimoto, HR Sanborn, and JE Stein. 1996. Accumulation and dose-response of hepatic DNA adducts in English sole (*Pleuronectes vetulus*) exposed to a gradient of contaminated sediments. Aquatic Toxicology 36: 1-16.

Gewurtz, SB, R Lazar, and GD Haffner. 2000. Comparison of polycyclic aromatic hydrocarbon and polychlorinated biphenyl dynamics in benthic invertebrates of Lake Erie, USA. Environ. Toxicol. Chem. 19(12): 2943-2950

Gibson, GG and P Skett. 1986. Introduction to drug metabolism. Chapman and Hall. New York.

Gobas, FAPC and D Mackay. 1987. Dynamics of hydrophobic organic chemical bioconcentration in fish. Environ. Toxicol. Chem. 6: 495-504.

Gobas, FAPC and HA Morrison. 2000. Bioconcentration and biomagnification in the environment. *in:* Boethling RS, D Mackay, eds. 1999. Handbook of Property Estimation Methods for Chemicals: Environmental and Health Sciences. CRC, Boca Raton, FL, USA.

Gobas, FAPC and LG MacLean. 2003. Sediment-water distribution of organic contaminants in aquatic systems: the role of organic carbon mineralization. Environ. Sci. Technol. 37: 735-741.

Gobas, FAPC, DCG Muir, and D Mackay. 1988. Dynamics of dietary bioaccumulation and faecal elimination of hydrophobic organic chemicals in fish. Chemosphere 7(5): 943-962.

Gobas, FAPC, JB Wilcockson, RW Russell, GD Haffner. 1999. Mechanisms of biomagnifcation in fish under laboratory and field conditions. Environ. Sci. Technol. 33: 133-141.

Gobas, FAPC, JR McCorquodale and GD Haffner. 1993a. Intestinal-absorption and biomagnification of organochlorines. Environ. Toxicol. Chem. 12(3): 567-576.

Gobas, FAPC, X Zhang and R Wells. 1993b. Gastrointestinal magnification: the mechanisms of biomagnification and food chain accumulation of organic chemicals. Environ. Sci. Technol. 27: 2855-2863.

Gobas, FAPC. 1993. A model for predicting the bioaccumulation of hydrophobic organic chemicals in aquatic food webs: application to Lake Ontario. Ecol. Model. 69: 1-17.

Gunnarsson, JS and M Skold. 1999. Accumulation of polychlorinated biphenyls by the infaunal brittle stars *Amphiura filiformis* and *A. chiajei*: effects of eutrophication and selective feeding. Mar. Ecol. Prog. Ser. 186: 173-185.

Gustaffson, O, F Haghseta, C Chan, J Macfarlane and PM Gschwend. 1997. Quantification of the dilute sedimentary soot phase: implications for PAH speciation and bioavailability. Environ. Sci. Technol. 31: 203-209.

Harris, GE. 1999. Assessment of the assimilative capacity of Kitimat Arm British Columbia: A case study approach to the sustainable management of environmental contaminants. Ph.D. Thesis, Resource and Environmental Management. Simon Fraser University. October 1999.

Hawker, DH and DW Connell. 1988. Octanol-water partition coefficients of polychlorinated biphenyl congeners. Environ. Sci. Technol. 22: 382-387.

Higgs, DA, JS MacDonald, CD Levings, and BS Dosanjh. 1995. Chapter 4 - Nutrition and feeding habits in relation to life history stage. *in:* Groot, C, L Margolis, and WC Clarke (eds.). 1995. Physiological ecology of Pacific salmon. UBC Press, Vancouver.

IARC (International Agency for Research on Cancer). 1982. IARC Monographs on the Evaluation of the Carcinogenic Risk of Chemicals to Humans. IARC: Lyons, France, Vol. 29, p. 16.

Ikonomu, MG, MP Fernandez, W Knapp, and P. Sather. 2002. PCBs in Dungeness crab reflect distinct source fingerprints among harbour/industrial sites in British Columbia. Environ. Sci. Technol. 36: 2545-2551

IRIS (Integrated Risk Information System). 1994. Benzo(a)pyrene (BaP) (CASRN 50-32-8) – full IRIS summary. US Environmental Protection Agency. http://www.epa.gov/iris/subst/0136.htm.

Iverson, SJ, KJ Frost, and SLC Lang. 2002. Fat content and fatty acid composition of forage fish and invertebrates in Prince William Sound, Alaska: factors contributing to among and within species variability. Mar. Ecol. Prog. Ser. 241: 161-181.

Jackson, LJ, AS Trebitz, an dKL Cottingham. 2000. An introduction to the practice of ecological modeling. Bioscience 50(8): 694-706.

James, MO and PJ Little. 1984. 3-methylcholanthrene does not induce in vitro xenobiotic metabolism in spiny lobter, or affect in vivo disposition of benzo(a)pyrene. Comp. Biochem. Physiol. 78C: 241-245.

James, MO. 1989. Biotransformation and disposition of PAH in aquatic invertebrates. In: Varanasi, U (ed.). 1989. Metabolism of polycyclic aromatic hydrocarbons in the aquatic environment. CRC Press. Boca Raton.

Jonker, MTO and A Koelmans. 2002. Sorption of Polycyclic Aromatic Hydrocarbons and Polychlorinated Biphenyls to Soot and Soot-like Materials in the Aqueous Environment: Mechanistic Considerations. Environ. Sci. Technol.2002, 36,3725-3734.

Kaag, NHBM, EM Foekema, MCT Scholten, and NM Van Staalen. 1996. Comparison of contaminant accumulation in three species of marine invertebrates with different feeding habits. Environ. Toxicol. Chem. 16: 837-842.

Kane-Driscoll, S and AE McElroy. 1996. Bioaccumulation and metabolism fo benzo(a)pyrene in three species of polychaete worms. Environ. Toxicol. Chem. 15(8): 1401-1410.

Kane-Driscoll, SB and AE McElroy. 1997. Elimination of sediment-associated benzo(a)pyrene and its metabolites by polychaete worms exposed to 3-methylcholanthrene. Aquat. Toxicol. 39: 77-91.

Kitamaat Village Council. 2003. Kitimat Village Council – history. Kitamaat Village , BC. http://www.haisla.net/history.htm

Kitimat Chamber of Commerce. 2003. Kitimat: A planned community. Kitimat, BC. www.visitkitimat.com/kitimat.htm

Krahn, MK, LD Rhodes, MS Myers, LK Moore, WD MacLeod Jr., and DC Malins. 1986. Associations between metabolites of aromatic compounds in bile and the occurrence of hepatic lesions in English sole (Parophrys vetulus) from Puget Sound, Washington. Arch. Environ. Contam. Toxicol.. 15: 61-67.

Kristensen, E. 1989. Oxygen and carbon dioxide exchange in the polychaete *Nereis virens*: influence of ventilation activity and starvation. Marine Biology. 101: 381-388.

Landrum, PF and D. Scavia. 1983. Influence of sediment on anthracene uptake, depuration and biotransformation by the amphipod *Hyallella azteca*. Can. J. Fish. Aquat. Sci. 40: 298-305.

Lasker, R. 1966. Feeding, growth, respiration, and carbon utilization of a euphausiid crustacean. J. Fish. Res. Bd. Canada. 23: 1291-1317.

Lee, RF and ML Neuhauser. 1976. Fate of petroleum hydrocarbons taken up from food and water by the blue crab *Callinectes sapidus*. Mar. Biol. 37: 363-370.

Linkov, I, D Burmistrov, J Cura and T Bridges. 2002. Risk-based management of contaminated sediments: consideration of spatial and temporal patterns in exposure modeling. Environ. Sci. Technol. 36:238-246

Little, PJ, MO James, JB Pritchard and JR Bend. 1985. Temperature-dependent disposition of [14C] benzo[a]pyrene in the spiny lobster, *Panulirus argus*. Toxicol. Appl. Pharm. 77: 325-333.

Livingstone, DR. 1991. Organic xenobiotic metabolism in marine invertebrates. Advances in Comparative and Environmental Physiology. Vol. 7, Chp. 2, pp: 46 – 185.

Livingstone, DR. 1992. Persistent pollutants in marine invertebrates. *In:* Walker, CH and DR Livingstone (eds.). 1992. Persistent Pollutants in Marine Ecosystems. SETAC Special Publications Series. Pergamon Press. Oxford, England.

Livingstone, DR. 1998. The fate of organic xenobiotics in aquatic ecosystems: quantitative and qualitative differences in biotransformation by invertebrates and fish. Comparative Biochemistry and Physiology-Part A 120: 43-49.

Lotufo, GR. 1998. Bioaccumulation of sediment-associated fluoranthene in benthic copepods: uptake, elimination and biotransformation. Aquat. Toxicol. 44: 1-15.

Mackay, D and A Fraser. 2000. Bioaccumulation of persistent organic chemicals: mechanisms and models. Environmental Pollution 110: 375-391.

Mackay, D, W Shiu, K Ma. 1999. Physical-chemical properties and environmental fate handbook. CRC Press LLC.

Mackay, D. 1991. Multimdia Environmental Fate Models: the Fugacity Approach. CRC Press/Lewis Publishers, Boca Raton, FLA.

Mackintosh, CM and J Maldonado. 2003. PCB concentration data for sediments and organism tissues from False Creek, BC.

Mackintosh, CM. 2003. Distribution of phthalate esters in a marine food web. REM 699 Research Project. Report no. 295. Simon Fraser University, School of Resource and Environmental Management.

Malins, DC, MM Krahn, MS Myers, LD Rhodes, DW Brown, CA Krone, BB McCain and S Chan. 1985. Toxic chemicals in sediments and biota from a creosote-polluted harbor: relationships with hepatic neoplasms and other hepatic lesions in English sole (*Parophrys vetulus*). Carcinogenesis 6(10): 1463-1969.

Marsden, ID. 1999. Respiration of the surf clam *Paphies donacani* from New Zealand. Hydrobiologia 405: 179-188.

McCarty, LS and D Mackay. 1993. Enhancing ecotoxicological modeling and assessment. Environ. Sci. Technol. 27(9): 1719-1728.

McDonald, DG , CM Wood and BR McMahon. 1980. Ventilation and oxygen consumption in the Dungeness crab, *Cancer magister*. J. Expt. Zool. 213: 132-136.

McElroy, A, K Leitch and A Fay. 2000. A survey of *in vivo* benzo[a]pyrene metabolism in small benthic marine invertebrates. Mar. Env. Res. 50: 33-38.

McElroy, AE, JM Cahill, JD Sisson and KM Kleinow. 1991. Relative bioavailability and DNA adduct formation of benzo(a)pyrene and metabolites in the diet of winter flounder. Comp. Biochem. Physiol. 100C: 29-32.

McElroy, AE. 1985. *In vivo* metaoblism of benz[a]anthracene by the polychaete Nereis virens. Marine Environmental Research. 17: 133-136

Meador, JP, JE Stein, WL Reichert, and U Varanasi. 1995. Bioaccumulation of polycyclic aromatic hydrocarbons by marine organisms. Reviews of Environmental Contamination and Toxicology. Vol. 143: 79 – 165

Mining Association of British Columbia. 2003. Mining, who needs it? Vancouver, BC. www.mining.bc.ca/mwni/chapter02-05.html

Morrison, HA, DM Whittle CD Metcalfe and AJ Niimi. 1999. Application of a food web bioaccumulation model for the prediction of polychlorinated biphenyl, dioxin and furan congener concentrations in Lake Ontario aquatic biota. Can. J. Fish. Aquat. Sci. 56: 1389-1400.

Morrison, HA, FAPC Gobas, R Lazar, and GD Haffner. 1996. Development and verification of a bioaccumulation model for organic contaminants in benthic invertebrates. Environ. Sci. Technol. 30: 3377-3384.

Morrison, HA, FAPC Gobas, R Lazar, DM Whittle and GD Haffner. 1997. Development and verification of a benthic/pelagic food web model for PCB congeners in Western Lake Erie. Environ. Sci. Technol. 31: 3267-3273.

Myers, MS, JT Landahl, MM Krahn, LL Johnson and BB McCain. 1990. Overview of studies on liver carcinogenesis in English sole from Puget Sound: evidence for a xenobiotic chemical etiology I: pathology and epizootiology. Sci. Tot. Environ. 94: 33-50.

Myers, MS, LL Johnson, OP Olson, CM Stehr, BH Horness, TK Collier, and BB McCain. 1998b. Toxicopathic hepatic lesions as biomarkers of chemical contaminant exposure and effects in marine bottomfish species from the Northeast and Pacific Coasts, USA. Mar. Poll. Bull. 37(1-2): 92-113.

Myers, MS, LL Johnson, T Hom, TK Collier, JE Stein and U Varanasi. 1998a. Toxicopathic hepatic lesions in subadult English sole (*Pleuronectes vetulus*) from Puget Sound, Washington, USA: relationships with other biomarkers of contaminant exposure. Marine Environmental Research 45(1): 47-67.

Nagpal, NK. 1993. Ambient water quality criteria for polycyclic aromatic hydrocarbons (PAHs). Province of British Columbia. Ministry of Environment, Lands and Parks. Water Quality Branch .Water Management Division. February, 1993

Nichols JW, PN Fitzsimmons, FW Whiteman, DW Kuehl, BC Butterworth, and CT Jenson. 2001. Dietary uptake kinetics of 2,2 ',5,5 '-tetrachlorobiphenyl in rainbow trout. Drug Metabolism and Disposition 29(7): 1013-1022

NOAA (National Oceanic and Atmospheric Administration). 2000. Sampling and analysis plan for Kitimat environmental assessment. Prepared for: Haisla First Nation, Kitamaat Village, BC, Canada. By: Northwest Fisheries Science Center, National Marine Fisheries Service, NOAA. Seattle WA

Oakey, T and D Pauly. 1999. A trophic mass-balance model of Alaska's Prince William Sound ecosystem, for the post-spill period 1994-1996 – 2nd edition. Fisheries Centre Research Reports Volume 7, No. 4. Fisheries Centre, University of British Columbia.

Paine, MD, PM Chapman, PJ Allard, MH Murchoch and D Minifie. 1996. Limited bioavailability of sediment PAH near an aluminum smelter: contamination does not equal effects. Environ. Toxicol. Chem. 15: 2003-2018.

Parkerton, TF. 1993. Estimating toxicokinetic parameters for modeling the bioaccumulation of non-ionic organic chemicals in aquatic organisms. Ph.D. Dissertation. Graduate Program in Environmental Science. Rutgers University. New Brunswick, NJ.

Pauly, D and V Christensen. 1996. Mass balance models of north-eastern Pacific ecosystems. Fisheries Centre Research Reports Vol. 4, No. 1. Fisheries Centre, University of British Columbia, Canada. ISSN 1198-6727

Payne, SA, BA Johnson, and RS Otto. 1999. Proximate composition of some north-eastern Pacific forage fish species. Fish. Oceanogr. 8(3): 159-177.

Reichert, WL, BL Eberhart and U. Varanasi. 1985. Exposure of two species of deposit feeding amphipods to sediment-associated [3H]benzo[a]pyrene: uptake, metabolism and covalent binding to tissue molecules. Aquat. Toxicol. 6: 45-56.

Reichert, WL, MS Myers, K Peck-Miller, B. French, BF Anulacion, TK Collier, JE Stein, and U Varanasi. 1998. Molecular epizootiology of genotoxic events in marine fish: linking contaminant exposure, DNA damage and tissue-level alterations. Mutation Research. 411: 215-225.

Seth, R, D Mackay and J Muncke. 1999. Estimating the organic carbon partition coefficient and its variability for hydrophobic chemicals. Environ. Sci. Technol. 33: 2390-2394

Sharpe, S and D Mackay. 2002. A framework for evaluating bioaccumulation in food webs. Environ. Sci. Technol. 34: 2373-2379.

Shaw, GR and DW Connel. 2001. DNA adducts as a biomarker of polycyclic aromatic hydrocarbon exposure in aquatic organisms: relationship to carcinogenicity. Biomarkers 6: 64-71.

Sijm, DTHM and A Opperhuizen. 1989. Biotransformation rates of xenobiotic compounds in relation to enzyme activities – a critical review. Toxicological and Environmental Chemistry 23: 181-190.

Simpson, CD, CF Harrington, WR Cullin, DA Bright and KJ Reimer. 1998. Polycyclic aromatic hydrocarbon contamination in marine sediments near Kitimat, British Columbia. Environ. Sci. Technol. 32: 3266-3272.

Skoglund, RS and DL Swackhamer. 1999. Evidence for the use of organic carbon as the sorbing matrix in the modeling of PCB accumulation in phytoplankton. Environ. Sci. Technol. 33: 1515-1519

Skoglund, RS, K Stange and DL Swackhamer. 1996. A kinetics model for predicting the accumulation of PCBs in phytoplankton. Environ. Sci. Technol. 30: 2113-2120.

Stevens, BG, DA Armstrong and R Cusimano. 1982. Feeding habits of the Dungeness crab, *Cancer magister*, as determined by the index of relative importance. Marine Biology 72: 135-145.

Thomann, RV and J Komlos. 1999. Model of biota-sediment accumulation factor for polycyclic aromatic hydrocarbons. Environ. Toxicol. Chem. 18(5): 1060-1068.

Thomann, RV, JP Connolly, and TF Parkerton. 1992. An equilibrium model of organic-chemical accumulation in aquatic food webs with sediment interaction. Environ. Toxicol. Chem. 11(5): 615-629.

Thomann, RV. 1989. Bioaccumulation model of organic chemical distribution in aquatic food chains. Environ. Sci. Technol. 23: 699-707

Tracey, GA and DJ Hansen. 1996. Use of biota-sediment accumulation factors to assess similarity of nonionic organic chemical exposure to benthically-coupled organisms of differing trophic mode. Arch. Environ. Contam. Toxicol. 30: 467-475.

UNECE (United Nations Economic Council of Europe). 1998. Convention on Long Range Transboundary Air Pollution (1979) and its 1998 Protocols on Persistent Organic Pollutants. New York, USA and Geneva, Switzerland: United Nations. Report No. ECE/EB.AIR/66. ISBN: 9211167248. 91 p. Avaialble from: United Nations publication sales no. E.99.II.E.21.

US EPA (United States Environmental Protection Agency). 1998. Guidelines for ecological risk assessment. EPA/630/R-95/002F. April 1998. Risk Assessment Forum, USEPA. Washington, DC.

Vallack, HW, DJ Bakker, I Brandt, E Brostrom-Lunden, A Brouwer, KR Bull, C Gough, R Guardans, I Holoubek, B Jansson, R Koch, J Kuylenstierna, A Lecloux, D Mackay, P McCutcheon, P Mocarelli, RDF Taalman. 1998. Controlling persistent organic pollutants - what next?. Environmental Toxicology and Pharmacology. 6(3): 143-175.

Van der Linde, A, A J Hendriks, and DTHM Sijm. 2001. Estimating biotransformation rate constants of organic chemicals from modelled and measured elimination rates. Chemosphere 44: 423-435.

Varanasi, U (ed.). 1989. Metabolism of polycyclic aromatic hydrocarbons in the aquatic environment. CRC Press. Boca Raton.

Varanasi, U, JE Stein and M Nishimoto. 1989a. Biotransformation and disposition of PAH in fish. *In:* Varanasi, U (ed.). 1989. Metabolism of polycyclic aromatic hydrocarbons in the aquatic environment. CRC Press. Boca Raton.

Varanasi, U, M Nishimoto, WM Baird, TA Smolarek. 1989b. Metabolic activation of PAH in subcellular fractions and cell cultures from aquatic and terrestrial species. In: Varanasi, U (ed.). 1989. Metabolism of polycyclic aromatic hydrocarbons in the aquatic environment. CRC Press. Boca Raton.

Varanasi, U, WL Reichert, JE Stein, DW Brown, HR Sanborn. 1985. Bioavailability and biotransformation of aromatic hydrocarbons in benthic organisms exposed to sediment from an urban estuary. Environ. Sci. Tech. 19: 836-841.

Wang, W and NS Fisher. 1999. Assimilation efficiencies of chemical contaminants in aquatic invertebrates: a synthesis. Environ. Toxicol. Chem. 18(9): 2034-2045

Wania, F and D Mackay. 1995. A global distribution model for persistent organic chemicals. Science of the Total Environment 160/161: 211-232.

Wania, F and D Mackay. 1999. The evolution of mass balance models of persistent organic pollutant fate in the environment. Environ. Pollut. 100: 223-240.

WCED (World Commission on Environment and Development). 1987. Our Common Future. Oxford University Press.

Weston, DP. 1990. Hydrocarbon bioaccumulation from contaminated sediment by the deposit-feeding polychaete *Abarenicola pacifica*. Mar. Biol. 107: 159-169.

Winsor, MH, BL Boese, H Lee, RC Randall and DT Specht. 1990. Determiniation of the ventilation rates of interstitial and overlying water by the clam, *Macoma nasuta*. Environ. Toxicol. Chem. 9: 209-213.

Xie, W, W Shiu, and D Mackay. 1997. A review of the effect of salts on the solubility of organic compounds in seawater. Mar. Env. Res. 44(4): 429-444.

APPENDIX A - Derivation of the Expression for Estimating F_{sc} (Equation 42)

For PAH congeners, the fraction of chemical associated with soot carbon in sediments (F_{sc}) was calculated using Equation 42 (see text). Equation 42 was derived using mass balance principles according to the following series of equations.

On a dry-weight basis, PAHs in sediments are expected to be present only in the sorptive phases of sediment. These include sediment organic carbon and soot carbon. Thus, the total mass of chemical in sediments, on a dry weight basis can be represented as:

$$M_s = M_{oc} + M_{sc} \qquad [46]$$

where M_s is the total mass of a given PAH congener (g), M_{oc} is the mass of chemical associated with organic carbon (g) and M_{sc} is the mass of chemical associated with soot carbon (g). M_s, M_{oc} and M_{sc} will depend on the respective concentrations (C) in each phase (i.e., whole sediment, organic carbon or soot carbon) and the volume (V) of each phase. With substitution of these terms, Equation 46 becomes:

$$C_s V_s = C_{oc} \cdot (V_s \cdot \phi_{oc}) + C_{sc} \cdot (V_s \cdot \phi_{sc}) \qquad [47]$$

where C_s, C_{oc} and C_{sc} are respective chemical concentrations in sediment (g/kg sediment), organic carbon (g/kg OC) and soot carbon (g/kg SC), V_s is the mass of sediment solids (kg) and ϕ_{oc} and ϕ_{sc} are respective dry-weight fractions of organic carbon and soot carbon in sediments.

Assuming equilibrium between sediment organic carbon and soot carbon, the expected chemical concentrations in organic carbon and soot carbon can be related based on the octanol-water partition coefficient (K_{ow}) and the soot-carbon-water partition coefficient (K_{sc}) such that:

$$\frac{K_{sc}}{K_{ow} \cdot 0.35} = \frac{C_{sc}/C_w}{C_{oc}/C_w} = \frac{C_{sc}}{C_{oc}} \qquad [48]$$

and,

$$C_{oc} = \frac{C_{sc} \cdot K_{ow} \cdot 0.35}{K_{sc}} \qquad [49]$$

where C_w is the theoretical concentration of chemical in water at equilibrium with either octanol or soot carbon (g/kg), and 0.35 represents the sorptive capacity of organic carbon relative to octanol (see Seth et al., 1999). Substitution of Equation 49 into Equation 47 then yields:

$$C_s V_s = \frac{C_{sc} \cdot K_{ow} \cdot 0.35}{K_{sc}} \cdot (V_s \cdot \phi_{oc}) + C_{sc} \cdot (V_s \cdot \phi_{sc}) \qquad [50]$$

Finally, given that:

$$F_{sc} = \frac{M_{sc}}{M_s} = \frac{C_{sc} \cdot (V_s \cdot \phi_{sc})}{C_s V_s} \qquad [51]$$

it is possible to reduce and solve Equation 50 for F_{sc} such that:

$$F_{sc} = \frac{C_{sc} \cdot (V_s \cdot \phi_{sc})}{C_s V_s} = \frac{1}{1 + (K_{ow} \cdot 0.35/K_{sc}) \cdot (\phi_{oc}/\phi_{sc})} \qquad [52]$$

Thus, for each PAH congener it is possible to estimate the fraction of chemical associated with soot carbon in sediments (F_{sc}) using only chemical properties (K_{ow} and K_{sc}) and the dry-weight fractions of organic carbon (ϕ_{oc}) and soot carbon (ϕ_{sc}) in sediments.